Condensates in group field theory

The emergence of cosmological evolution and matter

Xiankai Pang

München 2023

Condensates in group field theory

The emergence of cosmological evolution and matter

Xiankai Pang

Dissertation
der Fakultät für Physik
der Ludwig-Maximilians-Universität
München

vorgelegt von
Xiankai Pang
aus Shandong Province, China

München, den 16.06.2023

Erstgutachter: Dr. Daniele Oriti
Zweitgutachter: Dr. Michael Haack
Tag der mündlichen Prüfung: 28.07.2023

Zusammenfassung

In der Theorie der Gruppenfeldtheorie (GFT) der Quantengravitation löst sich das übliche Raum-Zeit-Kontinuum mikroskopisch in diskrete Bausteine auf. Eine große Herausforderung besteht darin, wie man aus diesen fundamentalen nicht-raumzeitlichen Freiheitsgraden die auf dem Raum-Zeit-Kontinuum basierende Physik extrahieren kann. Im Allgemeinen besteht jeder makroskopische Bereich des Raumes aus zahlreichen Bausteinen, und er kann aus Mean-Field Kondensatzuständen extrahiert werden.

Innerhalb von GFT, welche über $SU(2)$-Gruppen definiert ist, kann das Kondensat durch Spins unterschiedlicher Darstellungen charakterisiert werden. Im kosmologischen Sektor kann man das Kondensat jedoch von einem bestimmten Typ wählen, dessen Spins identisch sind. Dadurch kann die kombinatorische Struktur der GFT-Wechselwirkung ignoriert werden, was zu einer effektiv einfacheren Dynamik führt. Wir bezeichnen verschiedene Spins als Moden, und wir extrahieren die kosmologische Entwicklung unter Beitrag mehrerer Moden.

Zu früher kosmologischer Zeit herrscht Dominanz von kinetischen Termen, die zu Beschleunigungsexpansionen unmittelbar nach dem Bounce führen. Diese frühen Beschleunigungen sind aber auch mit allen Moden nicht von langer Dauer. Wechselwirkungsterme sind für die späte Beschleunigung notwendig. Insbesondere bei zwei Kondensatmoden können wir eine phantomähnliche Expansion rein quanten-gravitativen Ursprungs erhalten, auch ohne Phantom-Materie. Ein solches Verhalten kann durch die effektive equation of state aufgezeigt werden, aus der wir auch die ungefähre Position des Phantom-Übergangs, der im Ein-Moden-Fall fehlt, erhalten. Dieser erfolgt bei einer niedrigen Rotverschiebung, weswegen die Einbeziehung der zweiten Mode nur zu späten Zeiten zu Modifizierungen führt. Solche Modifikationen können den aktuellen Hubble-Wert H_0, der aus Daten abgeleitet wurde, erhöhen und somit zur Entlastung der H_0-Spannung aufgrund von Quantengravitationseffekten beitragen.

Darüber hinaus können wir durch die Berücksichtigung inhomogener Störungen in Kondensaten des Boulatov-Modells, einer 3d-GFT, die Dynamik eines Materiefeldes in Form einer generalisierten Version des Amit-Roginsky (AR)-Modells erhalten. Im Gegensatz zum kosmologischen Sektor berücksichtigen wir dabei die kombinatorischen Strukturen der Wechselwirkungsterme.

Hierfür betrachten eine Klasse von Lösungen, um die perturbiert werden soll, und wählen passende Störungen für den Angleich an die AR Freiheitsgrade. Die AR-Dynamik emergiert im Kondensat unter zwei zusätzlichen Bedingungen, und die resultierende Wirkung

ist eine Summe von AR-Modellen mit verschiedenen Spins. Diese Verallgemeinerung bricht melonische Dominanz im large-N Grenzwert, aber kann in bestimmten Näherungen wiederhergestellt werden.

Abstract

As a theory of quantum gravity, in group field theory (GFT) the usual spacetime dissolves microscopically into discretized building blocks. A major challenge is to understand how the familiar laws of physics based on continuous spacetime can emerge from these fundamental, non-spatio-temporal elements. Generally, any macroscopic region of the spacetime consists numerous number of building blocks, and the spacetime continuum can be extracted from condensate states at the mean field level.

In GFT over $SU(2)$ group, the corresponding condensate can be characterized by spins of different representations. For the cosmological sector, one can choose the condensate as a particular type whose spins are identical, such that the combinatorial structure of the GFT interaction can be ignored, which provides a simpler dynamics effectively. Different spins are referred to as 'modes', and we want to study the cosmological evolution when multiple modes contribute.

At early times, the dynamics of GFT is primarily governed by kinetic terms, resulting in accelerated expansion right after the cosmic bounce. However, these early-time accelerations are not long-lasting even when all modes are taken into account. Late-time acceleration requires interaction terms, and in particular, when we consider two condensate modes, we can obtain phantom-like evolution that arises purely from quantum gravity, without any phantom matter. Such behaviour can be revealed through the effective equation of state, from which the position of phantom crossing can be determined approximately. The crossing occurs at a low red shift, which indicates that the inclusion of the second mode modifies the single mode evolution only at late times. Such modifications can increase the current Hubble value H_0 inferred from data, which shed some lights in alleviating the H_0 tension based on quantum gravity effects.

Furthermore, by considering inhomogeneous perturbations over the condensates of the Boulatov model, a 3d GFT, we are able to get the dynamics of a matter field, in the form of a generalized version of the Amit-Roginsky (AR) model. Unlike the cosmological sector, the combinatorial structures of the interaction terms will be taken into account. We consider a class of solutions to the equation of motion, which serves as the condensate function to be perturbed, and choose suitable forms of perturbations to match the AR degrees of freedom. The AR dynamics will emerge when the condensate satisfies two additional conditions, and the resulting action will be a summation over the original AR model of different spins. This generalization breaks the melonic dominance in the large-N limit, but it can be restored under certain approximations.

Contents

List of Acronyms

AR Amit-Roginsky

CMB cosmological microwave background

CPS coherent peaked state

EoS equation of state

EPRL Engle-Pereira-Rovelli-Livine

F2PR fully 2-particle reducible

FLRW Friedmann-Lemaître-Robertson-Walker

GFT group field theory

GR general relativity

LQC loop quantum cosmology

LQG loop quantum gravity

NF2PR not fully 2-particle reducible

PR Ponzano-Regge

PW Peter-Weyl

QFT quantum field theory

QM quantum mechanics

TGFT tensorial group field theory

Chapter 1

Introduction

The quantization of gravity is one of the most important and challenging open problems in theoretical physics. Despite several decades of efforts after the birth of general relativity (GR) and quantum mechanics (QM), we are still far from a complete theory of quantum gravity [1–3], which even made one to suspect that whether gravity needs to be quantized or not[1]. Indeed, it's very difficult to verify quantum gravity theories experimentally, as in practice the Planck scale (where quantum gravity effects are expected to be relevant) is much greater than we can reach in the lab[2]. And even conceptually, we are lacking of conclusive proofs but only tentative arguments and beliefs that gravity should be quantized as other fundamental forces do [12–18]. However, there is no doubt that in Planck scale, where one needs to take into account both GR and QM, our understanding of space and time should be changed completely.

For example, according to QM, when trying to probe shorter distances one needs higher energy (density), while according to GR, when the energy density is high enough there would be black holes, which prevents us from obtaining any useful information, as the results of an experiment that tries to measure distance smaller than Planck length will be hidden inside the horizon [19, 20]. Furthermore, when calculating Feynman diagrams with loops in quantum field theory (QFT), one needs to integrate over virtual particles with arbitrarily large energy, and hence lead to the formation of black holes as well [21]. The problem is, when black holes are formed, they can evaporate into particles of all possible species according to Hawking radiation [22, 23]. Such processes are not possible in ordinary QFT without gravity, and hadn't been observed so far. In other words, GR and QM won't be able to tell us what will happen in Planck scale, therefore, their combination will certainly lead to new physics. The search of quantum gravity theories is one, and a

[1] In fact, it already takes decades of work to show that the first approach to quantum gravity, *perturbative quantum GR*, that tries to incorporate methods from usual QFT, fails as the resulting theory is not renormalizable [2, 4–8].

[2] Very recently, using methods from quantum information theory, it's argued that the quantum nature of gravity can be revealed if gravity can entangle two previously non-entangled systems [9–11]. But still, such *table-top* experiments are quite hard, as they require the preparation of two massive objects that have long enough decoherence time to be entangled [9, 10].

promising one, of the efforts to reveal what such new physics would look like.

At the same time, due to the extensive pursuit of quantizing gravity over a long period, numerous quantum gravity theories have emerged, offering valuable insights into the microscopic structure of spacetime [1]. Perturbatively, drawing from the experiences gained in conventional QFT, one can attempt to decompose the spacetime metric into a fixed background and a dynamic perturbation, leading to the theory of 'gravitons', which are massless spin-2 particles. However, as mentioned earlier, this theory turns out to be non-renormalizable, rendering it unsuitable as a fundamental theory. On the other hand, the asymptotic safety approach [24] takes a non-perturbative path in quantizing gravity, following the methods employed in QFT. Alternatively, string theory can be regarded as a generalization of the perturbative approach, where point-like objects are extended to string-like entities, introducing additional degrees of freedom and uncovering numerous non-perturbative phenomena [25].

However, in this thesis we will not follow the approaches above that emphasis the particle aspect of quantum gravity. Instead, our analysis based on the canonical approaches, that apply the quantization techniques from QM to the gravitational field, or spacetime, thus resulting a background independent quantization. Following this route, one can arrive at loop quantum gravity (LQG) [26], or it's path integral formulation, spin foam models [27] and tensorial group field theory (TGFT) [28, 29]. The later is the main focus of the current thesis.

Indeed, without a complete theory of quantum gravity, we are not able to imagine the exact picture of the physics in Planck scale, but the existing yet to be complete theories can already provide us insightful glimpses for the microscopic structure of spacetime. Generally, many quantum gravity approaches suggest that at the microscopic level, the usual notion of spacetime continuum disappears [30], instead the discrete structure of one sort or another would appear, and the macroscopic spacetime we are experiencing every day should emerge from such abstract, non-spatio-temporal entities [31]. Therefore, it's a common problem faced by many quantum gravity theories to recover the usual description of the universe in terms of a smooth spacetime and fields living on it, and their dynamics governed by (a possibly modified version of) GR and effective QFT. The task is simpler in approaches that in fact *start* from the same mathematical structures of effective field theory, like asymptotic safety or string theory, which can still make use to a large extent of the usual intuition and tools of spacetime physics (however, they may have then a harder time providing a precise description of the fundamental degrees of freedom of the underlying spacetime itself). On the other hand, for theories that take these abstract, non-spatio-temporal building blocks as a starting point, one faces a more serious challenge. And the more distant their candidate fundamental entities are from the usual notion we are familiar with, the harder to recover the spacetime continuum from these quantum gravity theories. The set of such challenges is often referred to as the issue of the *emergence of spacetime* in quantum gravity [31].

As we have mentioned, the main approach followed by this thesis, TGFT, belong to this second kind of quantum gravity approaches, with their fundamental interaction processes represented as simplicial complexes (of one dimension higher) [28, 29, 32–37]. In this respect, however, they have the advantage that, despite their fully background independent

and non-spatio-temporal character, they can still rely on tools from QFT to investigate the emergence of spacetime from their quantum dynamics. This has been one important motivation in the study of renormalization group flows and critical behaviour of numerous TGFT models [32, 34–36, 38, 39]. TGFTs can also rely, for solving the same issue, on the additional quantum geometric data labelling their fundamental quanta and enriching their quantum dynamics. Indeed, while this makes their quantum states and amplitudes more involved, it also provides a guideline for their spatio-temporal interpretation, and makes even the simplest types of approximation schemes geometrically rich enough to be interesting. From a phenomenological point of view, however, the 'tensorial' nature of the field is not quite important, and we will focus on a subclass of TGFTs, the group field theory (GFT) [28, 29, 40].

1.1 GFT condensates and cosmology

In chapter 2, we will give a short overview of the GFT formalism. Here we just note the fact that, as we have mentioned, in GFT the continuous spacetime dissolves into discrete building blocks, or quantas, and any macroscopic region of spacetime should emerge from a large number of these building blocks [29]. In this case, the methods from statistical mechanics can be applied, and one would expect that the actual spacetime should emerge from some kind of condensates (see equation (2.15) for a definition), in which the field operator has non-zero expectation value, in contrast to the vacuum state.

Based on these ideas, GFT condensate cosmology [41–51] provides a research programme aiming at the extraction of spacetime physics, in particular cosmology, from GFTs. It is based on the hypothesis that the emergent gravitational physics should be looked for in the hydrodynamic approximation of the full GFT quantum dynamics, and focuses in particular on condensate states, thus treating the universe as a peculiar quantum fluid, made out of GFT quantas. A large number of recent analyses in this context have shown not only the general viability of this strategy, but also that physically interesting results can be obtained already in the mean field (or Gross-Pitaevskii) approximation.

In particular, for very early time, when our universe is close to Planck scale and quantum gravity effects are expected to be important, it's shown that, already in the single mode[1] case, in GFT condensate cosmology the singularity is replaced by a bounce [41–43, 46], as one can expect from the cosmological sector of other approaches to quantum gravity, such as loop quantum cosmology (LQC) [52–54]. Shortly after the bounce, depend on the details of the value of GFT parameters, we either get a Friedman phase of the universe, in the sense that the equation of motion in the model has the same form as the Friedmann-Lemaître-Robertson-Walker (FLRW) equation with free massless scalar field, provides the expected classical limit [42, 43]; or we enter an inflationary phase of pure quantum gravitational origin without the need of inflaton, and it's possible to tune the GFT parameters to get a large enough number of e-folds suited for cosmological re-

[1] Here the term 'mode' is similar as Fourier mode in Fourier expansion except in GFT we are dealing with functions on groups and Peter-Weyl (PW) decomposition will be used.

quirements [45, 55]. These results suggest that GFT condensate cosmology can already reproduce some existing phenomenological or otherwise simplified models incorporating hypothetical quantum gravity effects or specific features of existing fundamental formalisms (such as LQC), hence provide a way to establish a solid connection between fundamental quantum gravity formalisms and effective continuum physics of the usual spacetime.

On the one hand, however, quantum gravity effects in cosmology do not need to be confined to the very early universe. Especially, in any emergent spacetime context notions like separation of scales or locality, on which usual effective field theory reasoning is based, are by definition approximate, and one should rather expect that the whole spacetime structure and dynamics, including large scale features, could be discovered to be of direct quantum gravity origin, as in the case of early universe.

On the other hand, although the ΛCDM model is very successful in describing the evolution of our universe using only a few parameters [56, 57], the smallness of the value of cosmological constant Λ [57, 58], i.e., the famous *cosmological constant problem*, remains a challenge to fundamental physics. Furthermore, more seriously, the ΛCDM model wasn't able to explain some recent observational results, especially for the data of supernova [59–61]. For example, many analyses show that we may currently be experiencing a phantom phase [59, 62, 63], caused by some *phantom dark energy* with equation of state (EoS) w less than -1, which is impossible in the ΛCDM model. Furthermore, we have the so called H_0 tension, which shows that the current value H_0 of the Hubble parameter inferred from the CMB [56] is smaller than the one from local measurements [61, 64]. And not so surprisingly, one can actually alleviate the H_0 tension by introducing a late time phantom phase in the expansion of the universe [60, 65, 66], which provides an evidence for the need to modify the expansion history of our universe.

Therefore, it's natural to ask whether these cosmological anomalies can be alleviated, or the late time acceleration can be extracted, with the help of quantum gravity effects. Such issues are not discussed extensively in the GFT community yet. And in this thesis we will try to fill this gap by showing that, when going beyond the single mode scenario, such as considering two modes in our GFT condensate cosmology model, the phantom phase can emerge naturally (see chapter 3 for details), without the need of any kind of phantom matter in the sense of particle physics.

The result is interesting for two reasons. First, a proper field theoretic modelling of phantom dark energy is challenging, if the phantom field is taken to be a fundamental component of the universe. In fact, the negative kinetic term needed to have $w < -1$ leads to vacuum instability, Lorentz violation or other pathology [67, 68]. Various solutions have been proposed, for example involving several scalar fields [69], but with no conclusive success. Second, in our model, on one hand the singularity in the very early universe can be resolved by a bounce, and on the other hand the phantom phase can emerge in late time. In fact, we can see in chapter 4 that in GFT condensate cosmology, when we have a non-vanishing cosmological constant today, there had to be a bounce instead of the big bang singularity. Therefore, in our formalism, the physics we are experiencing now and the physics of the far past can be brought together, showing the effects of quantities of very small scale, such as the Planck length, on observational results of very large scale,

the cosmological constant governing the accelerated acceleration of the whole universe at current stage. The fact that cosmological anomalies can be resolved using the Planck scale physics is also observed in LQC [70, 71].

1.2 Matter as perturbations over GFT condensates

Another open issue in GFT is how to incorporate matter fields into our formalism, which is important if we want to discuss the cosmological evolution in a more realistic manner, by including the real matter contents, such as the radiation and non-relativistic matter, into consideration. It's possible to couple directly the GFT with the free massless scalar field, such that we can get the correct semi-classical limit for both gravity and matter field [72]. There are also additional routes to get matter content in our formalism, for example we can extract matter from the condensate itself as perturbations [73].

On the other hand, the usage of homogeneous and isotropic condensate in the GFT condensate cosmology is successful in capturing the main feature of the cosmological evolution, but such simplification but also hides many detail structures of GFT, for example the non-local and combinatorial nature of the interaction kernel. **Going beyond homogeneity** requires us to be able to distinguish different points of the spacetime, or in other words, we need to have *relational rods* to set up spatial coordinates, similar as the relational clock used to track time evolution. Such rods can also be modelled using free massless scalar fields, which enables us to obtain a relational reference frame constructed from physical system [51, 74]. Based on this matter frame, we can introduce inhomogeneities into the condensate state, as a source of cosmological perturbation [51]. **Going beyond isotropy**, on the other hand, usually requires us to deal with non-equilateral tetrahedra instead of the equilateral ones [75, 76], such that the combinational nature of the kinetic and interaction term can be taken into account, which will certainly make the equation of motion complicate compared to the case of homogeneous and isotropic cosmological evolution.

For the first step to combine inhomogeneity and anisotropy, in chapter 5 we will consider a GFT model in 3d spacetime, the Boulatov model[1] [77]. In fact, this is the first GFT model that has been proposed, whose Feynman expansion around vacuum gives the Ponzano-Regge (PR) amplitudes [29], corresponds to a discretization of 3d gravity [78, 79]. Surprisingly, it turns out that inhomogeneous perturbations over anisotropic condensates can be viewed as a massive matter field, which is non-trivial as it's still unclear on how to incorporate a field with mass into the GFT formalism. The difficulty lies in the fact that to get the correct dynamics of both gravitation and the matter field in the continuum limit, the mass term of the matter field should be accounted by a non-trivial interaction term of GFT [72]. So far only the free massless scalar field that can be implemented consistently in GFT[2], and the results of chapter 5 provide another way of dealing with matter in quantum gravity theories, i.e., by viewing matter as emerged from the perturbations over condensate states, we can leave aside the necessity of coupling external matter to gravity.

[1] Which is easier to handle than the more realistic 4d models.

[2] That's why we always use them as relational time and rods.

The idea of extracting matter degree of freedom from gravity is not new. In particular, it's already shown that perturbations over classical solutions of GFT dynamics can be viewed as matter fields over flat spacetime in the 3d case [73] or the spacetime corresponds to deformed special relativity in the 4d case [80]. These works mainly considered the group representation of the GFT formalism, and haven't introduced the relational time and rods, which makes it difficult to interpret the resulting dynamics of the emerged matter fields in the usual language we are familiar with in ordinary QFT. Such obstacles can be overcome by introducing free massless scalar fields as physical frame, and working in the spin representation, such that the 'coordinate' degrees of freedom decouple from the group ones, which allows us to identify the dynamics of matter fields in the sense of QFT, and we will see in chapter 5 that the resulting field theory is a generalization of the so called Amit-Roginsky (AR) model [81, 82]. The model is interesting on its own as it's the only field theory we have known so far that has a cubic interaction but dominated by melonic graphs in the large N limit [82], and the results in chapter 5 suggests that two different type of fields, i.e., group field (which *generates* the spacetime continuum itself) on the one hand, and the AR model (which *lives* on the spacetime continuum) on the other, can be linked together in the GFT formalism.

1.3 An overview of the thesis

The thesis is organized as follows. In chapter 2, we will provide a brief introduction of the GFT formalism and its cosmological sector based on condensates. We can see that GFT can be second quantized, with quanta created by the creation operator $\hat{c}^\dagger_{\boldsymbol{x}}$ corresponds to a 4-valent vertex in LQG, which can be interpreted as a tetrahedron (see figure 2.1), and the volume operator can be written using creation and annihilation operators. The dynamics can be introduced using GFT action, where the time evolution is tracked by introducing a free massless field ϕ as a relational clock. Based on these structures, one can construct condensate states peaked on a given relational time ϕ_0 (see the definition (2.15) of coherent peaked state). Furthermore, we can focus on the isotropic and homogeneous sector of condensates, from which the cosmological evolution can be extracted. Such evolution can be written using the expectation value of the volume operator and its derivative respect to relational time. Finally, two primary results, i.e., the resolution of the big bang singularity and the emergence of classical limit are discussed.

Chapters 3 and 4 exhibit the applications of GFT condensate on cosmological evolution. In chapter 3 we discuss the effects when including more than one mode into GFT condensate cosmology formalism, with the promised phenomena of the emergence of phantom phase for late time expansion. We first introduce the effective EoS w whose dynamics is the central object of our analysis, summarize the main aspects of phantom dark energy, and rewrite previous results of GFT condensate cosmology in single mode case using EoS. In section 3.2, we consider the early universe dynamics right after the bounce, where the free part in the quantum gravity condensate dominates. We take all quantum geometric modes into account and show that the bounce is followed by an accelerated phase, but this phase

is not long-lasting in general. The role of GFT interactions is considered in section 3.3, where it's shown that with interaction terms in the effective GFT action, the phantom phase can emerge naturally accompanied by the de Sitter phase asymptotically, and it's also possible to obtain an inflationary scenario in early time while keeping the phantom phase in the late universe.

In chapter 4, we discuss the cosmological effects of the model we obtained in more detail. In section 4.1, we consider how to obtain the minimal value of EoS and the location of the minimum. The last part of section 4.1 shows the relation between cosmological constant and microscopic parameters of GFT. Section 4.2 shows how to introduce red shift z in the GFT formalism, which allows us to discuss the deviations of expansion history of our universe and the consequent effects on the current value H_0 of Hubble parameter. And it's shown that the inclusion of the second mode will actually increase H_0 when we try to infer the value from data.

Chapter 5 deals with the emergence of matter fields from the perturbations over GFT condensate. A brief review of the Boulatov model is given in section 5.1. In the following section we recall the AR model and study the condition on the perturbations of classical solutions of the equations of motion of the Boulatov model necessary to recover an effective action in a similar form as the AR model. Section 5.3 discusses the existence of a melonic dominance for our effective action. While it is unsettled for the moment whether it's the case in the most general setting, we exhibit additional conditions to enforce the melonic dominance of our generalized AR model.

For simplicity, if not specified we will use the unit such that $c = \hbar = 1$, where c is the speed of light and $\hbar$ is the Planck constant.

Chapter 2

Group field theory and cosmology

In this chapter we present some basics of the TGFT formalism and of quantum geometric models (i.e., GFTs) for 4d quantum gravity in particular, with a focus on the elements on which the extraction of cosmological dynamics is based. We only include the ingredients that are needed as immediate background of the work presented in this thesis, especially for chapter 3 and 4. For a more detailed introduction to TGFT we refer to existing reviews [28, 29, 33, 40]. For the basics of GFT condensate cosmology see instead the original work in [41, 42, 83, 84] and the reviews [43, 44, 47]. See also [48, 49] for the use of coherent peaked states for the study of relational observables and their dynamics, and for the discussion of their quantum fluctuations.

2.1 The formalism of group field theory

GFTs are quantum field theories defined over several copies of a Lie group G, which replaces the usual spacetime manifold of standard field theories and does not have, to start with, any spatiotemporal interpretation. The usual notion of space and time can only emerge from a proper limit or a suitable scenario, such as the condensate state with a large number of GFT quantas [29, 30]. In 4d quantum gravity models, the (usually complex) field is a tensorial map $\varphi:\ G^{\times 4} \to \mathbb{C},\ \varphi(g_v) = \varphi(g_1, \cdots, g_4)$, where the rank of the tensor is chosen equal to the dimension of the spacetime one intends to reconstruct [29]. GFTs are understood, in fact, as field theory formulations *of* spacetime, more precisely of the kinematics and dynamics of its fundamental constituents, rather than *on* spacetime as it is the case for usual QFTs. The basic quanta of the theory can be depicted as combinatorial 3-simplices, i.e. tetrahedra, labelled by the group-theoretic data, which encode their quantum geometry (assumed to be space-like). Quantum states and boundary data of such models will correspond to collections of such quanta. In the quantum geometric models proposed to date the relevant group manifold is $G = SL(2, \mathbb{C})$ or its rotation subgroup $SU(2)$, since the restrictions (for example the simplicity constraint [20, 85]) that the models impose on the group-theoretic data to ensure a proper geometric interpretation of the simplices allows (in the EPRL model [20, 86], for example) to map the two formulations of their quantum

geometry [85–88]. For details on the quantum geometric conditions, we refer to the cited literature. In the following we will take $G = SU(2)$.

Following these geometric restrictions, the field $\varphi(g_v)$ is required to be right invariant, $\varphi(g_v h) = \varphi(g_1 h, g_2 h, g_3 h, g_4 h) = \varphi(g_v)$, $\forall h \in G$, and therefore $\varphi(g_v) \in L^2(G^{\times 4}/G)$. A complete and orthonormal basis of $L^2(G^{\times 4}/G)$ is given in terms of $SU(2)$ Wigner representation functions contracted by group intertwiners; these are called spin network vertex functions. Such functions are obtained from the PW decomposition

$$\varphi(g_v) = \sum_{\boldsymbol{x}} c_{\boldsymbol{x}} \kappa_{\boldsymbol{x}}, \tag{2.1}$$

with $c_{\boldsymbol{x}} = \int \mathrm{d}^4 g \varphi(g_v) \kappa_{\boldsymbol{x}}(g_v)$ is the projection of field $\varphi(g_v)$ onto basis $\kappa_{\boldsymbol{x}}(g_v)$, defined as:

$$\kappa_{\boldsymbol{x}}(g_v) = \sum_{\boldsymbol{n}} \left\{ \left[\prod_{i=1}^{4} \sqrt{d(j_i)} D^{j_i}_{m_i n_i}(g_{v_i}) \right] \mathcal{I}^{\boldsymbol{j},\iota}_{\boldsymbol{n}} \right\} \in L^2(G^{\times 4}/G), \tag{2.2}$$

which are orthonormal under the normalized Haar measure $\int_G \mathrm{d}g = 1$, i.e.,

$$\int \mathrm{d}^4 g \kappa_{\boldsymbol{x}}(g_v) \kappa_{\boldsymbol{x}'}(g_v) \equiv \int \prod_i \mathrm{d}g_{v_i} \kappa_{\boldsymbol{x}}(g_v) \kappa_{\boldsymbol{x}'}(g_v) = \delta_{\boldsymbol{x},\boldsymbol{x}'}. \tag{2.3}$$

In equation (2.2), $D^j(g)$ is the Wigner matrix in the spin j representation of $SU(2)$, i.e., $D^j_{mn}(g) = \langle j, m | g | j, n \rangle$ represents the matrix element of the group element g under the representation of $SU(2)$ of spin j, and $\mathcal{I}^{\boldsymbol{j},\iota}_{\boldsymbol{n}}$ is the intertwiner, belong to the invariant space of tensor products of $SU(2)$ representations. More precisely, in the 4d case we have $\mathcal{I}^{\boldsymbol{j},\iota}_{\boldsymbol{n}} = \mathcal{I}^{j_1,j_2,j_3,j_4,\iota}_{\boldsymbol{n}} \in \mathrm{Inv}\{V_{j_1} \otimes V_{j_2} \otimes V_{j_3} \otimes V_{j_4}\}$, for representation space V_{j_i} labelled by spin j_i. For more details on the $SU(2)$ recoupling theory, see the nice introduction [89].

As shown in figure 2.1, these basis functions can be associated graphically to a 4-valent spin network vertex, i.e. a node with $d = 4$ open links associated with 4 spins $\boldsymbol{j} = (j_1, j_2, j_3, j_4)$, together with angular momentum projections $\boldsymbol{m}$, and the intertwiner quantum number ι associated instead to the node itself [90]. Geometrically, one can think the spin network vertex sitting inside the tetrahedron with the 4 links emanated from the node crossing its 4 triangular faces. Following the quantization of simplicial geometry for the tetrahedron (whose results are also consonant to the results obtained in the continuum canonical loop quantum gravity context), such spin network states are eigenstates of relevant geometric operators, with the spin labels j_i determining the areas of the four faces, while the intertwiner label specifying the volume of the tetrahedron.

Therefore, a GFT can be given based on either group elements of the representations, we will call the former *group representation* and the latter *spin representation*. Furthermore, there is an *algebra representation* based on the elements of Lie algebra $su(2)$ of the group $SU(2)$ [29], but such representation will not concern us in this thesis. In the following we will mainly work on the spin representation, where the calculations can be made more explicit. The resulting quantas, in the second quantization of GFT, correspond to spin network vertices in LQG, dual to the tetrahedra [90], as indicates by figure 2.1. The group representation, on the other hand, will also be used occasionally, in particular for writing down the GFT dynamics, where the action has a simpler form compared to the spin representation [29, 42].

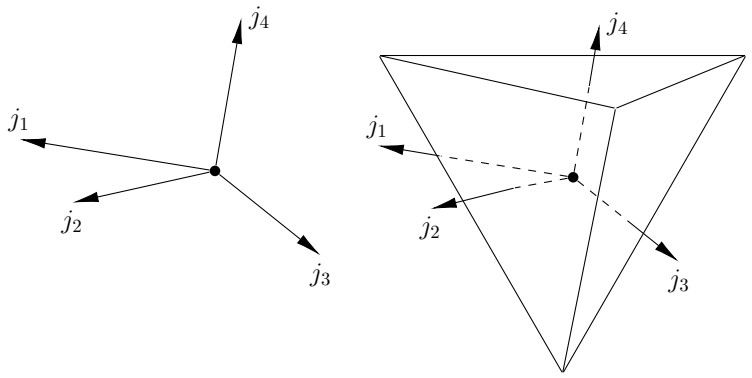

(a) 4-valent vertex (b) Dual tetrahedra

Figure 2.1: 4-valent vertex of a spin network and its dual tetrahedra.

2.1.1 Second quantization

GFTs can be dealt with in a second quantization language[1] by promoting the fields and their modes $c_{\boldsymbol{x}}$ to operators [90],

$$\hat{\varphi}(g_v) = \sum_{\boldsymbol{x}} \hat{c}_{\boldsymbol{x}} \kappa_{\boldsymbol{x}}(g_v), \ \hat{\varphi}^\dagger(g_v) = \sum_{\boldsymbol{x}} \hat{c}^\dagger_{\boldsymbol{x}} \bar{\kappa}_{\boldsymbol{x}}(g_v), \tag{2.4}$$

where the annihilation (creation) operator $\hat{c}_{\boldsymbol{x}}$ ($\hat{c}^\dagger_{\boldsymbol{x}}$), annihilates (creates) spin network node (or, equivalently, tetrahedron) labelled by $\boldsymbol{x} = (\boldsymbol{j}, \boldsymbol{m}, \iota)$. We also have the following commutation relations (assuming bosonic statistics)

$$\left[\hat{c}_{\boldsymbol{x}}, \hat{c}^\dagger_{\boldsymbol{x}'}\right] = \delta_{\boldsymbol{x},\boldsymbol{x}'}, \ [\hat{c}_{\boldsymbol{x}}, \hat{c}_{\boldsymbol{x}'}] = \left[\hat{c}^\dagger_{\boldsymbol{x}}, \hat{c}^\dagger_{\boldsymbol{x}'}\right] = 0. \tag{2.5}$$

The vacuum $|0\rangle$, which is the state with no spacetime structure (geometrical or topological), is defined by $\hat{c}_{\boldsymbol{x}} |0\rangle = 0, \ \forall \boldsymbol{x}$. By acting the creation operator $\hat{c}^\dagger_{\boldsymbol{x}}$ repeatedly on $|0\rangle$ we can construct the many-body states as usual, leading to the Fock space

$$\mathcal{F}(\mathcal{H}) = \bigoplus_{N=0}^{\infty} sym\left\{\mathcal{H}^{(1)} \otimes \cdots \otimes \mathcal{H}^{(N)}\right\}, \ \mathcal{H} = L^2\left(G^{\times 4}/G\right),$$

where N denotes the number of tetrahedra in each sector of the Fock space (again, the bosonic statistics is assumed). Extended topological structures, corresponding to simplicial complexes formed by glued tetrahedra, or equivalently by graphs formed by connected spin network vertices, can be put in precise correspondence with entangled many-body states

[1] This second quantized formulation, however, is not directly the result of quantizing by standard canonical methods the theory starting from the classical GFT action, due to the lack of external time parameters on which such standard methods would rely. In fact, alternative 'deparametrized' formulation of the same GFTs (after additional 'matter' degrees of freedom have been included; see the following sections) exist [91, 92]. This timeless formalism can also be derived by more standard canonical quantization methods from a 'frozen' perspective [93], looking at the GFT model as a peculiar constrained system.

inside the Fock space, with the graph structure encoding exactly the entanglement pattern among fundamental degrees of freedom [94].

For this formalism to be a compelling formulation of quantum gravity, one should be able to extract the dynamics of spacetime continuum, and with a proper limiting procedure, we should get classical GR. In particular, our universe, including its dynamical spacetime geometry, should be shown to emerge from the quantum dynamics of these more abstract fundamental entities. To do this, we need to construct geometrical operators, which can be used to characterize the geometric properties of the spacetime in a way we are familiar with. In the cosmological sector, second quantized versions of the various quantum geometric operators can be then constructed. To be more specific, we are going to need the volume operator, which is diagonal in the spin network basis with matrix elements depending on the intertwiner label ι. Therefore, we can write [49]

$$\hat{V} = \sum_{\boldsymbol{x},\boldsymbol{x}'} V(\iota,\iota')\delta_{\boldsymbol{x}-\{\iota\},\boldsymbol{x}'-\{\iota'\}}\hat{c}^{\dagger}_{\boldsymbol{x}}\hat{c}_{\boldsymbol{x}'}. \tag{2.6}$$

The total volume of the universe can be then be given as the expectation value of the volume operator in a condensate state, from which the continuous spacetime emerge. But before we can write equation in analogy as FLRW equation, which governs the cosmological evolution, we need to know how localize the building blocks, and in particular, to track the evolution. Because as we emphasized before, in general there is no coordinate system *a priori* in quantum gravity theories. In the following, we will tackle this issue by coupling free massless scalar fields χ_a to GFT as relational frame, such that the usual notion of spacetime manifold can be extracted.

2.1.2 Relational description

In a diffeomorphism invariant context, there is no preferred coordinate frames to begin with. A convenient strategy to localize the building blocks is relational one in which appropriate internal dynamical degrees of freedom of the theory are used as physical frames, including rods and clock, with respect to which the location and evolution of the others are defined [95, 96]. In many applications, and in GFT cosmology in particular, the role of such a physical frame is played by non-interacting (and minimally coupled) scalar fields χ_a ($a = 0,\ 1,\ 2,\ 3$ in our 4d case). Such degrees of freedom of scalar fields are added to the quantum geometric ones in the fundamental definition of the GFT model. For the matter frame to work, the first step is to extend the definition of GFT field to be the map $\varphi : G^{\times 4} \times \mathcal{R}^{\times 4} \to \mathcal{C}$, and then the GFT action should be extended to include appropriate coupling of the new degrees of freedom. The main guideline for constructing such extended dynamics is in fact the same as for the pure geometry models: the GFT model is defined in such a way that its perturbative expansion produces a sum over simplicial complexes weighted by an appropriate discrete path integral for gravity, now coupled to free massless scalar fields [41, 42, 72]. We will see how to use these requirements to fix the GFT kinetic terms in next subsection.

Let us stress that, while the interpretation of the new degrees of freedom, just like that of the quantum geometric ones, is guided by the role they play at the discrete level corresponding to GFT quanta and Feynman amplitudes, their actual physical meaning and properties should be determined by the role they play at some effective continuum level. The GFT cosmology programme is exactly aimed at extracting such effective description and controlling the emerging physics of these quantum gravity models.

After quantization, the field operators will also be χ_a dependent, in particular the commutation relation between annihilation and creation operator becomes [42, 51]

$$\left[\hat{c}_{\boldsymbol{x}}(\chi_a), \hat{c}^\dagger_{\boldsymbol{x}'}(\chi'_a)\right] = \delta_{\boldsymbol{x},\boldsymbol{x}'}\delta^{(4)}(\chi_a - \chi'_a),\ [\hat{c}_{\boldsymbol{x}}(\chi_a), \hat{c}_{\boldsymbol{x}'}(\chi'_a)] = \left[\hat{c}^\dagger_{\boldsymbol{x}}(\chi_a), \hat{c}^\dagger_{\boldsymbol{x}'}(\chi'_a)\right] = 0. \quad (2.7)$$

Correspondingly, the definition of other observables will include their dependence on scalar field degrees of freedom. For example, the volume operator, counting the contribution from each GFT quantum, becomes

$$\hat{V} = \int \mathrm{d}^4\chi \hat{V}(\chi_a) = \int \mathrm{d}\phi \sum_{\boldsymbol{x},\boldsymbol{x}'} V(\iota,\iota')\delta_{\boldsymbol{x}-\{\iota\},\boldsymbol{x}'-\{\iota'\}}\hat{c}^\dagger_{\boldsymbol{x}}(\chi_a)\hat{c}_{\boldsymbol{x}'}(\chi_a). \quad (2.8)$$

Without introducing inhomogeneities, it's enough to work with homogeneous condensate. In this case, when acting on the condensate, the dependence on rods (indicated by χ_i (with $i = 1,\ 2,\ 3$) fields) of the volume operator has no effects either. Therefore, for simplicity we can keep only the dependence on relational time[1] $\chi_0 = \phi$, such that

$$\hat{V} = \int \mathrm{d}\phi \hat{V}(\phi) = \int \mathrm{d}\phi \sum_{\boldsymbol{x},\boldsymbol{x}'} V(\iota,\iota')\delta_{\boldsymbol{x}-\{\iota\},\boldsymbol{x}'-\{\iota'\}}\hat{c}^\dagger_{\boldsymbol{x}}(\phi)\hat{c}_{\boldsymbol{x}'}(\phi). \quad (2.9)$$

The relational strategy would then suggest to look for a definition of a relational observable corresponding to the volume of the universe *at given clock time*, with the role of clock played by the scalar field, and a first definition could be given by the quantity $\hat{V}(\phi)$ entering the above expression. Indeed, this has been the definition adopted in much of the GFT cosmology literature. Recently, an effective relational strategy has been proposed, in which relational observables correspond to the expectation values of the generic GFT operators in appropriately selected 'clock-peaked' states. We are going to illustrate this effective strategy in the following, after discussing the dynamical aspects of the theory.

2.1.3 Dynamics

Classically, the dynamics of a given GFT model is specified by the action [42, 43, 45, 51]

$$\begin{aligned} S(\bar{\varphi},\varphi) = &\int \mathrm{d}g_{v_1}\mathrm{d}g_{v_2}\mathrm{d}^4\chi_{v_1}\mathrm{d}^4\chi_{v_2}\bar{\varphi}(g_{v_1},\chi_{a,v_1})\varphi(g_{v_2},\chi_{a,v_2})K(g_{v_1},g_{v_2};(\chi_{a,v_1}-\chi_{a,v_2})^2) \\ &-\sum_{n,m}^{\infty}\lambda_{n+m}\int \mathrm{d}^4\chi \left\{\left[\prod_{i=1}^{m}\mathrm{d}g_{v_i}\bar{\varphi}(g_{v_i},\chi_a)\right]\left[\prod_{j=1}^{n}\mathrm{d}h_{v_j}\varphi(h_{v_j},\chi_a)\right]\mathcal{V}_{n+m}(g_v,h_v)\right\}, \end{aligned} \quad (2.10)$$

[1] Following the original paper [42], we let the relational time $\chi_0 = \phi$ for an easier comparison with previous results.

where $K(g_{v_1}, g_{v_2}; (\chi_{a,v_1} - \chi_{a,v_2})^2)$ and $\mathcal{V}_{n+m}(g_v, h_v) = \mathcal{V}_{n+m}(g_{v_1}, \cdots, g_{v_m}, h_{v_1}, \cdots, h_{v_n})$ are kinetic and interaction kernels respectively, whose explicit form can be determined by requiring that its Feynman expansion provides the correct amplitudes obtained in spin foam models [42], for example the Engle-Pereira-Rovelli-Livine (EPRL) model [85, 86, 97]. It's worth emphasizing that the kinetic term K only depends on the square $(\chi_{a,v_1} - \chi_{a,v_2})^2$ of the differences between the relational times associated to two building blocks (tetrahedra labelled by v_1 and v_2), respectively. This is because that the Lagrangian density of a free massless scalar field minimally coupled to gravity[1],

$$\mathcal{L} = \frac{1}{2}\sqrt{-g}g^{\mu\nu}\partial_\mu\chi_a\partial_\nu\chi_a, \tag{2.11}$$

is invariant under the translation $\chi_{a,v} \to \chi_{a,v} + c_a$ for some constants c_a and the reflection $\chi_{a,v} \to -\chi_{a,v}$. These two symmetries have to be restored when we take the classical limit, hence it's natural to assume they are valid also at the quantum level in the GFT [42]. By further assuming that the differences $\chi_{a,v_1} - \chi_{a,v_2}$ is small, we can consider a derivative expansion of the kinetic term [42, 49]. When acting on the coherent peaked state (CPS), which we will discuss in subsection 2.2.1, terms other than the first two will be suppressed in the presence of the peaking function (usually taken as Gaussian) [49]. Furthermore, the first two terms correspond to mass term and the derivative terms $\partial/(\partial\chi_a)$, respectively [42, 49]. In particular, in the homogeneous case, we can ignore the rods and focus only on the time derivative $\partial/(\partial\chi_0) = \partial/(\partial\phi)$.

Given that the kinetic term are fixed by symmetry considerations, a GFT is mainly defined by specify the interaction term $\mathcal{V}_{n+m}$, whose explicit form won't concern us in the cosmological sector of the thesis as the work is done in an effective level. In chapter 5, however, the combinatorial detail of the interaction term would be important, and we will write down the action (5.7) of *Boulatov model* [73, 77] explicitly, as an example of what the interactions would look like.

Note that we have adopted a notation reminiscent of quantum many-body physics, indicating that different interactions involving varying numbers of 'spacetime atoms' are possible, and restricted to the case of pure quantum geometric data for simplicity of notation. The interaction kernels are generically non-local with respect to such quantum geometric data, in the sense that arguments in each interacted group field φ are not simply identified to each other. When scalar field degrees of freedom are present, on the other hand, typical interaction kernels are going to be local in them. The quantum dynamics can be extracted from the partition function[2]

$$Z = \int \mathcal{D}\varphi\mathcal{D}\bar{\varphi}\mathrm{e}^{-S(\bar{\varphi},\varphi)},$$

[1] $g^{\mu\nu}$ represents the metric of the spacetime under consideration, and there is no summation over the subscript a.

[2] This partition function can be seen as the result of rewriting in path integral form a 'generally covariant equilibrium partition function' of quantum statistical type for a system of quantized simplices; see [98, 99].

from which we get the Schwinger-Dyson equations [41, 43]

$$0 = \int \mathcal{D}\varphi\mathcal{D}\bar{\varphi}\frac{\delta}{\delta\bar{\varphi}}\left[O(\bar{\varphi},\varphi)\mathrm{e}^{-S(\bar{\varphi},\varphi)}\right] = \left\langle \frac{\delta O(\bar{\varphi},\varphi)}{\delta\bar{\varphi}} - O(\bar{\varphi},\varphi)\frac{\delta S(\bar{\varphi},\varphi)}{\delta\bar{\varphi}}\right\rangle, \tag{2.12}$$

where the vacuum expectation value $\langle\cdots\rangle$ is defined as

$$\langle O(\bar{\varphi},\varphi)\rangle = \int \mathcal{D}\varphi\mathcal{D}\bar{\varphi}O(\bar{\varphi},\varphi)\mathrm{e}^{-S(\bar{\varphi},\varphi)}.$$

When quantum fluctuations are small, a mean field approximation is expected to be valid. This means that at the leading order we need only consider the simplest one in the series of Schwinger-Dyson equations

$$\left\langle \sigma \left| \frac{\delta\hat{S}(\hat{\varphi}^\dagger,\hat{\varphi})}{\delta\hat{\varphi}^\dagger}\right| \sigma\right\rangle = 0$$

for any state $|\sigma\rangle$. In particular, if $|\sigma\rangle$ is an eigenstate of the field operator, i.e.,

$$\hat{\varphi}(g_v,\chi_a)\,|\sigma\rangle = \sigma(g_v,\chi_a)\,|\sigma\rangle \tag{2.13}$$

for some eigenfunction $\sigma(g_v,\phi)$, the dynamics can be expressed as equation of motion for $\sigma(g_v,\phi)$ obtained from the effective action

$$S(\bar{\sigma},\sigma) = \langle\sigma|S(\hat{\varphi}^\dagger,\hat{\varphi})|\sigma\rangle. \tag{2.14}$$

This approximation can also be seen as corresponding to approximating the full quantum effective action of the field theory with its classical one, since the resulting equations of motion are the ones obtained from the classical action replacing the GFT field with the function $\sigma(g_v,\phi_a)$. In the context of quantum many-body system, specifically quantum liquids, this is the Gross-Pitaevskii approximation of the condensate hydrodynamics for the condensate wave function $\sigma(g_v,\phi_a)$.

With geometrical operators (from which we can extract geometric properties) and condensate state (from where the homogeneous universe emerges) in hand, we are able to track the evolution of our universe by considering the expectation values. The remaining issue is to construct the suitable condensate state $|\sigma\rangle$ that captures our universe correctly, as we will do in the following.

2.2 GFT condensate cosmology

As being mentioned, in this thesis we won't consider inhomogeneities in the context of cosmology, therefore for simplicity we will ignore the relational rods in the following discussion, and focus only on the relational time $\chi_0 = \phi$. We will see in chapter 5 when we consider perturbations, the relational rods have to be used to define inhomogeneity. Until that, it's enough to work solely with clock ϕ.

In principle, arbitrary wave function can be used to define the condensate state, as long as the resulting $|\sigma\rangle$ is an eigenstate of the field operator, as indicated by equation (2.13). But in general this way the quantum fluctuations are not controlled [48, 49]. For a better control of the fluctuations, the wave function σ needs to be chosen such that the resulting condensate state is peaked on a given relational time ϕ_0, which lead us to the notion of *coherent peaked state* [49]. Furthermore, although the universe extracted from condensate states is homogeneous by definition, it's in general not isotropic. We will see later that imposing isotropy will further simplify our analysis by allowing us to split the contributions to cosmological evolution into *modes*, whose dynamics are decoupled from each other under our choice of interaction kernel.

2.2.1 Coherent peaked states

In our framework, the evolution of the universe can be expressed as the change of a spatial slice of spacetime with respect to relational time ϕ. In order to introduce this dependence of observables on the value of our clock and to get a better control over the quantum fluctuations, we should work with states peaked on a fixed relational time ϕ_0 [49]. The same states should support the extraction of expectation values of geometrical observables, whose non-vanishing indicates that a large number of fundamental GFT quantas are required, such that the spacetime continuum can emerge with good approximations [42]. These two considerations lead to the use of the coherent peaked state (CPS):

$$|\sigma_\varepsilon;\phi_0,\pi_0\rangle = \mathcal{N}(\sigma)\exp\left(\int(\mathrm{d}g)^4\mathrm{d}\phi\sigma_\varepsilon(g_v,\phi;\phi_0,\pi_0)\hat{\varphi}^\dagger(g_v,\phi)\right)|0\rangle\,, \tag{2.15}$$

with $\mathcal{N}(\sigma)$ is some normalization constant and $|0\rangle$ is the vacuum state. The condensate wave function $\sigma_\varepsilon(g_v,\phi;\phi_0,\pi_0)$ is peaked on $\phi=\phi_0$ and can be written as [48]

$$\sigma_\varepsilon(g_v,\phi;\phi_0,\pi_0) = \eta_\varepsilon(\phi-\phi_0,\pi_0)\tilde{\sigma}(g_v,\phi), \tag{2.16}$$

where $\eta_\varepsilon(\phi-\phi_0,\pi_0)$ is a *peaking function* (usually taken as a Gaussian, see equation (52) in [49]) around ϕ_0 with a typical width given by ε, and π_0 is a further parameter controlling the fluctuations of the operator corresponding to the conjugate momentum of the scalar field ϕ. We further require that, the *reduced condensate function* $\tilde{\sigma}(g_v,\phi)$, which is the actual dynamical variable in the hydrodynamic approximation, should not modify the peaking property of $\sigma_\varepsilon(g_v,\phi;\phi_0,\pi_0)$, such that the peaking function $\eta_\varepsilon(\phi-\phi_0,\pi_0)$ fully determines the peaking structure of the condensate state. It remains true, of course, that the condensate state (2.15) is an eigenstate of GFT field operator

$$\hat{\varphi}(g_v,\phi)\,|\sigma_\varepsilon;\phi_0,\pi_0\rangle = \sigma_\varepsilon(g_v,\phi;\phi_0,\pi_0)\,|\sigma_\varepsilon;\phi_0,\pi_0\rangle\,. \tag{2.17}$$

One further condition imposed on the condensate wave function, motivated by geometric considerations [41, 42, 49, 100], is invariance under both right and left diagonal group actions

$$\tilde{\sigma}(hg_vk,\phi) = \tilde{\sigma}(g_v,\phi),\ \forall h,\ k\in SU(2). \tag{2.18}$$

2.2.2 Imposing isotropy

In the context of GFT condensate cosmology, it's usually assumed that the condensate wave function $\tilde{\sigma}$ takes the form of [42]

$$\tilde{\sigma}(g_I, \phi) = \sum_j \tilde{\sigma}_j(\phi) \bar{\mathcal{I}}^{j,\iota_+}_{\boldsymbol{m}} \mathcal{I}^{j,\iota_+}_{\boldsymbol{n}} d(j)^2 \prod_{l=1}^{4} D^j_{m_l n_l}(g_l), \tag{2.19}$$

where we write j for $\boldsymbol{j} = (j_1, j_2, j_3, j_4) = (j, j, j, j)$, and similarly for $\boldsymbol{m}$, $\boldsymbol{n}$; $\mathcal{I}^{j,\iota_+}_{\boldsymbol{m}}$ is the intertwiner labelled by ι_+; $d(j) = 2j + 1$ is the dimension of the spin j representation and $D^j_{m_l n_l}(g_l)$ are the Wigner representation functions. The dependence on relational time is then only encoded in $\tilde{\sigma}_j(\phi)$ for each mode. Geometrically, such a restriction corresponds to a tetrahedron with equal areas of the four faces (see figure 2.1) and a volume as large as possible. The latter fact is the reason why we use ι_+ instead of ι [42, 49].

Following [42], we will call these condensates as the *isotropic* ones. Since locally the equilateral tetrahedron is the most isotropic one compared to other kind of tetrahedra. But this doesn't mean that the isotropic spacetime can only emerge from such condensates, as there are many ways to implement isotropy. In particular, the Friedmann universe can emerge from condensates labelled by spins not equal to each other, corresponding to non-equilateral tetrahedra [76]. This is what one can expect as even an isotropic spacetime admits anisotropic triangulations.

Therefore, in the current thesis, notions like *isotropic* and *anisotropic* are only defined locally, not necessarily related to the corresponding property of the emerged spacetime. More precisely, isotropic condensates refer to the ones whose wave function is labelled by identical spins, geometrically corresponding to the equilateral tetrahedra in the 4d case, for example. While on the contrary, anisotropic condensates indicate the fact when labelling the condensate function there is at least one spin that is different from others, such that the combinatorial details of the interaction terms would be important in determining its behaviour. We emphasize that it's possible for an isotropic space to emerge from the anisotropic condensates, as we can see in chapter 5.

Note that, given the definition (2.15) of annihilation operator $\hat{c}_{\boldsymbol{x}}$, we have

$$\hat{c}_{\boldsymbol{x}}(\phi) \left|\sigma_\varepsilon; \phi_0, \pi_0\right\rangle = \eta_\varepsilon(\phi - \phi_0, \pi_0) \tilde{\sigma}_j(\phi) \bar{\mathcal{I}}^{j,\iota_+}_{\boldsymbol{m}} \left|\sigma\right\rangle, \tag{2.20}$$

i.e., only for $j_1 = j_2 = j_3 = j_4 = j$ the action of $\hat{c}_{\boldsymbol{x}}$ with $\boldsymbol{x} = (\boldsymbol{j}, \boldsymbol{m}, \iota)$ is not vanishing.

In summary, when imposing isotropy the dynamics of GFT in the cosmological sector will be encoded in a collection of functions $\tilde{\sigma}_j(\phi)$, which we call *modes*, each of them can be labelled by a single spin j[1]. By a suitable choice of the interaction kernel, the equations of motion for different modes will decouple from each other, which simplifies further our analysis of the cosmological evolution.

[1] In the following we usually call it mode j for short.

2.2.3 Effective dynamics

Having fixed the peaking function $\eta_\varepsilon(\phi-\phi_0,\pi_0)$, the dynamics of the condensate is encoded in the evolution of the reduced condensate function $\tilde{\sigma}(g_v,\phi)$. Furthermore, using the fact (2.17) that the CPS $|\sigma_\varepsilon\rangle$ is an eigenstate of the field operator, the effective action, from which the dynamics for each mode can be extracted, reads at mean field level [49]

$$\begin{aligned} S(\bar{\tilde{\sigma}},\tilde{\sigma}) &= \int \mathrm{d}\phi_0 \langle \sigma_\varepsilon;\phi_0,\pi_0|S(\hat{\varphi}^\dagger,\hat{\varphi})|\sigma_\varepsilon;\phi_0,\pi_0\rangle, \\ &= \int \mathrm{d}\phi_0 \left\{ \sum_j \left[\bar{\tilde{\sigma}}_j(\phi_0)\tilde{\sigma}''(\phi_0) - 2\mathrm{i}\tilde{\pi}_0 \bar{\tilde{\sigma}}_j(\phi_0)\tilde{\sigma}_j'(\phi_0) - \xi_j^2 \bar{\tilde{\sigma}}_j(\phi_0)\tilde{\sigma}_j(\phi_0) \right] + \mathcal{V}(\bar{\tilde{\sigma}},\tilde{\sigma}) \right\}, \end{aligned} \tag{2.21}$$

where $\tilde{\pi}_0 = \dfrac{\pi_0}{\varepsilon\pi_0^2-1}$, ξ_j is an effective parameter encoding the details of the kinetic term of the fundamental GFT action (in the isotropic restriction), and $'$ denotes derivative with respect to ϕ_0. Finally, $\mathcal{V}(\bar{\tilde{\sigma}},\tilde{\sigma})$ is the interaction kernel, also determined by the underlying GFT model. We refer to [49], and references cited therein, for more details.

The interaction term for quantum geometric GFT models remains quite involved also in the isotropic restriction, and the corresponding dynamics is difficult to handle even at this mean field level. For this practical reason, most analyses so far have neglected the contribution coming from such interaction terms, which are expected to be anyway subdominant with respect to the kinetic part[1]. In this work, on the other hand, we want to focus exactly on how these interaction terms affect the effective cosmological dynamics, especially at late times.

For doing so, we adopt a rather phenomenological approach, modelling these interactions with a simple, rather general form, used also in previous work [45]:

$$\mathcal{V}(\bar{\tilde{\sigma}},\tilde{\sigma}) = \sum_j \left(\frac{2\lambda_j}{n_j} |\tilde{\sigma}_j(\phi_0)|^{n_j} + \frac{2\mu_j}{n_j'} |\tilde{\sigma}_j(\phi_0)|^{n_j'} \right), \tag{2.22}$$

where λ_j and μ_j are interaction couplings correspond to each mode j satisfy that $|\mu_j| \ll |\lambda_j| \ll |m_j^2|$, and we assume that $n_j' > n_j > 2$. Albeit definitely simpler than full-blown quantum geometric models, this choice still captures several relevant features of the same, and hopefully key aspects of what we may expect to be universal effective behaviour. We emphasize that at this stage our effective action is not derived from some underlying GFT model. We choose the interaction kernel to be equation (2.22) as it is easy to handle and also has a similar structure of some microscopic GFT theories, such as the one corresponding to EPRL model [42]. In this sense, any GFT model that can reproduce such effective action (under mean-field approximation or with some quantum corrections) would lead to the same evolution of the universe that we will explore below.

[1] This is also needed, in fact, for the perturbative form of the GFT quantum dynamics, where the connection with spin foam models and lattice gravity path integral is established, to be of any relevance.

Note that there is no cross term among different modes in the action, therefore the equations of motion for different modes, labelled by j, decouple from each other. This would simplify the analysis quite a bit. At the same time, some models like the EPRL model decouple different modes in the isotropic restriction [42]. For more general GFT actions, different modes can couple to each other (for example [101], in the Riemannian setting) and the analysis would be more involved, we leave the study of behaviour of coupled modes for future work.

In [45] this kind of interactions has been studied in the case in which only a single spin mode contributes, and it has been shown that they affect the effective universe dynamics in interesting ways. For example, it allows us to obtain an inflationary phase in the early universe, accompanied by a contraction phase of the universe after the inflation, hence results in a cyclic evolution [45].

Chapter 3 of this thesis improves the result obtained in [45], by considering the contribution of more than one mode, and proved even more interesting results; in particular, we will show that we can obtain an effective dark energy dynamics at late times, produced directly from the underlying quantum gravity dynamics, without introducing any kind of additional matter-like field. This way some pathologies faced by many phantom dark energy models from the QFT perspective, such as the stability issue [68], can be avoided.

Before analysing the resulting dynamics for the universe volume, obtained from this effective condensate action, let us recast it in a more convenient hydrodynamic form by writing down the relevant equations of motion[1]. Varying the action (2.21) with respect to $\bar{\tilde{\sigma}}_j$ we get [46, 49]

$$\tilde{\sigma}_j'' - 2\mathrm{i}\tilde{\pi}_0\tilde{\sigma}_j - \xi_j^2\tilde{\sigma}_j + 2\lambda_j|\tilde{\sigma}_j|^{n_j-2}\tilde{\sigma}_j + 2\mu_j|\tilde{\sigma}_j|^{n_j'-2}\tilde{\sigma}_j = 0. \tag{2.23}$$

Decomposing $\tilde{\sigma}_j(\phi) = \rho_j(\phi)\exp[\mathrm{i}\theta_j(\phi)]$ with real functions, ρ_j (condensate density) and θ_j (condensate phase), the last equation splits to two equations, correspond to imaginary and real parts respectively. Note that our system has a global $U(1)$ symmetry, in the sense that the effective action is invariant under the phase transformation $\theta_j(\phi) \to \theta_j(\phi) + \alpha_j$ for any real constants α_j, the imaginary part of equation (2.23) can be written as the conservation condition $Q_j' = 0$ for the conserved quantities Q_j for each mode. These conserved quantities can be written in terms of modulus and phase functions as following [42, 49]

$$Q_j = (\theta_j' - \tilde{\pi}_0)\rho_j^2. \tag{2.24}$$

The modulus part of equation (2.23) then becomes [42, 45, 49]

$$\rho_j'' - \frac{Q_j^2}{\rho_j^3} - m_j^2\rho_j + \lambda_j\rho_j^{n_j-1} + \mu_j\rho_j^{n_j'-1} = 0, \tag{2.25}$$

where $m_j^2 = \xi_j^2 - \tilde{\pi}_0^2$ is now both a function of the fundamental parameters of the model (through ξ_j) and of the parameter ε characterizing the non-ideal nature of our clock. This

[1] Since following equations only depend on ϕ_0 and thus is no risk of confusion, for notation simplicity in the following we will drop the subscript 0 and use ϕ to represent the relational time for a given spatial slice.

equation can be directly integrated once, which gives another conserved quantity [42], as a result of the symmetry of the system under 'clock-time translation' $\phi \to \phi + c$ [45, 49],

$$E_j = \frac{1}{2}(\rho_j')^2 - \frac{1}{2}m_j^2\rho_j^2 + \frac{Q_j^2}{2\rho_j^2} + \frac{\lambda_j}{n_j}\rho_j^{n_j} + \frac{\mu_j}{n_j'}\rho_j^{n_j'}. \tag{2.26}$$

As we will see, the total volume of the universe, as an expectation value of the volume operator in condensate state $|\sigma\rangle$, can be expressed as a sum over modes j, and the resulting dynamics can be derived based on equations (2.25) and (2.26).

2.3 Volume dynamics

Combining the definitions of the volume operator (2.9) and the condensate state (2.15), we see that the expectation value of $\hat{V}$ at a given time takes the form (we restored the subscript 0 for given relational time ϕ_0 for the moment to avoid confusion)

$$\begin{aligned} V(\phi_0) &= \langle\sigma_\varepsilon;\phi_0,\pi_0|\hat{V}|\sigma_\varepsilon;\phi_0,\pi_0\rangle \\ &= \langle\sigma_\varepsilon;\phi_0,\pi_0|\int \mathrm{d}\phi \sum_{\boldsymbol{x},\boldsymbol{x}'} V(\iota,\iota')\delta_{\boldsymbol{x}-\{\iota\},\boldsymbol{x}'-\{\iota'\}}\hat{c}^\dagger_{\boldsymbol{x}}(\phi)\hat{c}_{\boldsymbol{x}'}(\phi)|\sigma_\varepsilon;\phi_0,\pi_0\rangle \\ &\approx \sum_j V_j\rho_j(\phi_0)^2, \end{aligned} \tag{2.27}$$

where $\rho_j = |\sigma_j|$ is the modulus of reduced condensate function $\tilde{\sigma}$, $V_j \propto l_p^3 j^{3/2}$ is the volume contribution from each quantum (tetrahedron) in the spin j representation, and we have used the intertwiner normalization condition $\sum_{\boldsymbol{m}} \mathcal{I}^{j,\iota_+}_{\boldsymbol{m}}\bar{\mathcal{I}}^{j,\iota'_+}_{\boldsymbol{m}} = \delta_{\iota_+,\iota'_+}$. The approximation amounts to keeping only the dominant contribution to the saddle point approximation of the peaking function coming from our choice of state [49].

The dynamics of the universe volume can now be obtained by differentiating $V(\phi)$ respect to relational time and then substituting the equations (2.25) and (2.26) for ρ_j, writing them in the form of modified FLRW equations [42]

$$\left(\frac{V'}{3V}\right)^2 = \left[\frac{2\sum_j V_j\sqrt{2E_j\rho_j^2 - Q_j^2 + m_j^2\rho_j^4 - \frac{2}{n_j}\lambda_j\rho_j^{n_j+2} - \frac{2}{n_j'}\mu_j\rho_j^{n_j'+2}}}{3\sum_k V_k\rho_k^2}\right]^2, \tag{2.28}$$

$$\frac{V''}{V} = \frac{2\sum_j V_j\left[2E_j + 2m_j^2\rho_j^2 - \left(1+\frac{2}{n_j}\right)\lambda_j\rho_j^{n_j} - \left(1+\frac{2}{n_j'}\right)\mu_j\rho_j^{n_j'}\right]}{\sum_k V_k\rho_k^2}. \tag{2.29}$$

Note that we only consider the expansion phase, so we chose the sector $\rho_j' \geq 0$ when we substituted equation (2.26).

We will focus on these two equations (2.28) and (2.29) in the following discussion, by writing them in the form of standard cosmological equations in terms of an effective EoS in relational language, and analysing its behaviour when the universe volume grows.

The late time behaviour of the model, we will see, is particularly interesting and can naturally describe a dark energy-driven acceleration, generated solely by pure quantum gravity effects.

At this stage, we would like to emphasize that our approach, especially the work in chapter 3 and chapter 4, is phenomenological, where we started from the effective action (2.21) (with the effective interaction kernel (2.22)) in its general form, rather than derive it from some fundamental GFT model, in the sense that the model is not restricted to a condensate setting. GFT coherent states, as introduced above, might not provide a good approximation to the effective GFT dynamics when the interactions are strong [92]. But in the current work the use of CPS is to provide an easy way to explain the essential concepts in GFT cosmology, and to give a template of how to extract effective dynamics using mean-field approximation. The essential part is the condensation of a large number GFT quantas, i.e. the building blocks of spacetime, such that the continuum limit can be extracted. Suppose the true ground state is given by $|\Omega\rangle$, such that the expectation value of the field operator $\sigma(g_v, \phi) = \langle\Omega|\hat{\varphi}|\Omega\rangle$ does not vanish, then the full effective action, including all quantum corrections, can still be written in the form of $S = S(\bar{\sigma}, \sigma)$, just as in our case where we used the coherent state. We see this as the form that the quantum effective action of some interesting model takes, after including (some) quantum corrections, rather than taking it literally as the classical mean field dynamics of a model, and hoping that it is not spoiled by quantum corrections, despite having strong interactions.

So, from this point of view, our analysis and results remain rather generic and hopefully robust. The main limitation comes, however, from the explicit form we use for the expectation value of the total volume. In using equation (2.27), we actually assumed that $\langle\Omega|\hat{c}^\dagger_{\boldsymbol{x}}(\phi)\hat{c}_{\boldsymbol{x}}(\phi)|\Omega\rangle = \langle\Omega|\hat{c}^\dagger_{\boldsymbol{x}}(\phi)|\Omega\rangle\,\langle\Omega|\hat{c}_{\boldsymbol{x}}(\phi)|\Omega\rangle$, which is only exactly true for coherent states. In general, there should be quantum fluctuations, marking the difference between the actual ground state and the coherent state, and hence the expectation value of the total volume would be given by

$$V(\phi_0) = \langle\Omega|\hat{V}|\Omega\rangle = \sum_j V_j \rho_j(\phi_0)^2 + \chi(\phi)^2, \tag{2.30}$$

with $\chi(\phi)^2$ specifies the fluctuations. Even though such fluctuations do not vanish for a general ground state, we can expect that they would be suppressed (at least in relative terms) when there are a large number of quantas, which is the case when we try to recover the continuum universe. Furthermore, for the evolution the ground state $|\Omega\rangle$ should be (relational) time-dependent, which means that the fluctuations $\chi(\phi)^2$ should also depend on the relational time ϕ. When plugged into the equation of motion, we can expect that such fluctuations should also be suppressed over time, to give a stable ground state, such that the system remains in the condensate phase. Therefore, as a leading order approximation, we use the GFT field coherent state as our starting point, to be then improved by the effects of fluctuations on the expectation value of the universe volume. We leave a detailed analysis of fluctuations in the interacting case to future work.

Despite these caveats, however, the approximation we are using can already provide fruitful results. For example, the Big Bang singularity can be replaced by a bounce, and short after that, a classical limit that captures correctly the Friedmann dynamics will emerge [42].

Bounce. At very early time, the volume is small (so is the modulus ρ_j for each mode), and the dynamics can be well approximated by the free evolution, ignoring the contribution from interactions. One can verify that, as long as one of the Q_j's is non-zero, the corresponding ρ_j cannot reach 0, so that the square root in equation (2.28) is real. Consequently, the total volume will not reach 0 and the classical big bang singularity is replaced by a bounce [42]. More concretely, in the case where only one mode j_0 contributes, the modified FLRW equation (2.28) can be simplified to give (where the parameters correspond to mode j_0, which are omitted for simplicity) [42]

$$\begin{aligned}\left(\frac{V'}{3V}\right)^2 &= \frac{4\left(m^2\rho^4 + 2E\rho^2 - Q^2\right)}{9\rho^4},\\ &= \frac{4m^2}{9} + \frac{8V_{j_0}E}{9V} - \frac{4V_{j_0}^2Q^2}{9V^2}.\end{aligned} \tag{2.31}$$

It can be seen that for non-vanishing Q_{j_0}, V' vanishes for finite volume V, indicates that there should be a bounce. Furthermore, in chapter 3 we will see that when all modes are taken into account, as they should be for the very early universe, there is still a bouncing scenario, hence the appearance of the bounce is quite general in our formalism.

In fact, as it's shown in [49], with the help of CPS, even if all the Q_j's vanish, the bouncing scenario is obtained for a large class of parameters (those for which (2.26) does not vanish for at least one j), and can thus be considered a rather general, albeit not universal, consequence of the quantum gravity dynamics described by the GFT model.

Classical limit. As the volume grows, but before the GFT interactions become relevant, we reach a regime where the dynamics can be well approximated by the FLRW equation in the presence of a free massless field [42, 49]. In fact, when ρ_j is large $\rho_j^2 \gg E_j/m_j^2$ and $\rho_j^3 \gg Q_j^2/m_j^2$ while not so large such that $|\mu_j|\rho_j^{n_j'-2} \ll |\lambda_j|\rho_j^{n_j-2} \ll m_j^2$, equations (2.28) and (2.29) can be approximated by

$$\left(\frac{V'}{3V}\right)^2 = \left(\frac{2\sum_j V_j m_j \rho_j^2}{3\sum_k V_k\rho_k^2}\right)^2, \quad \frac{V''}{V} = \frac{\sum_j V_j\left(4m_j^2\rho_j^2\right)}{\sum_k V_k\rho_k^2}.$$

If at least for a dominant spin mode $m_{\tilde{j}} \approx \text{const}$[1], we can *define* $m_{\tilde{j}}^2 \equiv 3\pi G$ in terms of an effective dimensionless Newton constant G, and the equation takes the form of the FLRW equation with a free massless scalar field in relational time [42, 46, 49]

$$\left(\frac{V'}{V}\right)^2 = \frac{V''}{V} = 12\pi G.$$

[1] Note that this is just a sufficient condition, not a necessary one.

Furthermore, it can be shown that in the free case the lowest spin mode j_0 will dominate quickly [102], therefore it is sufficient that $m_{j_0}^2 = 3\pi G$ to recover the FLRW equation. This means that one can obtain the correct classical limit after the end of the bouncing scenario from the effective GFT condensate hydrodynamics, before the GFT interactions start to take over.

Let us also stress that the above results have been obtained by several different strategies, beyond the specific one we illustrated above, thus confirming their solidity [91, 92]. Moreover, quantum fluctuations of the relevant geometric observables can be analysed in some detail [48]; the analysis confirms that fluctuations are naturally suppressed at late times, thus the semi-classical limit is reliable, and it allows putting precise constraints on the range of values of the various parameters in the model, for which the same quantum fluctuations remain under control in the bounce region at early times, and for which the relational evolution remains valid as well, i.e. the chosen clock remains a good one.

The important issue becomes, then, how the GFT interactions modify the effective dynamics. This is the issue we will tackle in the next chapter, extending the first analyses of this issue, performed in [45, 103, 104].

2.4 Summary

In this chapter we presented a short overview of the GFT formalism and the application of condensates in its cosmological sector. It's been argued that GFTs are theories of spacetime itself, from which the continuum physics can emerge. As many other quantum gravity theories, in GFT there is no notion of space and time coordinates *a priori*, and we explained how to reintroduce such concepts using the relational description. More precisely, we can use free massless scalar fields as relational rods and clock. And in the cosmological sector, we only consider the homogeneous condensates, or in other words, the condensate wave function should be independent of spatial coordinates. Therefore, for condensate cosmology it's enough to have clock without taking into account relational rods.

Moreover, a further simplification comes from the fact that we only consider a special type of condensates, the *isotropic* ones, such that the wave function can be characterized by identical spins, corresponds to equilateral tetrahedron geometrically (in the 4d case). With such restriction the combinatorial structure in the interaction term can be ignored, leaving us a simpler action at the effective level. In particular, the equation of motion for different modes decouple from each other, which is a basis for us to be able to consider contributions to the cosmological evolution from only a few modes. The resulting volume dynamics is in a form of the modified FLRW equation, from which we can already see that the big bang singularity is replaced by a bounce scenario and a suitable classical limit can be extracted from the single modes case.

Noting that FLRW equation describes an isotropic universe, which justifies our introduction of the isotropic condensates. But we need to emphasize again that in this thesis we only define *isotropic* or *anisotropic* condensate locally (or microscopically), in the sense

that we call a condensate isotropic if it can be specified by identical spins. This is not a necessary consequence of the fact that our universe being isotropic. In fact, we will see in chapter 5 that, even the *anisotropic* condensate[1] is able to provide us the flat space, which is isotropic (in the macroscopic sense). But before that, let's first consider the cosmological consequences of GFT condensates in chapters 3 and 4.

[1] In the microscopic sense, i.e., in the condensate function there is at least one spin that is different from others.

Chapter 3

Phantom-like dark energy from GFT condensates

Since its discovery [105, 106], the accelerating expansion of our universe, and the full characterization of its features, remain main challenges for modern cosmology [57]. The simplest candidate for the source of the acceleration would be the cosmological constant Λ [57, 107], which lead us to the standard ΛCDM model. But the smallness of the observed value of Λ [108], compared to the theoretical expectations from vacuum energy of QFT [57, 109] or from the renormalization flow of couplings in GR [58, 110, 111], making it difficult to find a compelling origin of the cosmological constant. More seriously, as we have discussed, the standard cosmological model is challenged by several recent observations, for example there should be a phantom phase ($w < -1$), which is impossible in the ΛCDM model.

To go beyond that and address the possible phantom-like evolution, one can introduce dynamical dark energy models [112], which basically means considering additional matter fields (whose properties are peculiar in the sense that they should have negative pressure) other than those found in the standard model of particle physics. Another route, besides the more particle-theoretic approach, is to modify gravity theory [113]. In particular, the quantum gravity effects can be viewed as modifications to GR at the effective level. For example, the acceleration of universe can be reproduced within the formalism of asymptotically safe cosmology [114], of Dvali-Gabadadze-Porrati braneworld model [115], and of condensate cosmology in GFT [50], without the need of dark energy or cosmological constant. On the other hand, even if some dark energy fields do exist, their behaviour may change due to the inclusion of gravity. For instance, some future singularities, that would be encountered because there is no graceful exit of the phantom phase with solely phantom dark energy field, could be avoided if one considers the quantum gravity effects [116].

In this thesis, particularly in this chapter, we adopt a similar approach of modifying gravity. However, our modifications to General Relativity (GR) stem from quantum gravity effects. Since our objective is to derive the cosmological evolution, it is natural to employ a phenomenological approach. We focus on an effective description within the hydrodynamic approximation, taking into account the fundamental quantum dynamics of spacetime constituents. In this context, the condensate introduced in the previous chapter

plays a central role. It allows us to extract the expectation values of relevant operators and track their evolution with respect to the relational time ϕ.

Specifically, we will demonstrate that phantom-like dark energy can naturally emerge from GFT condensate cosmology. What is remarkable is that this is achieved without the need to introduce any specialized phantom matter. The cosmological acceleration is generated by the interaction terms of the effective GFT action, and to get a phantom phase while keeping our universe stable, so we can avoid future singularities such as Big Rip [67, 117, 118], we need to consider contributions from at least two condensate modes. Then it's natural to ask how the inclusion of multiple modes will change the early time evolution as well, which served as an insurance to show that without interaction terms, we can't get a long-lasting acceleration phase no matter how many modes are included in the analysis. Before stepping into the detailed discussion, however, we need first to find a proper quantity/observable that characterizes correctly the cosmological evolution. As we will see in the following, the suitable choice for GFT condensate cosmology is w, the effective equation of state.

3.1 Effective equation of state

The volume dynamics (2.28) and (2.29) obtained for GFT condensate cosmology, in fact contain already all the information we need to describe the evolution of our universe. However, they are not suitable for the comparison between our GFT cosmology results with the standard ones obtained using more particle-theoretic approaches, as in the former we are using the relational time ϕ while in the latter the cosmic time is usually used. The value of the EoS, which can be derived from volume and its derivatives as well as keeping all the relevant information (see appendix A.1), is independent of the clock we are chosen. Furthermore, some observational results, such as that fact that we may be experiencing a phantom phase now, are inferred directly from the value of EoS [59]. Therefore, in the following we will choose the effective EoS as the main quantity to reveal the characteristics of the cosmological evolution.

In a homogeneous universe, for example, the matter content is assumed to be a perfect fluid and can be characterized by its energy density ρ and pressure p in a commoving frame. The fluid then couples to the geometry, determining the cosmological evolution, through its EoS $w = p/\rho$. For example, if the expanding universe is dominated by a fluid with $w < -1/3$, then the expansion will be accelerating. Current cosmological observations give a value $w \simeq -1$, thus we are indeed experiencing an accelerating expansion phase of the universe. On the other hand, the usual matter content from the standard model would give $w = 1/3$ for relativistic particles and $w = 0$ for non-relativistic particles, certainly neither of which is able to generate the acceleration. As we have emphasized, although a small positive cosmological constant could reproduce exactly $w = -1$ that could account the current accelerating expansion of our universe, such a model won't able to explain the preferred value of $w < -1$ inferred from supernova data [59]. Some form of dynamical dark energy model has to be considered.

To see that the required phantom phase arises naturally in GFT condensate cosmology, we need to consider the behaviour of the EoS corresponds to the GFT interaction. Or more conveniently, we can introduce an effective EoS, deducted from the FLRW equation, to represent the evolution history of our universe.

For a homogeneous and isotropic metric with scale factor $a(t)$, the Hubble parameter can be given by $H = \dot{a}/a$ with the $\dot{}$ represents the derivative respect to cosmic time t. Then the effective EoS can be defined as $w = -1 - 2\dot{H}/(3H^2)$. In the GFT (and more generally, quantum gravity) context, we cannot rely at the fundamental level on any time coordinate or direction. We can use, instead, a relational definition of time in terms of a physical clock, for example a free massless scalar field ϕ, as discussed in section 2. In appendix A.1 we show that using this definition of relational time, the effective EoS w has the form

$$w = 3 - \frac{2VV''}{(V')^2}, \tag{3.1}$$

where V is the total volume and the $'$ indicates the derivative with respect to the relational time ϕ, and we chose the time gauge, in which the volume $V = a^3$ for scale factor a.

Using this effective EoS, all the effects produced on the evolution of the universe by the underlying quantum gravity dynamics can be described as if they were due to some effective matter field ψ satisfying $w_\psi \equiv p_\psi/\rho_\psi = w$, with p_ψ and ρ_ψ its pressure and energy density, respectively.

We emphasize that the field ψ introduced this way is just a convenient rewriting of what remains due to the fundamental quantum gravity dynamics. As such, it is not required to possess the usual features of well-behaved matter field theories defined on cosmological backgrounds, nor the desiderata of any effective QFT. For the same reason, we will not discuss possible Lagrangians for ψ, or dwell any further into its properties *qua matter field*.

One main advantage of introducing the fictitious field ψ, beside making the analysis of the volume evolution more practical, is that it helps to gain an intuitive understanding of quantum effects on geometry, or more precisely, on the scalar curvature, which is a rather tricky observable to define and compute in the fundamental quantum geometric GFT context. In fact, suppose the energy-momentum tensor of field ψ is given by $T_{\mu\nu}$, then tracing the Einstein equation we see that the scalar curvature in a universe dominated by ψ can be given by $R = -T^\mu_\mu = -(1+3w_\psi)\rho_\psi$, where we used the fact that $T^\mu_\mu = \rho_\psi + 3p_\psi$ in the commoving frame. In particular, this helps to identify potentially singular regimes. For example, if $\rho_\psi \to \infty$, we see that the scalar curvature diverges as well (except for $w \neq -1/3$, which, as we can see in subsection 3.1.1, will not lead to a divergent energy density anyway); these correspond to *Big Rip*-like singularities, which is relevant for dark energy models [117–120], and on which we are going to have more to say in the following.

3.1.1 The evolution of ψ

Now we recall the evolution of an effective field ψ endowed with the EoS w. We stress once more that we intend this to be only an illustration of which properties a field of this type

would have in the context of standard GR and effective QFT, making use of all the auxiliary structures (topological manifold, coordinates, gauge conditions, etc.) that are useful tools in such context. It is not a determination of the physical properties of a physical field, corresponding to fundamental degrees of freedom and observables of our quantum gravity formalism, but only an effective rewriting of quantum 'pre-geometric' gravity degrees of freedom, which are not described in terms of similar auxiliary structures. For example, we could *define* an energy density for the effective field ψ from the EoS w and the universe volume V and study its properties, but there is no independent fundamental observable corresponding to it, in the GFT algebra of (2nd quantized) observables.

Having clarified this important point, the energy density ρ_ψ satisfies the conservation equation $\dot{\rho}_\psi + 3H(1+w)\rho_\psi = 0$. Using the standard definition of Hubble parameter in time gauge $H = \dot{a}/a = \dot{V}/(3V)$, this equation can be rewritten as

$$\frac{\mathrm{d}\rho_\psi}{\mathrm{d}V} + \frac{1+w}{V}\rho_\psi = 0, \tag{3.2}$$

which can indeed be taken as a definition of the energy density in terms of quantities corresponding to GFT observables. For constant w, equation (3.2) can be easily solved, and the solution is given by

$$\rho_\psi = \frac{\rho_{\psi 0}}{V^{1+w}},$$

with the $\rho_{\psi 0}$ is the constant of integration. For $w > -1$, the energy density ρ_ψ decreases as the volume grows, and tends to vanish when volume is large, as one can expect for any ordinary matter in the sense of particle physics; for $w = -1$, the energy density is a constant, corresponding to a cosmological constant, and would tend to dominate over any other fluids with $w > -1$ at late times; for $w < -1$, on the other hand, ρ_ψ increases as the volume becomes larger, and would tend to diverge for $V \to \infty$. Such a large energy density with $w < -1$ will tear apart every thing in the universe, leaving no bound system at all even when the size of the universe is finite, before the total volume diverges, as discussed in [118][1]. Furthermore, when ρ_ψ diverges, the scalar curvature $R = -(1+3w_\psi)\rho_\psi$ would approach to infinity as well, lead to Big Rip-like singularities.

The above discussion gives a first intuition for the possible late time evolution of our universe, and of various issues constituting the dark energy problem. It should be clear, however, that things are so simple only under the assumption of constant EoS w. Any dark energy model which is based on a *dynamical* EoS would require a more detailed analysis.

A particularly interesting class of dark energy models is in fact based on fields with EoS less than -1, producing a *phantom (dark) energy*, which is well compatible with present observational constraints. And when the EoS became dynamics, i.e., not a constant any more, it's possible to avoid the Big Rip-like singularities even if the evolution is phantom-like, as it happens for our GFT condensate cosmology model.

[1] We thank Dr. Che-yu Chen for pointing out this reference.

3.1.2 Phantom energy

The mentioned feature of phantom energy compared to other field-theoretic models with $w > -1$, i.e. that its energy density increases as the universe volume grows, is the root of various difficulties in constructing a viable field theoretic model of phantom energy. In fact, $w < -1$ requires negative kinetic energy and leads to a violation of various energy conditions [67, 68, 121]. The negative kinetic energy is also unbounded from below, and straightforward introductions of a regularizing cut-off would lead, in general, to violations of Lorentz symmetry [122].

While these are serious difficulties for such field-theoretic phantom models, phantom energy cannot be ruled out based on cosmological data. On the contrary, several observations *favour* an EoS less than -1 [59, 62, 63, 123]. In addition, it has been recently shown that the existence of phantom energy may alleviate the H_0 tension [65, 124], i.e. the fact that the value of the Hubble parameter when estimated from local observations of supernova [64] is larger that what is deduced from CMB data [56]. These results suggest possible discrepancies between the cosmological observation and the underlying matter field description of particle physics. See [61] for a recent review of cosmological tensions.

Therefore, we seem to be facing a situation in which a phantom-like evolution of the observed (late) universe struggles to find a compelling theoretical description. From our quantum gravity viewpoint, based on a formalism in which spacetime is naturally seen as emergent, the difficulties of a formulation of phantom energy in terms of a field theory framework is not particularly worrying. We expect the whole background cosmological dynamics, including its large-scale features, to be determined by the underlying quantum gravity dynamics, and no fundamental phantom field needs to be part of the story. On the other hand, our task is, first of all, to match cosmological observations, which is a difficult challenge for all fundamental quantum gravity approaches, and for this aim an effective phantom dark energy would be suitable. Indeed, we will show in the following how phantom-like dark energy can emerge from our GFT condensate model.

For completeness, we mention that one can also tackle the phantom energy problem in the context of modified gravity theories. That is, one can attribute the accelerated expansion of the universe to a modification of the underlying gravitational dynamics, with respect to GR, for example as the $f(R)$ theory [125], rather than to new exotic matter components. In such a way, one can bypass the difficulties of constructing a well-defined matter field theory of phantom energy. This second approach is much closer in spirit to the one we take within our quantum gravity framework, and the emergent cosmological dynamics we extract from the fundamental quantum dynamics of 'spacetime constituents' could in principle be recast also in terms of some effective modified gravity theory.

Big Rip singularity. In the phantom phase, we have $w < -1$ and the energy density (or Ricci scalar in the case of pure gravity) increases as volume grows, and it's possible (if the phantom phase lasts long enough) that such energy density can increase to infinity

and tears apart everything in our universe[1] [117, 118]. Such behaviour, however, can be changed dramatically in the presence of quantum gravity effects. For example, in the early universe, even ordinary matter with $w > -1$ can have phantom like behaviour due to discreteness of quantum geometry [126]. And at late times, quantum gravity effects can dissolve the Big Rip singularity in the presence of phantom matter with $w < -1$, as studied in the LQC context [116] and also in semi-classical analyses [127]. Here we will not consider the coupling between quantum gravity and matter, since the accelerated phase with effective EoS $w < -1$ will emerge from pure quantum gravity effects in our model, and the Big Rip singularity can be avoided due to a non-trivial time dependence of w.

Indeed, as mentioned above, when w is time dependent the evolution of (any effective) ρ_ψ can be rather involved. In particular, if w approaches to -1 fast enough, the phantom energy density does not diverge but increases to a constant value, and the Big Rip singularity can be avoided. For example, consider ρ_ψ as a cosmological constant plus some matter component with negative energy density, inversely proportional to the volume [128]. This corresponds to a field ψ with $w_\psi < -1$, but that approaches -1 at large volume, so that asymptotically we reach a de Sitter spacetime. This is referred to as *phantom analogues of de Sitter space* in [128]. In subsections 3.3.2 and 3.3.3 we will see how exactly this kind of behaviour emerges from our model of GFT condensate cosmology.

3.1.3 w from single-mode GFT condensates

Before moving on to our new analysis of multiple modes contributions to GFT cosmological dynamics in the presence of interactions, let us rewrite some earlier results in terms of w, as an illustration on how the information of universe evolution can be read out from EoS. The result of [45] is equivalent to a study of the behaviour of the effective w under the assumption that only a single mode j contributes to the dynamics, which is partially justified as the asymptotic dominance of a single mode when the universe expands is expected also in the general case. The generalization of these results, i.e., including contribution from other modes, constitutes an important part of this thesis.

As we will explain in the following, the presence of other modes changes the way in which w approaches the asymptotic value, which is of important physical relevance, on top of making the dynamics much richer in any intermediate regime. But still, the analysis in [45] is already important to show how GFT interactions can have very interesting consequences on the emergent cosmological dynamics, as we are going to discuss in this subsection.

With only a single mode j, substituting (2.28) and (2.29) in the definition (3.1) we obtain the EoS

$$w = \frac{-3Q^2 + 4E\rho^2 + m^2\rho^4 + \left(1 - \frac{4}{n}\right)\lambda\rho^{n+2} + \left(1 - \frac{4}{n'}\right)\mu\rho^{n'+2}}{-Q^2 + 2E\rho^2 + m^2\rho^4 - \frac{2}{n}\lambda\rho^{n+2} - \frac{2}{n'}\mu\rho^{n'+2}}, \tag{3.3}$$

[1] For a matter field with $w < 0$, its pressure would be negative. So intuitively, instead of squeezing things together, the fields modelling dark energy (correspond to $w \simeq -1$) will tend to tear things apart. And when the energy density, hence the absolute value of the pressure, is large enough, no stable bound structure can exist any more [117, 118].

where for simplicity we dropped the subscript j labelling different modes. Furthermore, for a single mode the total volume[1] $V = V_{j_0}\rho^2$, which enables us to get the evolution EoS as a function of the total volume, $w = w(V)$, even without solving the equation of motion. This greatly simplifies the analysis.

Early time acceleration in the free case. At early times, the module ρ of the condensate is small (since the total volume is small), therefore the interaction terms can be ignored. Here we set $\lambda = \mu = 0$ in equation (3.3), then w is simply

$$w = \frac{-3Q^2 + 4E\rho^2 + m^2\rho^4}{-Q^2 + 2E\rho^2 + m^2\rho^4}.$$

Similarly, the equation of motion (2.28), when constraining to the free case with a single mode, simplifies to equation (2.31). At the bounce, we should have $V' = 0$, which requires the equation

$$-Q^2 + 2E\rho^2 + m\rho^4 = 0,$$

from which we can get the value of ρ at the bounce

$$\rho_b = \frac{1}{m}\sqrt{\sqrt{E^2 + m^2Q^2} - E}.$$

Putting the value ρ_b back into w we see that its denominator vanishes while its numerator is negative, therefore near the bounce we have $w \to -\infty$, means that right after the bounce the expansion of our universe is accelerating, as we expect in general from a bouncing scenario[2]. However, we can show that this accelerating phase ends quickly, i.e., the volume at the end of acceleration is not large compared to the volume at the bounce [45]. The situation is similar even if we consider the contributions from all modes, as we shall see in section 3.2.

It is worth mentioning that even if $w \to -\infty$ at the bounce, we do not run into singularities due to the quick end of the acceleration phase and the fact that the total volume has a minimum value $V_b > 0$. To see this we first note that for a single mode (assumed to be mode j_0), the total volume can be given by $V = V_{j_0}\rho^2$, therefore the EoS can be rewritten as

$$w = \frac{-3Q^2V_{j_0}^2 + 4EV_{j_0}V + m^2V^2}{-Q^2V_{j_0}^2 + 2EV_{j_0}V + m^2V^2}.$$

Then we substitute this EoS into the conservation equation (3.2) for the fictitious field ψ, we get the solution

$$\rho_\psi = \frac{\tilde{\rho}_{\psi\infty}}{V^2} + \frac{2E_0V_{j_0}}{V^3}\frac{\tilde{\rho}_{\psi\infty}}{m^2} - \frac{Q^2V_{j_0}}{V^4}\frac{\tilde{\rho}_{\psi\infty}}{m^2},$$

[1] Here j_0 represents the mode that being dominated, which we restored to avoid confusions.

[2] The universe should expand which requires $V' > 0$ after the bounce, and at the bounce we have $V_b' = 0$, therefore we should also have $V_b'' > 0$. Since the volume V_b at the bounce is also positive, from the definition (3.1) of w we see that $w \to -\infty$ at the bounce is a general feature.

where $\tilde{\rho}_{\psi\infty}$ is defined such that $\rho_\psi V^2 \to \tilde{\rho}_{\psi\infty}$ as the total volume $V \to \infty$. Since the volume $V \geq V_b > 0$ is bounded below, we see that the energy density ρ_ψ remains finite, hence there are no singularities. We also note that at the bounce we have $\rho_\psi(V_b) = 0$.

Emergence of the FLRW universe. As we have explained in section 2.3, the classical limit emerges already in the free case for large volume, where the module ρ is also expected to be large, hence we can consider the expansion respect to ρ. At leading order in $1/\rho$, we have a constant value $w = 1$, corresponds to the EoS of a free massless scalar field $\chi_0 = \phi$, the one we introduced as the relational time in chapter 2. In fact, substituting $w = 1$ back into its definition (3.1), simple algebraic manipulation shows that

$$\frac{V''}{V} - \left(\frac{V'}{V}\right)^2 = \frac{VV'' - (V)^2}{V^2} = \frac{\mathrm{d}}{\mathrm{d}\phi}\left(\frac{V'}{V}\right) = 0,$$

hence $V'/V = \text{const}$ which characterizes the FLRW equation using the relational language in the presence of a free massless field [42].

At the next order of $1/\rho$, we can approximate w as

$$w = 1 + \frac{2E}{m^2\rho^2}, \tag{3.4}$$

confirming that the effective EoS approaches 1 at large volume. Furthermore, for $E > 0$, w approaches this asymptotic value from above; see figure 3.1. This is not the case when we consider more than one mode, as we shall see in subsection 3.2.3.

An emergent inflationary phase from quantum gravity. The next question is how the single-mode interactions change this picture, in particular concerning the early acceleration after the bounce. As showed in [45], one can indeed get a long-lasting accelerated phase, in contrast to the free condensate. Furthermore, with two interaction terms this acceleration can end properly, and the time that the acceleration lasts can be adjusted by tuning couplings λ and μ [45]. What is missing, however, is a subsequent FLRW phase, which is of course also crucial for a proper cosmological model.

Now let's consider how to show the emergence of the long-lasting accelerated phase through the evolution of the effective EoS. Since we assumed that $|\mu| \ll |\lambda|$, there is an intermediate range, where $m^2\rho^4$ and $\mu\rho^{n'+2}$ are both small compared to $\lambda\rho^{n+2}$, and the behaviour of w is determined by the λ term. The case with $\lambda > 0$ will give an additional root of the denominator of w, corresponds to the maximum value of ρ and lead to a cyclic universe very quickly after the bounce. Therefore, we need only consider the case with $\lambda < 0$, where to the leading order we obtain $w = 2 - n/2$. We see that for $n \geq 5$ the EoS $w < -1/3$, which corresponds to an accelerating phase. In absence of other interactions, this accelerated phase would simply not end. Otherwise, as ρ increases further, the μ term becomes important compared to the λ term. If $\mu > 0$, ρ' will vanish again (besides the point of minimal volume reached at the bounce), corresponding to the maximum value of

ρ determined approximately by (other terms can be ignored when volume is very large)

$$\frac{2}{n}\lambda\rho^{n+2} = \frac{2}{n'}\mu\rho^{n'+2},$$

near which $w \to \infty$. This means the accelerating phase dominated by the λ term stops. By adjusting the values of the couplings λ and μ we can make this phase lasts long enough to account the observational constraints [45]. The magenta dash-dotted line in figure 3.4 shows the behaviour of w when $\mu > 0$ and we see that there is a nice inflationary phase with $w = -1/2$. However, as anticipated, this inflationary phase ends when the volume approaches its maximal value, being quickly followed by a contracting phase, with no FLRW phase in between. The important take home message, however, is that interesting large scale cosmological dynamics, like a long-lasting inflationary (or more generally, accelerated) phase can be produced purely from fundamental quantum gravity dynamics, without the need of any exotic matter field (here, an inflaton).

Phantom crossing. Finally, in this simpler single-mode context, we can ask whether anything like a phantom-crossing can also be obtained as a result of the quantum gravity dynamics.

As we explained above, when $w < -1$ we have phantom energy. For a dynamical w, it is possible for w to change from $w > -1$ to $w < -1$, a phenomenon called *phantom crossing* [129]. In our case, if $\mu < 0$, ρ can keep growing until the μ term dominates, with the asymptotic behaviour of the EoS given by

$$w \to 2 - \frac{n'}{2} + (n' - n)\,\frac{n'\lambda}{2n\mu}\rho^{n-n'}.$$

Since $n' > n$, we see that for $n \geq 5$, we have $w < -1/3$ as ρ grows and the acceleration does not stop. And in contrast to the $\mu > 0$ case, where the volume has a maximum value after which the universe starts to collapse, when $\mu < 0$ the total volume can grow forever. Note that $n' > n$ and that both λ and μ are negative, thus we conclude that w approaches its asymptotic value from above. For $n' = 6$, we have $w \to -1$, which mimics the behaviour of a cosmological constant. Since w approaches this value from above, we have $w > -1$ after the end of early accelerating phase (which is dominated by the free parameters of the condensate). We conclude that for a single mode with $n' \leq 6$, w cannot cross the phantom divide $w = -1$. This is illustrated in figure 3.4 by the black solid line.

On the other hand, for $n' > 6$ with $\mu < 0$, the asymptotic value of w would be less than -1, so phantom crossing is possible. But now the energy density of the fictitious field ψ with effective EoS w will diverge as the volume of the universe grows. When the volume is large enough, this energy density would produce a Big Rip singularity [117]. In section 3.3, we will show that in contrast to the single mode case considered here, when including another mode into the contribution of the cosmological evolution, we can get an EoS w that crosses the phantom divide, and that, instead of a Big Rip singularity, the *phantom analogues of de Sitter space* [128] is obtained.

Table 3.1 summarizes the influence of parameters in our model on the behaviour of the cosmological evolution. Note that the early accelerating phase can be regarded as inflation only when there is a graceful exit, or in other words, such phase has to end properly at some point, which is not possible for the last row in the table, where $\mu < 0$.

		Inflationary phase	FLRW phase	Cyclic behaviour	Late time acceleration	Phantom crossing	Big Rip
$\lambda > 0$				✓			
$\lambda < 0$	$\mu > 0$	$n \geq 5$	$\lvert\lambda\rvert$ small	✓			
	$\mu < 0$		$\lvert\lambda\rvert$ small		$n' \geq 5$	$n' > 6$	$n' > 6$

Table 3.1: The influence of parameters on the cosmological evolution in single mode case. The blank cell indicates there is no such behaviour, the check mark ✓ means such behaviour would occur, while other non-empty cells suggest that the behaviour would show up for the given range for the parameters.

3.2 Acceleration in early time

Previously, we have seen that in our model of GFT condensate cosmology, a single mode won't able to generate the phantom phase while avoiding the Big Rip-like singularity. For such a phase to emerge the inclusion of other modes is necessary [50]. But before we discuss the details of the emergence, we will show in this section that the interactions are also necessary, in the sense that, even with multiple modes, without interaction terms there won't be a long-lasting phantom phase.

Another reason for the study of multiple modes in the free case is that, in the early universe, where the volume is small, and the free terms are dominated compared to the interaction ones, we have no reason to expect one mode to dominate over the others, so we should include the contributions from several modes into account. The inclusion of other modes won't change much of the result we discussed in last section, such that the accelerating expansion is still not long-lasting and the asymptotic value of w remains 1. What will change, however, is the way that w approaches to its asymptotics. In particular, for the two modes case, w will approach 1 from below (see figure 3.1), which is not possible in the single mode case. This provides some insights to the interacting case as well, where the asymptotic value is -1 and when approaching it from below, we necessarily enter a phantom phase. Section 3.3 will provide more details on the issue of late time behaviour and phantom crossing.

3.2.1 Accelerated expansion in the free condensate

In the region we are going to consider we require that $\rho_j' \geq 0$, and then the condition $V' = 0$ for the volume at the bounce corresponds to requiring $\rho_j' = 0,\ \forall j$. The value of ρ_j

at the bounce can be obtained by solving the equation $\rho'_j = 0$, where ρ'_j is obtained from the definition (2.26) of the GFT 'energy' E_j as

$$\rho'_j(\phi) = \frac{1}{\rho_j}\sqrt{2E_j\rho_j^2 - Q_j^2 + m_j^2\rho_j^4 - \frac{2}{n_j}\lambda_j\rho_j^{n_j+2} - \frac{2}{n'_j}\mu_j\rho^{n'_j+2}}. \tag{3.5}$$

In the free case, at the bounce we have

$$\rho_{bj} = \frac{1}{m_j}\sqrt{\sqrt{E_j^2 + m_j^2Q_j^2} - E_j}.$$

Given the initial value $\rho_j(0) = \rho_{bj}$, the differential equation (3.5) can be solved [46, 102]

$$\rho_j(\phi) = \frac{1}{m_j}\sqrt{\sqrt{E_j^2 + m_j^2Q_j^2}\cosh(2m_j\phi) - E_j}. \tag{3.6}$$

Then the total volume (2.27) becomes

$$V = \sum_j V_j\rho_j^2 = \sum_j \frac{V_j\sqrt{E_j^2 + m_j^2Q_j^2}}{m_j^2}\cosh(2m_j\phi) - \sum_j \frac{V_jE_j}{m_j^2}. \tag{3.7}$$

At the bounce we have $\phi = 0$, where the volume is simply $V_b = c_1 - c_2$, with two constants c_1 and c_2 are given by

$$c_1 = \sum_j \frac{V_j\sqrt{E_j^2 + m_j^2Q_j^2}}{m_j^2},\ c_2 = \sum_j \frac{V_jE_j}{m_j^2}. \tag{3.8}$$

We can see that $c_1 > c_2 > 0$.

The volume should be convergent, in the sense that V is finite at any given relational time ϕ. In appendix A.2 we show that this is equivalent to the requirement that $\sum_j \frac{V_j}{m_j^2}\sqrt{E_j^2 + m_j^2Q_j^2}$ converges and all the m_j's are bounded. A direct consequence is that at sufficiently large ϕ, the volume is dominated by the mode with the largest value of $m_j = m$. This largest value defines, in this regime, the effective Newton's constant $m^2 = 3\pi G$, and the dynamics reduces to the standard Friedmann equation with the matter content given by the free massless scalar field [42]. There are general arguments suggest that m_j is monotonically decreasing with j, so that, at large volume, it is the smallest spin mode that eventually dominates [102].

3.2.2 Upper bound of the number of e-folds

Now we are ready to check if the inclusion of all modes can make the acceleration phase after the bounce last long enough to be of phenomenological significance as a quantum gravity-induced inflation, even in the free case.

For simplicity, we introduce a function $P(\phi)$ to characterize the acceleration

$$P(\phi) = -\frac{(V')^2}{2}\left(w + \frac{1}{3}\right), \tag{3.9}$$

which in the free case has the form

$$\begin{aligned} P(\phi) = &\sum_j 4V_j\sqrt{E_j^2 + m_j^2Q_j^2}\cosh(2m_j\phi)\sum_k \frac{V_k}{m_k^2}\left[\sqrt{E_k^2 + m_k^2Q_k^2}\cosh(2m_k\phi) - E_k\right] \\ &-\frac{5}{3}\sum_j \frac{2V_j}{m_j}\sqrt{E_j^2 + m_j^2Q_j^2}\sinh(2m_j\phi)\sum_k \frac{2V_k}{m_k}\sqrt{E_k^2 + m_k^2Q_k^2}\sinh(m_k\phi). \end{aligned} \tag{3.10}$$

The accelerating expansion requires $w < -1/3$, i.e. $P(\phi) > 0$, while the decelerating phase corresponds to $P(\phi) < 0$.

At the bounce, where $V' = 0$, we have simply

$$P(0) = \sum_j 4V_j\sqrt{E_j^2 + m_j^2Q_j^2}\,(c_1 - c_2) > 0, \tag{3.11}$$

with c_1 and c_2 defined in (3.8), while for large ϕ, the volume is dominated by a single mode, and equation (3.4) tells us that $w \to 1$ when volume is large. This implies $P(\phi) < 0$ at large volume. Therefore, there is a point where $P(\phi) = 0$ and the accelerating expansion stops. We now identify this point and show that the accelerating phase at this early state can not be long-lasting. More precisely, we will get an upper bound on the ratio V_e/V_b, where V_e is the volume when acceleration ends, and $V_b = c_1 - c_2$ is the volume at the bounce.

The time ϕ_e where the accelerating phase ends is determined by the requirement $P(\phi_e) = 0$. This equation is quite hard to solve for general m_j's. On the other hand, if the acceleration is long-lasting, ϕ_e would be large, and around this point $P(\phi)$ changes quickly. Therefore, we can introduce an approximated quantity $P_m(\phi)$, obtained by replacing $\cosh(2m_j\phi)$ and $\sinh(2m_j\phi)$ in (3.10) with $\cosh(2m\phi)$ and $\sinh(2m\phi)$ respectively, where m is the maximum value of m_j's (which is shown to exist due to the convergence of volume, see appendix A.2). We can write $P_m(\phi)$ as

$$P_m(\phi) = -\frac{4m}{3}\left[\cosh^2(2\sqrt{m}\phi)\left(5c_1'^2 - 3c_1c_1''\right) + \cosh(2\sqrt{m}\phi)(3c_1''c_2) - 5c_1'^2\right],$$

with c_1 and c_2 are given by equation (3.8) and the two new constants c_1' and c_2' are

$$c_1' = \sum_j \frac{V_j}{mm_j}\sqrt{E_j^2 + m_j^2Q_j^2},\ c_1'' = \sum_j \frac{V_j}{m^2}\sqrt{E_j^2 + m_j^2Q_j^2}. \tag{3.12}$$

We see that $c_1 > c_1' > c_1'' > 0$. The equation $P_m(\phi) = 0$ has a root ϕ_m and one has

$$\cosh(2m\phi_m) = \frac{-3c_1''c_2 + \sqrt{9c_1''c_2^2 + 20c_1'(5c_1'^2 - 3c_1c_1'')}}{2(5c_1'^2 - 3c_1c_1'')}. \tag{3.13}$$

Since $P(\phi)$ changes quickly near ϕ_e, we have approximately $\phi_e \approx \phi_m$, which in turn leads to $V_e = V(\phi_e) \approx V(\phi_m) < V_m(\phi_m)$. Here we define V_m similarly as P_m, i.e., replacing $\cosh(2m_j\phi)$ in the volume (3.7) with $\cosh(2m\phi)$, and therefore, at $\phi = \phi_m$ we have

$$V_m(\phi_m) = c_1 \cosh(2m\phi_m) - c_2.$$

Then the ratio between volume at the end of acceleration and the volume at the bounce satisfies

$$\frac{V_e}{V_b} < \frac{V_m(\phi_m)}{V_b} = \frac{-3c_1c_1''c_2 + c_1\sqrt{9c_1''c_2^2 + 20c_1'(5c_1'^2 - 3c_1c_1'')}}{2(5c_1'^2 - 3c_1c_1'')(c_1 - c_2)} - \frac{c_2}{c_1 - c_2}. \tag{3.14}$$

with c_1 and c_2 are given by equation (3.8). Under the conditions $c_1 > c_2 > 0$ and $c_1 > c_1' > c_1'' > 0$, $V_m(\phi_m)/V_b$ has a maximum value

$$\left.\frac{V_m(\phi_m)}{V_b}\right|_{max} = 1 + \frac{c_1}{c_2} + \frac{c_1}{c_2}\sqrt{\frac{c_1 + c_2}{c_1 - c_2}}.$$

Therefore, the original volume ratio with j dependent m_j has the upper bound

$$\frac{V_e}{V_b} < 1 + \frac{c_1}{c_2} + \frac{c_1}{c_2}\sqrt{\frac{c_1 + c_2}{c_1 - c_2}}, \tag{3.15}$$

with c_1 and c_2 are defined in equation (3.8).

The bound goes to infinity when $\frac{c_2}{c_1} \to 0$ or $\frac{c_2}{c_1} \to 1$. However, since the total volume V should be finite, both of c_1 and c_2 should be finite. Then, using their definition, we see that $\frac{c_2}{c_1} \to 0$ would require $E_j \to 0$ for all j while $\frac{c_2}{c_1} \to 1$ would require $Q_j^2 \to 0$ (m_j cannot vanish otherwise c_1 and c_2 would diverge) for all j. Therefore, for general configurations corresponding to non-vanishing Q_j and E_j for some j, the bound on the number of e-folds would not be large. While for vanishing Q_j and E_j we need to find a different bound to reach a reliable conclusion, it is clear that this would correspond to a rather special case, thus of limited interest, especially in a phenomenological setting like we have considered in this thesis.

We conclude that the expansion of the universe becomes decelerating quickly after the bounce, confirming the results of [45] in a more general setting by including multiple modes into consideration.

It is worth emphasizing that this initial accelerating expansion is in fact a general feature of a bouncing universe, not necessarily linked to any inflationary-like scenario. Inflation as usually understood should instead start later, during the radiation dominating phase [55]. Such later inflationary acceleration can indeed be reproduced as it has been shown in the previous section, recalling the results of [45], when accounting for GFT interactions in our condensate. As we discussed, however, single-mode interactions which are strong enough to be relevant shortly after the bounce, and before a FLRW phase produced by the free GFT dynamics, end up preventing that such a FLRW phase is realized after the inflationary one,

in contrast to a physically viable cosmological model. One may wonder if the contribution from multiple modes changes this picture. A moment of reflection, together with the analysis we present in the next section, would convince that this may only be possible in the presence of somewhat extreme fine-tuning of parameters and a very special behaviour of the condensate density, since in practice it would require that the contributions from the two interaction terms for the two modes approximately cancel for a long enough period in the evolution of our universe, after the inflationary phase, so to effectively reproduce the free dynamics and its FLRW phase. A situation of this type, even if possible in principle, would be of little interest, unless somehow governed by some symmetry principle or some other generic feature of the underlying quantum gravity model. Lacking this, we do not consider it further in the following.

We discuss instead in detail the role of GFT interactions in producing an accelerated expansion at even later times, in the next section. The important point to stress here is that, as long as the interaction couplings are small compared to 'mass' term m_j, the behaviour of condensates can be well approximated by free solutions. Therefore, a very short-lived accelerated expansion after the bounce followed by a decelerating phase remains a general feature even in the presence of interactions. We are going to use this feature to ensure that, whatever the detailed late time evolution of the universe in our model is, an extended FLRW phase can be realized, before quantum gravity interactions become relevant, as required by observations.

3.2.3 Equation of state after the end of acceleration

More precisely, after the end of the post-bounce acceleration, the expansion itself does not stop and the volume of universe keeps growing. According to the free solution (3.6), for large ϕ the module ρ_j increases exponentially. Therefore, the mode with largest m_j dominates quickly as the volume growing, which means the EoS will soon be dominated by this single mode as well[1]. As we have already discussed, w will have the asymptotic value $w = 1$ as in the single mode case, corresponding to the EoS of the free massless scalar field that we are using as relational time. However, the inclusion of other modes changes the precise way in which w approaches to the asymptotic value. Taking the two-modes case as an example (for simplicity, we write $\rho_{1,2} \equiv \rho_{j_1,j_2}$ etc.). Assuming $m_1 > m_2$ and hence at large volume we have $\rho_1 > \rho_2$, then w can be expanded as

$$w \to 1 + \frac{2V_2\rho_2^2}{V_1\rho_1^2}\left(2\sqrt{\frac{m_2}{m_1}} - 1 - \frac{m_2}{m_1}\right).$$

Since $2\sqrt{m_1/m_2} < 1 + m_2/m_1$, we see that $w < 1$ which means that the EoS approaches the asymptotic value (which is 1 here) from below, in contrast with the single mode case. In figure 3.1 we compare the behaviour of w for free condensate in the two-modes and

[1] In fact, as one can show that the mode has largest m_j usually corresponds to $j = 1/2$, i.e., the smallest spin possible [102]. Therefore, for the free case the large volume behaviour is usually dominated by the modes with small spin [102]. We will see later in section 3.3.1 that this is also true in the interacting case.

single-mode cases. At small volume near the bounce, $w < 0$ and its absolute value is large; this corresponds to large acceleration right after the bounce. With the increase in volume, w grows quickly and becomes larger than $-1/3$ soon, where the accelerated expansion stops. Then w keeps growing and reaches its maximum value, after which w starts to decrease. This behaviour is true for both the two-modes and single-mode cases. As the volume grows further, the evolution of w starts to differ in the two cases. In the two-modes case, w has a minimum value, which is smaller than 1, after which w starts to increase again, and reaches $w = 1$ from below. In the single-mode case, instead, there is no local minimum, and w keeps decreasing, and approaches the asymptotic value $w = 1$ from above. Something similar will happen in the interacting case. We will see that, for interactions of order 6, the asymptotic value will be the phantom divide where $w = -1$. Therefore, at large volume we have $w < -1$ and the phantom divide is crossed.

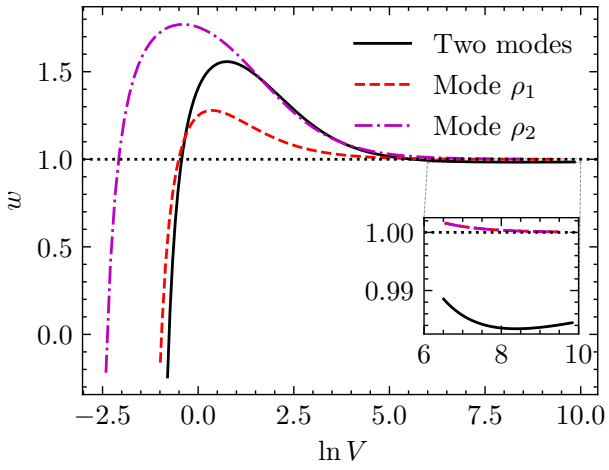

Figure 3.1: The behaviour of w for different modes in the free case. Black solid line considers contributions from both ρ_1 and ρ_2. Red dashed line shows the evolution of w of mode ρ_1, while magenta dash-dotted line shows ρ_2 case. For the convenience we also plotted the constant $w = 1$ using black dotted line. In the little box we showed the finer structure at large volume. We see that $w < 1$ in the two modes case, while $w > 1$ in both the single mode case ρ_1 and ρ_2. At large volume the value of w for ρ_1 and ρ_2 are so close that they can't be distinguished from each other in the plot. Parameters are $V_1 = 1/3, m_1^2 = 3,\ E_1 = 5,\ Q_1^2 = 9, V_2 = 1/2,\ m_2^2 = 2,\ E_2 = 9,\ Q_2^2 = 2.25$.

3.3 Late time accelerated expansion

We now turn to the main focus of our analysis, i.e. the emergent cosmological dynamics of interacting multi-modes condensates at late times.

In the last section, we have seen that for a free condensate, the accelerated expansion only lasts for a short while after the bounce. As volume increases, the quantum gravity

condensate would then be descried by a FLRW universe filled with a single massless scalar field. For large condensate densities (and thus volume), however, we expect the interactions to be relevant.

We first discuss how to solve the equation of motion for each mode, at least approximately. Then we extract the asymptotic behaviour of the effective EoS w in the two-modes case, showing that it is possible for the phantom divide to be crossed, thus producing a phantom-like dark energy purely from quantum gravity effects. In contrast to the single mode case, moreover, the phantom crossing does not lead to a Big Rip singularity. Finally, we also show that it is possible to produce at late times a more involved, if maybe less phenomenologically interesting, combination of inflation-like and phantom-like evolution in our model.

3.3.1 Large ρ behaviour of the interacting condensate

With interactions being included, the equation (3.5) becomes much harder to solve, and in general the solution cannot be written in a close analytic form. Nevertheless, under our assumption that $|\mu_j| \ll |\lambda_j| \ll m_j^2$, the equation of motion can be solved piece-wisely. For simplicity, we first assume $\mu_j = 0$; then for $\lambda_j < 0$ and ρ_j is large, the equation (3.5) can be approximated as

$$\rho_j'(\phi) = \sqrt{\frac{-2\lambda_j}{n_j}}\rho(\phi_j)^{\frac{n_j}{2}}. \tag{3.16}$$

This equation is much easier to solve than the exact one. The solution has the form

$$\rho_j(\phi) = \left(\frac{2}{n_j-2}\sqrt{\frac{-2\lambda_j}{n_j}}\right)^{-\frac{2}{n_j-2}} \frac{1}{(\phi_{j\infty}-\phi)^{\frac{2}{n_j-2}}}, \tag{3.17}$$

where $\phi_{j\infty}$ is a constant of integration, determined by initial conditions. It's true that for each mode j, the module ρ_j will diverge when $\phi \to \phi_{j\infty}$, which will lead to a divergent volume as well. In other words, the total volume of our universe will diverge even at a finite relational time ϕ, which may indicate some kind of future singularity such as the Big Rip, where the volume diverges at a finite cosmic time t [117]. However, as we will discuss in section 3.3.3, in our case the volume divergence at finite relational time ϕ does not necessarily imply the existence of the Big Rip singularity. As one can see that the cosmic time t could be infinite, like the total volume, even when the relational clock ϕ takes finite value. Therefore, the divergence of volume still happens at the infinite cosmic time t, which has no problem at all. In fact, if we consider the fictitious field ψ with EoS equals to w, then for $n \leq 6$ its energy density ρ_ψ will remain finite for $V \to \infty$; see subsection 3.3.3 for more details.

The value of $\phi_{j\infty}$ in the approximate solution (3.17) can be fixed by matching the solution (3.17) with the free one (3.6). In general, for the matching to be meaningful, the

matching point[1] ρ_{j0} should be the one where solutions (3.6) and (3.17) are both expected to be valid. Here, we choose ρ_{j0} such that the 'mass' term equals to the interaction term around it,

$$m_j^2\rho_{j0}^2 = \frac{-2\lambda_j}{n_j}\rho_{j0}^{n_j}, \tag{3.18}$$

In other words, near ρ_{j0}, the two approximations we used, i.e., ignoring interactions in obtaining (3.6) while only keeping them in obtaining (3.17), to solve the dynamical equation reach their limit of validity. Solving equation (3.18) provides us the value ρ_{j0} of module of the condensate at the matching point

$$\rho_{j0} = \left(\frac{n_j m_j^2}{-2\lambda_j}\right)^{\frac{1}{n_j-2}}. \tag{3.19}$$

Assuming that the free solution (3.6) is valid up to ρ_{j0} for each individual j, then ϕ_{j0} can be determined by inverting equation (3.6), which gives

$$\phi_{j0} = \frac{1}{2m_j}\text{arccosh}\frac{E_j + m_j^2\rho_{j0}^2}{\sqrt{E_j^2 + m_j^2 Q_j^2}}. \tag{3.20}$$

Taking (ϕ_{j0}, ρ_{j0}) as an initial condition for the differential equation (3.16), inserting them into the solution (3.17), and noting the fact that $\text{arccosh}x \to \ln(2x)$ when $x \to \infty$, we can get an approximate value of the constant $\phi_{j\infty}$ as

$$\phi_{j\infty} = -\frac{\ln[-\lambda_j/(2m_j^2)]}{(n_j-2)m_j} + \frac{1}{2m_j}\ln\left[\frac{n_j^{\frac{2}{n_j-2}}(2m_j^2)}{\sqrt{E_j^2 + m_j^2 Q_j^2}}\right] - \frac{\ln 2 - 1}{m_j}\frac{2}{n_j-2}. \tag{3.21}$$

At this point, we need to emphasize that equation (3.21) is only an approximation, obtained by matching two approximate solutions (3.6) and (3.17), to the exact value of $\phi_{j\infty}$. More specifically, the matching condition (3.18) is only approximate and shouldn't be valid in a more accurate setting. In principle, the accuracy can be improved by a finer matching, in the sense that splitting the range of interest into more pieces, making suitable approximations to the exact equation (2.26) in each region, getting the approximate solutions, and matching them near each border of the splitting. The procedure is lengthy and not quite useful in our setting as it's hard to find a physical meaning for the matching points in such a finer splitting.

Fortunately, there is another way to improve our approximation. In fact, the accuracy of our approximate result (3.21) of $\phi_{j\infty}$ can be improved with the help of exact solutions in special cases. As showed in appendix A.3, for $n_j = 4$ the equation of motion (3.5) can be

[1] Don't confuse ρ_{j0} with ρ_{j_0}. The former refers initial value (indicates by 0) for mode ρ_j, while the latter indicates mode ρ_{j_0} with spin j_0. That's why in equation (3.19) the value of ρ_{j0} is determined by parameters of mode j instead of j_0 or $j0$.

solved using elliptic functions. Then using the fact that $|\lambda_j|$ is small, an expansion of $\phi_{j\infty}$ can also be obtained. By comparing with the result in (3.21), we see that an additional term $\frac{\ln 2 - 1}{m_j}\frac{2}{n_j - 2}$ should be added, and the corrected form of $\phi_{j\infty}$ becomes

$$\phi_{j\infty} = -\frac{\ln[-\lambda_j/(2m_j^2)]}{(n_j-2)m_j} + \frac{1}{2m_j}\ln\left[\frac{n_j^{\frac{2}{n_j-2}}(2m_j^2)}{\sqrt{E_j^2 + m_j^2 Q_j^2}}\right]. \tag{3.22}$$

One can check that when using the corrected value (3.22) of $\phi_{j\infty}$ in solution (3.17), the matching condition (3.18) is not valid any more, which is normal as the condition is an approximate one after all.

To see how well the correction (3.22) works, we can compare this form of $\phi_{j\infty}$ for a given mode j with its numerical value, obtained by solving the equation of motion (3.5) numerically and substituting a large ρ_j (here taken to be $\rho_j = 10^8$) into the solution. The result is shown in figure 3.2. We see that our formula also works for non-integer n_j and, despite various approximations, the result is quite accurate at the order of λ_j. For comparison, we also plot the original ϕ_∞, given by (3.21) without correction, which shows that the additional term indeed improves the accuracy of our result, especially for small n.

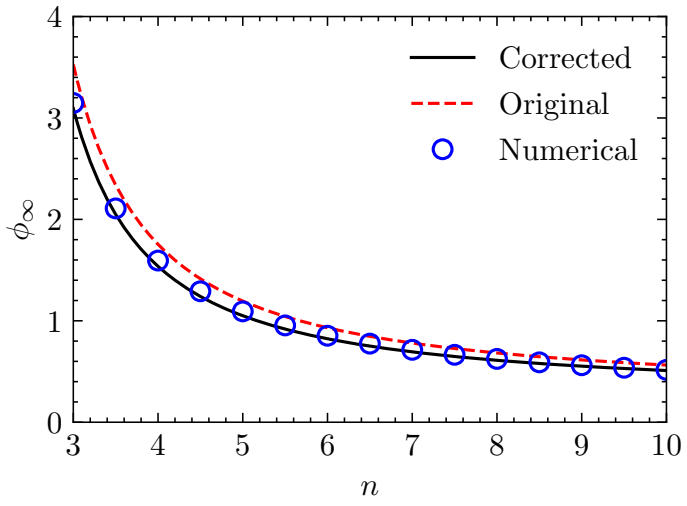

Figure 3.2: Asymptotic value ϕ_∞ for different n. Black solid line is obtained from equation (3.22), the corrected value of ϕ_∞. Red dashed line is the uncorrected value of ϕ_∞, given by equation (3.21). Blue circles show the numerical results obtained by solving the equation of motion (3.5) numerically (with $\mu_j = 0$) and set ρ to be large. Parameters are $m^2 = 2,\ E = 9,\ Q^2 = 2.25,\ \lambda = -0.1$.

It is clear from equation (3.22) that, for each mode j, the corresponding $\phi_{j\infty}$ is different. Note that $\rho_j(\phi)$ diverges when $\phi = \phi_{j\infty}$, hence the total volume $V = \sum_j V_j \rho_j^2$ will diverge

when ϕ reaches $\phi_\infty = \min\{\phi_{j\infty}\}$, the smallest one of the different $\phi_{j\infty}$'s corresponding to different modes. Moreover, before ϕ reaches ϕ_∞ but the total volume V is large enough, the mode with $\phi_{j\infty} = \phi_\infty$ will become dominate. In other words, the asymptotic behaviour of w is fixed by the single mode case, and the inclusion of other modes can only modify the way of how w can reach its asymptotic value, similar as we have observed before in the free case where the volume is small and interactions can be ignored.

To the leading order of λ_j, we have

$$\frac{\partial\phi_{j\infty}}{\partial m_j} = \frac{\ln[-\lambda_j/(2m_j^2)]}{(n_j-2)m_j^2}.$$

For small $|\lambda_j|$, this derivative is less than 0, thus large m_j will give small $\phi_{j\infty}$. Therefore, also with interactions the condensate dynamics tends to be dominated by the mode with largest m_j, which in general corresponds to small-j modes, as one can expect from the result of free case.

We emphasize that the solution (3.17) only works for negative couplings. In fact, if we add another interaction term $\mu_j > 0$, even under the assumption that $|\mu_j| \ll |\lambda_j|$, so that the contribution of μ_j to the value of $\phi_{j\infty}$ can be ignored, the behaviour of ρ_j at late times changes considerably. Explicitly, for $\mu_j > 0$, from equation (3.5) we see that, besides the bounce, $\rho_j'(\phi) = 0$ has an additional solution for some large ρ_j, determined by $\frac{2}{n_j}\lambda_j\rho_j^{n_j+2} = \frac{2}{n_j'}\mu_j\rho_j^{n_j'+2}$, which corresponds to the maximum value of ρ_j (and thus of the volume) at late times. After that, to ensure ρ_j' is real, we should require that ρ_j starts to decrease, and it leads to a periodic evolution of ρ_j and thus a cyclic universe (as in [45]). Since $|\mu_j| \ll |\lambda_j|$, we can take the value of ϕ approximately as $\phi \approx \phi_{j\infty}$ where ρ_j first reaches its maximum. Therefore, in the case with $\mu_j > 0$, instead of being the largest value that ϕ can reach (as in the single interaction case), $\phi_{j\infty}$ now should be regarded as a half-period in the evolution of ρ_j, indicating that ρ_j actually starts to decrease for $\phi > \phi_j$. On the other hand, for $\mu_j < 0$, ρ_j can keep growing until ϕ reaches $\phi_{j\infty}$ where ρ_j diverges.

We will see in section 3.3.4 how the combination of two modes with opposite sign of μ_j makes it possible for the effective EoS to cross the phantom divide $w = -1$.

3.3.2 Phantom crossing in the two-modes case

In this section we consider how the presence of two interacting modes, each with an individual contribution to the cosmological dynamics of the type we have illustrated above, can shape it in very interesting ways at late times.

For simplicity, we use $\rho_{1,2}$ to indicate ρ_{j_1,j_2} and similarly for other parameters. Although in previous sections we have seen that at sufficiently large volume there will be only one mode dominating also in the interacting case, we will see that the inclusion of a second mode does change the behaviour of the effective EoS w, and in particular how the asymptotic value is approached, which is of direct cosmological relevance.

To begin with, we consider the case in which two modes both have a single interaction term, i.e., we set $\mu_1 = \mu_2 = 0$. Since the coupling λ_1 and λ_2 are small, w will be dominated

by the free part of condensate at small volume, and it will approach $w = 1$ from below as volume grows. This is the needed FLRW universe of the standard cosmological model, reached after the phase close to the big bang, here replaced by a quantum bounce. When the volume becomes larger further, the interaction term for both modes increasingly contributes to the condensate dynamics, until, for large enough values of ρ_j (and thus of the volume), w will be dominated by the interaction terms instead. If further assuming that $n_1 = n_2 = n$, and keeping only interaction terms in the expression for w, we will see that w only depends on the ratio $r = \rho_2/\rho_1$ (as it was the case also in the free one we have discussed in section 3.2.3), and we have

$$\begin{aligned} w &= 3 - \frac{(2+n)(V_1 + r^2 V_2)(V_1\lambda_1 + r^n V_2 \lambda_2)}{2\left(V_1^2\lambda_1 + r^{2+n}V_2^2\lambda_2 - 2r^{1+\frac{n}{2}}V_1V_2\sqrt{\lambda_1\lambda_2}\right)} \\ &= 2 - \frac{n}{2} - \left(\frac{n}{2}+1\right)\frac{V_1V_2r^2\left(r^{n/2-1} - \sqrt{\lambda_1/\lambda_2}\right)^2}{\left(\sqrt{\lambda_1/\lambda_2}V_1 + V_2 r^{n/2+1}\right)^2}. \end{aligned} \tag{3.23}$$

Since the parameters are all real and both couplings λ_1 and λ_2 are assumed to be negative, we see that $w \leq 2 - \frac{n}{2}$. Recall that when the volume is large, one of the two modes will dominate over the other, and then we have $r \to 0$ or $r \to \infty$. In either case w will approach $2 - \frac{n}{2}$ from below, in contrast with the single mode case discussed in section 3.1.

There is a special case where $r = \left(\frac{\lambda_1}{\lambda_2}\right)^{\frac{1}{n-2}}$, for which $w = 2 - \frac{n}{2}$ is also a constant within the approximation we have made. From our solution (3.17) for each mode at large volume, we see that this indeed happens when $\phi_{1\infty} = \phi_{2\infty}$. In fact, when $\rho_2 = r\rho_1$ is proportional to ρ_1, we have $V = V_1\rho_1^2 + V_2\rho_2^2 = (V_1 + r^2V_2)\rho_1^2$, which is the same as the single mode case with a modified volume of the building blocks, $\tilde{V}_1 = V_1 + r^2V_2$. And therefore the EoS is the same as in the single mode case, which indeed approaches the asymptotic value from above.

In figure 3.3 we plot the different behaviour of w in the cases $\phi_{1\infty} < \phi_{2\infty}$ and $\phi_{1\infty} = \phi_{2\infty}$ using numerical solutions of equation of motion (2.25) in the single interaction case $\mu_j = 0$.

At small volume, the evolution is dominated by the free parameters, and the two case are identical. At a larger volume but when ϕ is still away from $\phi_{1\infty}$, the ratio $r = \rho_2(\phi)/\rho_1(\phi)$ changes slowly, and the behaviour of w in the two cases is still almost identical. As the volume grows further, ϕ approaches to $\phi_{1\infty}$, then in the case $\phi_{1\infty} < \phi_{2\infty}$, ρ_1 tends to ∞ and grows much fast than ρ_2, leads to $r \to 0$, and w approaches to the phantom divide $w = -1$ from below. In the same regime, but for $\phi_{1\infty} = \phi_{2\infty}$, we have $r = (\lambda_1/\lambda_2)^{\frac{1}{4}}$, so the last term in (3.23) vanishes[1], and w will approach $w = -1$ from above, as in the single mode case.

Now we consider the case $n = 6$ and assume that $\phi_{1\infty} < \phi_{2\infty}$. Then at large volume the first mode will dominate and $r \to 0$. Expanding w in equation (3.23) with respect to

[1] To plot the figure we have chosen $n = 6$ for its cosmological relevancies.

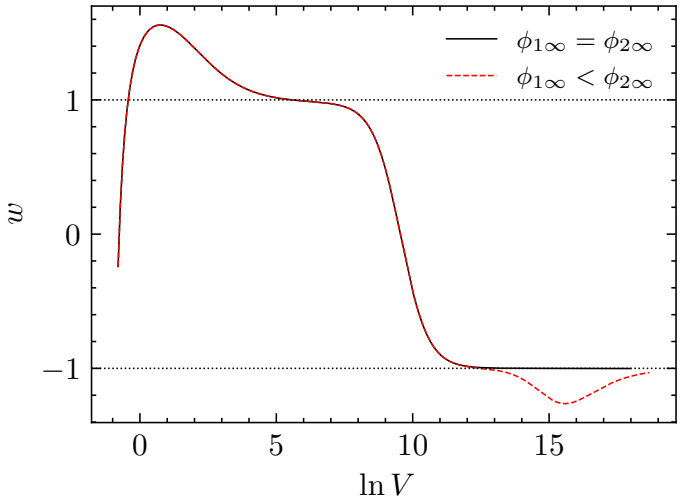

Figure 3.3: The behaviour of w in the two modes case, where both modes have only one interaction term. Black solid line shows the case where $\phi_{1\infty} < \phi_{2\infty}$, while for red dashed line we have $\phi_{1\infty} = \phi_{2\infty}$. Two black dotted lines show $w = 1$ and the phantom divide $w = -1$, respectively. Parameters are same as in figure 3.1 with additional ones are $\lambda_1 = -10^{-8}$, $\mu_1 = 0$, $\mu_2 = 0$, $n_1 = n_2 = 6$ and $\lambda_2 = -9.5 \times 10^{-8}$ for $\phi_{1\infty} < \phi_{2\infty}$, $\lambda_2 = -9.5725 \times 10^{-8}$ for $\phi_{1\infty} = \phi_{2\infty}$.

r gives simply

$$w = -1 - \frac{4V_2}{V_1} r^2 = -1 - \frac{4V_2}{V_1} \frac{\rho_2(\phi)^2}{\rho_1(\phi)^2}.$$

Therefore, when $n = 6$ the phantom divide $w = -1$ can be crossed at large volume and the corresponding effective field ψ behaves just like a phantom energy, whose energy density increases as the volume of universe grows.

This is our main result, showing how a phantom-like dark energy dynamics at late times can be produced, under rather general conditions (albeit in a simplified model, and of course in a specific regime of the full theory) purely from quantum gravity effects, i.e. as an effective description of the underlying quantum dynamics of spacetime constituents.

One may then worry about whether this effective phantom energy, like in many field theoretic models, leads to a Big Rip singularity at later times also in our model. We will discuss this issue in subsection 3.3.3, showing that the effective energy density ρ_ψ, *defined* from the EoS w, remains bounded in our model, tending towards to a finite value at asymptotically large volumes. To see this, we need some further approximation for the EoS w, which we anticipate below.

Since $\phi_{1\infty} < \phi_{2\infty}$, and for large volume we have $\phi \to \phi_{1\infty}$, we see that ρ_2 is nearly a

constant given by $\rho_2(\phi_{1\infty})$. Using the solution (3.17) for $n = 6$, we get

$$\rho_2(\phi_{1\infty}) = \left(\frac{1}{2}\sqrt{\frac{-\lambda_2}{3}}\right)^{-\frac{1}{2}} \frac{1}{(\phi_{2\infty} - \phi_{1\infty})^{\frac{1}{2}}}.$$

Furthermore, when $\phi \to \phi_{1\infty}$ the first mode ρ_1 would be much larger than ρ_2, hence in computing the total volume we can ignore ρ_2 and let $V = V_1\rho_1^2$. Inserting this approximate expression back in the expression for w, we get

$$w = -1 - \frac{b}{V}, \tag{3.24}$$

where $b = 4V_2\rho_2^2(\phi_{1\infty})$ is a constant. Notice again that $b > 0$, thus we have $w < -1$, and the phantom divide $w = -1$ had to be crossed somewhere.

We will see in chapter 4, as shown by figure 4.1, that our approximation (3.24) becomes accurate quickly after w passes its minimum and starts to increasing again, hence can be used to extract some cosmological observables, such as the changes of current Hubble parameter H_0 due to the appearance of the phantom phase (see section 4.2).

3.3.3 The Big Rip singularity

As we have emphasized, and in the presence of interactions, we can see from the solution (3.17) that, ρ_j becomes singular for $\phi = \phi_{j\infty}$, which means that the volume will also diverge at finite relational time $\phi_\infty = \min\{\phi_{j\infty}\}$. Now we are going to explain why this does not necessarily lead to a Big Rip singularity, which is usually expected to exist for a phantom like evolution, especially for constant EoS with $w < -1$. We will see that such singularities can be avoided in our setting due to the fact that w is dynamical and approaches to -1 very fast.

Let's consider the fictitious field ψ we introduced whose EoS equals to w given by equation (3.24). Its energy density ρ_ψ, *defined* by the EoS itself, satisfies the conservation equation (3.2). Substituting the approximated EoS (3.24) into equation (3.2), we get

$$\frac{\mathrm{d}\rho_\psi}{\mathrm{d}V} - \frac{b\rho_\psi}{V^2} = 0.$$

This equation can be solved in a close form

$$\rho_\psi = \rho_{\psi 0}\mathrm{e}^{-\frac{b}{V}} \approx \rho_{\psi 0} - \frac{\rho_{\psi 0}b}{V}, \tag{3.25}$$

where $\rho_{\psi 0}$ is a constant of integration, representing the asymptotic value of ρ_ψ when volume approaches to infinity.

Therefore, we see that in our model the energy density has a constant asymptotic value, which has the same effect as a cosmological constant, instead of blowing up when the volume is large. From this point of view, our model leads to a de Sitter spacetime asymptotically,

with no Big Rip-like singularities [118]. In fact, our model effectively belongs to the class of models considered in [128], where the Big Rip singularity is avoided even in presence of phantom matter by assuming that ρ_ψ can be obtained as a constant part plus some matter with negative energy density. Exactly this type of scenario is reproduced from the fundamental quantum gravity dynamics.

From the results above, one may suspect that the future singularities won't occur in the phantom scenario as long as the EoS $w \to -1$ for large volume, or putting it differently, the de Sitter spacetime with finite scalar curvature can be reached asymptotically if w has -1 as its limit. But we need to stress that it's *not* the case. The truth is, in order to obtain a de Sitter spacetime asymptotically, it's only necessary but not sufficient to require that w approaches to the phantom divide $w = -1$ at large volume. We need also to demand that w approaches to $w = -1$ fast enough, as it happens naturally in our case without further adjustments on the formalism or parameters.

To see that it's not trivial in avoiding the Big Rip-like singularities, we can assume that, when volume V is larger than some given V_0, the EoS is given approximately by

$$w = -1 - \frac{b}{\ln(V/V_0)},$$

which approaches to -1 as well for large V. Substituting this into the conservation equation (3.2), the evolution of the phantom energy density ρ_ψ now reads

$$\rho_\psi = \rho_{\psi 0} \left[\ln\left(\frac{V}{V_0}\right)\right]^b,$$

where $\rho_{\psi 0}$ is again a constant, now given by the energy density at volume $V = \mathrm{e}V_0$. In this case ρ_ψ diverges when $V \to \infty$, and the asymptotic de Sitter spacetime can't be obtained. Furthermore, as we discussed in subsection 3.1.2, when the energy density is large enough all bound systems in the universe will be destroyed at a finite volume and hence such kind of phantom evolution should be avoided [118].

3.3.4 Combining inflation-like and phantom-like acceleration

We have seen that we can reproduce naturally the late time acceleration behaviour of our observed universe by considering two condensate modes, for which has only one interaction term respectively. We also have reasons to expect that the late-time cosmological dynamics is dominated by a single interaction (that of the highest order, if more than one is allowed with comparable weights by the parameters of the model). Thus, we can claim some degree of generality for our main results.

However, it is interesting to ask how the late-time dynamics, after a FLRW phase, is affected by the presence of multiple interactions, for each mode. This could be relevant for further cosmological applications, but it also has purely theoretical motivations. For example, although $n = 6$ interactions are needed to reproduce phantom crossing, most quantum geometric GFT models include $n = 5$ interactions because they come from the simplicial construction of their (lattice gravity and spin foam) amplitudes [29].

So, we conclude our present analysis by considering briefly the case in which two spin modes both have two interactions, with the new couplings being μ_1 and μ_2.

When both μ_1 and μ_2 are less than 0, both modes would produce a divergent condensate density eventually and lead to a similar result as the previous single interaction case. On the other hand, when both μ_1 and μ_2 are positive, there would be a turning point for the condensate density for each mode, after which ρ_j starts to decrease, and the corresponding universe would become cyclic, as in the single mode case. The more interesting case, therefore, is when μ_1 and μ_2 have different signs.

We assume then that $\mu_1 < 0$ while $\mu_2 > 0$. As shown in [45], the mode ρ_2 alone can lead to a long-lasting inflationary-like phase. Now, with an additional mode ρ_1, we can have both the late time phantom-like acceleration and an inflationary-like phase before it.

With two interactions, we have three different cases according to the relative magnitude between $\phi_{1\infty}$ and $\phi_{2\infty}$. Since $\mu_2 > 0$, $\phi_{2\infty}$ would be the half-period of the ρ_2 mode rather than the maximum value that ϕ can reach as $\rho_2 \to \infty$. For $\phi_{1\infty} < \phi_{2\infty}$, the ρ_1 mode would increase faster than the ρ_2 mode, and dominates before inflation can end, leading to a similar dynamics as in the single interaction case. On the other hand, for $\phi_{1\infty} > \phi_{2\infty}$, ρ_2 will reach its maximum value before ρ_1 diverges. For large volume, but with $\phi < \phi_{2\infty}$, the ρ_2 mode would dominate and hence inflation can end. But since near $\rho_{2\infty}$, ρ_2 decreases very quickly, the total volume will also decrease for a while and then increase again when the ρ_1 mode takes over. Let us look at the resulting dynamics in more detail, considering the case where $\phi_{1\infty} = \phi_{2\infty}$ and assuming $n_1 = n_2 = 5,\ n_1' = n_2' = 6$.

Since the absolute value of the couplings $|\mu_{1,2}|$ is much less than $|\lambda_{1,2}|$, there would still be a region where the λ interaction terms dominate. Furthermore, we can also ignore the influence of μ terms on the value of $\phi_{j\infty}$, and the solution of each mode can still be given by equation (3.17) in this regime, with $\phi_{1\infty} = \phi_{2\infty}$. Then, as we discussed, in such case the ratio ρ_1/ρ_2 becomes a constant and the contribution from two modes cancels, leaves a constant EoS $w = -\dfrac{1}{2}$ in this region, corresponding to an inflationary-like phase.

As the volume increases, the μ terms become important. In this region, the EoS w will increase first, and inflation will end after $w > -1/3$. Afterwards, w decreases again to cross the phantom divide $w = -1$. At very large volume, the EoS can still be approximated by $w = -1 - b/V$, in the same form of (3.24), only this time with the constant b should be given by $b = 4V_2\rho_2^2(\phi_{2\infty}) = \dfrac{144}{25}\dfrac{V_2\lambda_2^2}{\mu_2^2}$, which can be determined with only the parameters from the second mode.

We compared the behaviour of w in two modes case and single mode case in figure 3.4. What needs to be stressed is that, although the inflationary phase can end, the exit is not as graceful as one would expect in the standard cosmology models, in the sense that there is no long-lasting Friedmann phase after the end of inflation in our case. As indicates by figure 3.4, w drops fast again after the end of inflation to enter the phantom phase. Therefore, our combination of inflationary and phantom phases is not as successful as one would expect, but nevertheless the result provides a template of how to make the combination possible in GFT condensate cosmology.

As in the single mode case, table 3.2 summarizes the effects of parameters on the evolution behaviour in the two modes case. As we have explained, the inflationary phase should be accompanied by a proper exit, hence such phase won't occur with only a single interaction term in each mode. Since the case of positive λ is already discussed in the single mode case, here we only consider the case $\lambda_1 < 0$ and $\lambda_2 < 0$. Furthermore, for simplicity we set $n_1 = n_2 = n$ and $n_1' = n_2' = n'$.

		Inflationary phase	Cyclic behaviour	Late time acceleration	Phantom crossing	Big Rip
Single interaction	$\phi_{1\infty} = \phi_{2\infty}$			$n \geq 5$	$n > 6$	$n > 6$
	$\phi_{1\infty} < \phi_{2\infty}$			$n \geq 5$	$n \geq 6$	$n > 6$
Two interactions	$\mu_1 > 0,\ \mu_2 > 0$	$n \geq 5$	✓			
	$\mu_1 < 0,\ \mu_2 < 0$			$n' \geq 5$	$n' \geq 6$	$n' > 6$
	$\mu_1 < 0,\ \mu_2 > 0$	$\phi_{1\infty} = \phi_{2\infty},\ n \geq 5$		$n' \geq 5$	$n' \geq 6$	$n' > 6$

Table 3.2: The influence of parameters on the cosmological evolution in two modes case. The meaning of symbols is the same as in table 3.1. There is no need to include FLRW phase, as it will always occur for the case considered in the current table.

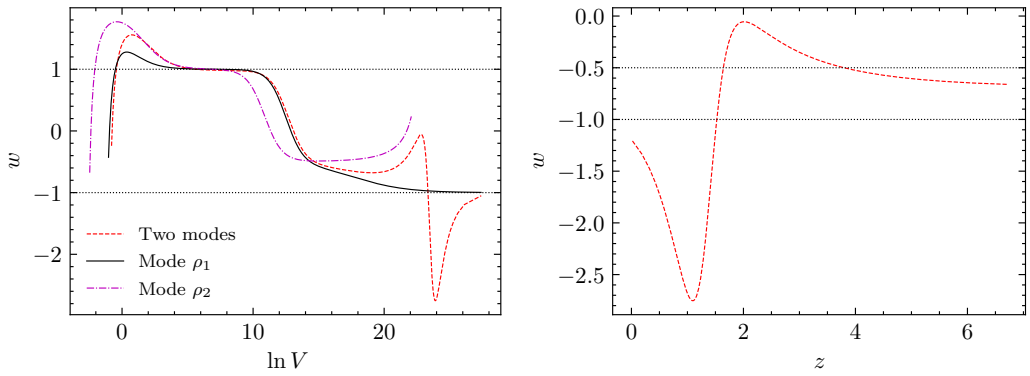

(a) Behaviour of w in the interacting case (b) w versus redshift in two modes case

Figure 3.4: The behaviour of w in the interacting case. As in figure 3.1, the black solid line shows w in two modes case, red dashed line shows single mode case with ρ_1, and magenta dash-dotted line shows single mode case with ρ_2. At large volume w for ρ_1 and ρ_2 differs significantly as the couplings μ_1 and μ_2 have different signs. The two black dotted lines represent $w = -0.5$ and $w = -1$ respectively. In 3.4(b) we plot the behaviour of w with respect to redshift z in the two modes case. The redshift is defined by $z = a_0/a - 1$, where scale factor $a = V^{1/3}$ and a_0 is its current value. Parameters are same as in figure 3.1 with additional ones are given by $\lambda_1 = -10^{-8},\ \mu_1 = -10^{-12},\ \lambda_2 = -1.4757 \times 10^{-7},\ \mu_2 = 1.2 \times 10^{-12}$ and $n_1 = n_2 = 5,\ n_1' = n_2' = 6$.

3.4 Summary

In this chapter, we have analysed the emergent cosmological dynamics corresponding to the mean field hydrodynamics of quantum gravity condensates, within the (tensorial) group field theory formalism. The main focus of the current work is the behaviour of the effective equation of state w when there are more than one condensate modes in the contribution to the cosmological evolution, which is an extension of previous works in the context of GFT condensate cosmology, where one usually considers only a single mode.

We argued that, the effective EoS is suitable for the study of cosmological evolution in the context of GFT condensate, and rewritten several previous results in terms of w. Then following the evolution of w, we first considered the free case in the GFT condensate dynamics, which corresponds to the early time in the universe evolution where the volume is small, hence the interaction terms in the effective GFT action can be ignored. The inclusion of multiple modes into consideration doesn't change much of the previous results, i.e., the big bang singularity can still be resolved by the bounce, followed by a short-lasting period of acceleration, and asymptotically the Friedmann phase will emerge, where $w = 1$ corresponds to the free massless scalar fields ϕ. What changes is the way w approaches to 1, yet this is not quite important as $w = 1$ is not a significant value in cosmology, partially because such a behaviour can be explained by the ϕ field without going beyond ordinary QFT. More importantly, our result can be viewed as a consistency check of the GFT condensate cosmology formalism, since near the bounce the total volume of our universe is small, there is no reason to expect that one mode can dominate over others, and we need to take all the modes into consideration. We have shown that, qualitatively the conclusions obtained from the analysis in the single mode case are still valid, which, on the other hand, shown the necessity of interactions in accounting the late time evolution of our universe.

After including interactions into the picture, the situation becomes more interesting. The main reason is that now the asymptotic value of w can be tuned by changing the order n of the interaction terms. In particular, when $n = 6$ we have $w = -1$ asymptotically, corresponds to the cosmological constant, which is certainly more interesting than the $w = 1$ case. To see the effects of GFT interactions to the evolution of w, especially in the two-modes case, we first solve the equation of motion (2.26) of the GFT condensate approximately in the large volume limit, from which we can see that for each mode j the solution diverges for some $\phi = \phi_{j\infty}$. Then we substitute the solutions (3.17) of the two modes under consideration to the definition (3.1) of the effective EoS for GFT cosmology to arrive at the result (3.23), which is less than -1 for $n = 6$, allowing us to obtain a phantom phase. The expression (3.23) can be further simplified by noting that w only depend on the ratio $r = \rho_2/\rho_1$, which towards to 0 when volume is large if $\phi_{1\infty} < \phi_{2\infty}$, therefore, the result can be expanded respect to r, which results in the simple expression (3.24). Since in our context of GFT condensate cosmology, the EoS we obtained approaches to $w = -1$ fast enough, one can show that the Big Rip-like singularities can be avoided. Finally, we showed that it's possible in our formalism to deal with inflationary and phantom phases simultaneously without the need of inflaton nor phantom dark energy.

It's fair to say that our results obtained in this chapter are mainly qualitative, for

example we have only shown the existence of the phantom phase or the non-existence of the future singularities, without paying much attention to the details of the phantom behaviour, such as how the phantom crossing close to us or what is the minimum value of w[1]. And we haven't considered the possible observational consequences of our results. These issues will be dealt with in the next chapter, where we will identify the minimum point of w, explain why the phantom crossing need to happen recently, and how the inclusion of the second mode will change the observed values of some quantity, such as the current value H_0 of the Hubble parameter.

[1] Since in our model w changes from values close to 1 to the asymptotic value -1, from below, there has to be a point where w reaches its minimum. As can be seen from figure 3.3.

Chapter 4

Observational consequences of the phantom phase

In the last chapter, we have seen that GFT interactions and the number of condensate modes that being taken into account are both relevant for the late time accelerating expansion of our universe. The extraction of the effective EoS from our GFT condensate cosmology model makes it easier to track the cosmological evolution and to compare the results with those obtained in other cosmological models. In particular, we have shown that a late time phantom phase, followed by an asymptotic de Sitter phase, exists in our GFT cosmology model.

As we have mentioned before, these results, although quite informative in extracting cosmological consequences of the quantum gravity effects from our GFT formalism, are only qualitative, and don't have observational relevance directly. In this chapter, we will try to fill this gap between our results and observations, by extracting approximately the minimum value of w, identifying cosmological constant in the de Sitter phase using GFT parameters, and showing that how the inclusion of a second condensate mode into consideration will change the current Hubble parameter H_0, compared to the single mode case. What's important is that the current value H_0 of the Hubble parameter can be observed directly. The last result indicates that quantum gravity effects might be helpful in alleviating the H_0 tension [60, 61], hence provides a window of testing quantum gravity theories using cosmological observations [3].

4.1 Behaviour of the effective equation of state

We have argued in section 3.3.1 that when ρ is large, we can ignore E_j, Q_j and m_j terms in the equation of motion (2.26), which provides us the approximated equation (3.16). Furthermore, for the cosmological relevance, we need a cosmological constant in the de Sitter phase, corresponds to $w = -1$, which requires interaction terms of order 6.

Therefore, by setting $n = 6$ in the solution (3.17) we get

$$\rho_j(\phi) = \frac{3^{1/4}}{\sqrt{2\sqrt{-\lambda_j}\,(\phi_{j\infty} - \phi)}}, \tag{4.1}$$

with $\phi_{j\infty}$ is a constant depend on parameters of each mode. It's worth emphasizing again that when the volume is very large, the mode with smallest $\phi_{j\infty}$ will dominate, and for $n = 6$ we have $w = -1$, corresponds to the asymptotic de Sitter spacetime. The appearance of other modes will modify the way we approach such an asymptotic regime, in particular, as we have discussed in section 3.3, with two-modes a phantom phase will emerge before the de Sitter spacetime shows up. More specifically, tracking the evolution of the EoS w (from the red dashed line of figure 3.3, for example), we see that near the end of the Friedmann phase, w decreases quickly from values close to 1 to values less than -1, and then increases again to reach the asymptotic value -1. Therefore, there have to be a point where $w = -1$ exactly, i.e., the point of phantom crossing, as well as a point where w reaches its minimum. We will see in the following that these two points are actually close to each other, and the latter can be given in a close analytical form in our formalism, at least approximately.

4.1.1 Location of phantom crossing

At the first sight, one may suspect that to get the position of phantom crossing we just need to substitute the solution (4.1) of ρ_j into the total volume (2.27), and then into the effective EoS (3.1) to get the relation $w = w(\phi)$. From which we can solve the equation $w(\phi) = -1$ to obtain the position where the phantom divide $w = -1$ is crossed. A moment of reflection shows that it's not as simple as one originally expects. In obtaining solutions in the form of (4.1) we have ignored free parameters like E_j, Q_j and m_j, therefore, when substituting them into w, we can only get an effective EoS depends only on the interaction couplings, or in other words, what we can obtain is in the form of (3.23). The problem is, for $n = 6$ the approximation (3.23) always gives $w < -1$ for any ρ_1 and ρ_2. Therefore, to get the position of phantom crossing, one has to restore, at least partially, the contributions from free parameters to the EoS, which requires us to solve the equation of motion (2.26) without ignoring the free parameters. But as we have mentioned before, the task is formidable at current stage[1].

One can work around this by noting that the phantom crossing has to occur between the end of Friedman phase (where $w \simeq 1$) and the point where w reaches its minimal value. Furthermore, as we can see below, that the latter two positions are actually close to each other, hence we can take the position of phantom crossing as the point where Friedman phase ends or w reaches its minimal value.

Minimal value of w. The alternative way proposed above depends on the assumption that the approximation (3.23) still has minimum value as the exact EoS, or putting it

[1] And that's the reason why we are looking approximate solutions of the form (3.17) in the first place.

differently, we assumed that the equation $w'(\phi) = 0$ respect to ϕ indeed has real positive roots even when we ignore the free parameters. This assumption can be verified if we can find the required root explicitly. In fact, taking derivative respect to relational time ϕ on both sides of effective EoS (3.1), we obtain

$$w' = -\frac{2\left[(V')^2 V'' - 2V(V'')^2 + VV'V'''\right]}{(V')^3}. \tag{4.2}$$

In the two modes case, the total volume (2.27) reduces to

$$V(\phi) = V_1\rho_1^2(\phi) + V_2\rho_2^2(\phi).$$

When the volume is large, substituting the total volume and the corresponding solutions (4.1) into the derivative (4.2) of EoS, we obtain

$$\begin{aligned} w' = &\frac{4V_1V_2(\lambda_1\lambda_2)^{\frac{3}{2}}(\phi_{2\infty}-\phi_{1\infty})^2}{\left[V_2\lambda_1\sqrt{-\lambda_2}(\phi_{1\infty}-\phi)^2 + V_1\sqrt{-\lambda_1}\lambda_2(\phi_{2\infty}-\phi)^2\right]^3} \\ &\times\left[V_2\lambda_1\sqrt{-\lambda_2}(\phi_{1\infty}-\phi)^2(2\phi+\phi_{1\infty}-3\phi_{2\infty}) + V_1\sqrt{-\lambda_1}\lambda_2(\phi_{2\infty}-\phi)^2(2\phi-3\phi_{1\infty}+\phi_{2\infty})\right]. \end{aligned} \tag{4.3}$$

We see that if $\phi_{1\infty} = \phi_{2\infty}$ then $w' = 0$ as we expected from equation (3.23), which gives constant value in this case. For $\phi_{1\infty} \neq \phi_{2\infty}$, demanding $w' = 0$ is equivalent to the requirement of the vanishing of the second line in the right hand side of equation (4.3), which provides us a cubic equation respect to ϕ

$$V_2\lambda_1\sqrt{-\lambda_2}(\phi_{1\infty}-\phi)^2(2\phi+\phi_{1\infty}-3\phi_{2\infty}) + V_1\sqrt{-\lambda_1}\lambda_2(\phi_{2\infty}-\phi)^2(2\phi-3\phi_{1\infty}+\phi_{2\infty}) = 0. \tag{4.4}$$

In principle, this equation can be solved exactly, but as one can imagine that the solution is lengthy as usual for cubic equations, and such a complex form might not be quite useful. So for now it would be sufficient to consider approximate solutions. In fact, at the minima the value of ϕ is close to $\phi_{1\infty}$, so we can assume that $\phi = \phi_{1\infty} - \delta$ and then expand w' with respect to δ. To the first order, we have

$$w' = \frac{4V_2\lambda_1(6\delta+\phi_{1\infty}-\phi_{2\infty})}{V_1\sqrt{\lambda_1\lambda_2}(\phi_{2\infty}-\phi_{1\infty})^2}. \tag{4.5}$$

Solving $w' = 0$ gives

$$\delta = \frac{\phi_{2\infty}-\phi_{1\infty}}{6}, \tag{4.6}$$

which results in

$$V_{\min,w} = -\frac{3\sqrt{3}\left(V_2\lambda_1\sqrt{-\lambda_2} + 7V_1\sqrt{-\lambda_1}\lambda_2\right)}{7\lambda_1\lambda_2\left(\phi_{2\infty} - \phi_{1\infty}\right)} = \frac{3\sqrt{3}}{7(\phi_{2\infty} - \phi_{1\infty})}\left(\frac{V_2}{\sqrt{-\lambda_2}} + \frac{7V_1}{\sqrt{-\lambda_1}}\right), \tag{4.7}$$

$$w_{\min} = \frac{V_2^2\lambda_1 + 2401V_1^2\lambda_2 - 1106V_1V_2\sqrt{\lambda_1\lambda_2}}{\left(V_2\sqrt{-\lambda_1} + 49V_1\sqrt{-\lambda_2}\right)^2} = -1 - \frac{1008V_1V_2\sqrt{\lambda_1\lambda_2}}{\left(V_2\sqrt{-\lambda_1} + 49V_1\sqrt{-\lambda_2}\right)^2}. \tag{4.8}$$

Note that $V_{\min,w}$ is of the same order as $1/\sqrt{\lambda_j}$, around which the mass term $m_j^2\rho_j^2$ and interaction term $\lambda_j\rho_j^6/3$ in the equation of motion (2.28) are of the same order, i.e., equation (3.18) is valid approximately, which indicates the end of the Friedman phase. Furthermore, the phantom crossing, where the EoS w starts to become less than -1, should happen before w reaches its minimum. And since $V_{\min,w}$ is close to the end of Friedman phase, we see that the universe becomes phantom like soon after Friedman phase ends, and w will reach its minimum soon after phantom crossing.

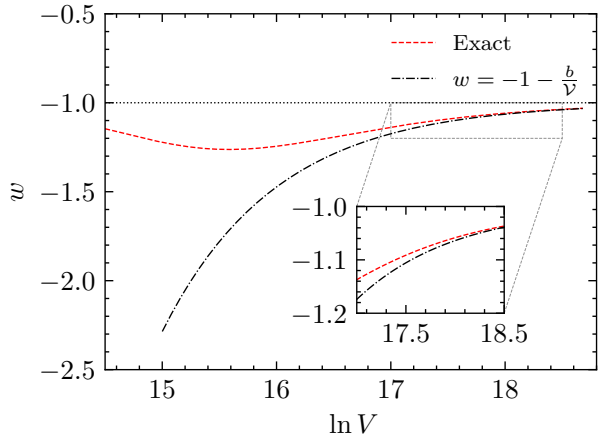

Figure 4.1: The comparison between the exact value and approximate value of EoS w. Red dashed line shows the exact numerical value of w, being part of the same line in figure 3.3 in the region specified here, while the black dash-dotted line shows the approximation (3.24). Parameters are the same as in figure 3.3.

Beyond the minimum. On the other hand, as can be seen from figure 4.1, the approximation (3.24) becomes accurate quickly after w reaches its minimum value and starts to increase. In fact, we can substitute $V_{\min,w}$ into our approximation (3.24), and obtain

$$w = -1 - \frac{56V_2\sqrt{-\lambda_1}}{3V_2\sqrt{-\lambda_1} + 21V_1\sqrt{-\lambda_2}} = -1 - \frac{56V_1V_2\sqrt{\lambda_1\lambda_2}}{3V_1V_2\sqrt{\lambda_1\lambda_2} - 21V_1^2\lambda_2}. \tag{4.9}$$

This is close to the minimal value (4.8), which means that w can be approximated using (3.24) soon after w passes its minimum value. Furthermore, the approximation (3.24) approaches to -1 quickly, which means that, in the phantom phase, w can only deviate from -1 significantly near its minimum.

We conclude that after phantom crossing, w will approach to its asymptotically value -1 quickly in our model. Therefore, if we are experiencing a phantom phase, the phantom crossing must happen recently. We emphasize that this is not trivial, as our model unifies two observational facts:

1. the phantom crossing happens recently, and

2. w deviates from -1 notably.

Our claim is that these two facts are related in our model, i.e., the reason why w may have a notable deviation from -1 is that phantom happens recently with a low red shift and vice verse.

Furthermore, since the phantom crossing only happens recently, the evolution of EoS w in the two modes case can be viewed as a slight modification of the single mode one at late times. Then the cosmological quantities, such as H_0, the current Hubble parameter, will also be modified slightly [66]. We will see in section 4.2 that in the presence of the phantom phase, H_0 will increase, which shed some light in alleviating the H_0 tension based on quantum gravity effects.

4.1.2 Explicit expression of cosmological constant as function of GFT quantities

Other than estimating the position of phantom crossing, our GFT model also allows us to identify the cosmological constant using microscopic parameters of GFT. In fact, note that long after the phantom crossing, we will enter the de Sitter regime asymptotically, at which the volume of the universe is very large, the interaction term in GFT will become dominant. In such region we can ignore the contributions from other terms and only keep interactions in the equation of motion (2.28). Furthermore, we have seen in chapter 3 that in such a region only a single mode dominates [50], where the canonical momentum π_ϕ of the relational time ϕ should be of the form [42]

$$\pi_\phi = Q_1.$$

On the other hand, for the free massless scalar field ϕ in a FLRW spacetime, the canonical momentum should have the form $\pi_\phi = V\dot{\phi}$ [45], which gives $\dot{\phi} = Q_1/V$. Substituting $\dot{\phi}$ into the relation (A.2) between Hubble parameter H and $\dot{\phi}$, we get the relation between H and the ratio V'/V in the single mode case [45, 50]

$$H = \frac{Q_1}{3}\frac{V'}{V}. \tag{4.10}$$

Therefore, in the asymptotic de Sitter regime we obtain

$$H^2 = \frac{8}{9}Q_1^2\left(\frac{-\lambda_1}{6V_1^2}\right) = \frac{1}{3}\left[\frac{4Q_1^2}{3V_1^2}(-\lambda_1)\right]. \tag{4.11}$$

Comparing this equation with the ΛCDM model at late time, we see that the cosmological constant is determined by the microscopic parameters of GFT model [45]

$$\Lambda = \frac{4Q_1^2}{3V_1^2}(-\lambda_1). \tag{4.12}$$

We would like to stress the following points of relation (4.12) between the cosmological constant Λ and GFT parameters

- Λ is determined by the parameters of a single mode despite that two modes are considered; this could have been expected since the asymptotic de Sitter regime is determined by mode ρ_1, after all;
- For a non-vanishing Λ, we see that $Q_1 \neq 0$, and hence the volume can never reach zero, which implying a bounce [42]. Although there is no evidence that Q_j's should be non-vanishing [49][1], we see now the cosmological constant would provide such a requirement that the Q_1 can't be zero and hence lead to a bounce [42], which resolves the Big Bang singularity. In other words, besides the CMB, which indicates that that our universe was in a hot dense state in the far past, we see now that the non-vanishing cosmological constant Λ itself would be a remnant of the expansion history of our universe in the very beginning. A similar situation also happens in the inflationary scenario [130, 131];
- Λ doesn't depend on m_j, hence the mass renormalization of GFT model will not change the value of cosmological constant;
- Since V_1 is the volume of a spacetime quanta, and Q_1 is an integral constant from the equation of motion, they are both remain the same under renormalization. Hence, Λ will strongly depend on the interaction coupling, whose renormalization will possibly lead to a small value of cosmological constant. A detailed analysis of the renormalization of coupling will leave to future work.

4.2 The deviation of Hubble parameter H_0 compared to single mode case

In the previous section we have seen how to identify the cosmological constant with microscopic parameters of GFT. However, if we are experiencing a phantom phase as we mentioned before, it could be hard to observe the cosmological constant Λ directly, because

[1] See, for example, equation (75) in [49].

its value given by equation (4.12) is an asymptotic one, which is not directly accessible as we haven't reached the future de Sitter regime yet. On the other hand, by fitting the observed data [59], we can get the preferred evolution of w, from which we can identify its minimal point as well, which can be compared to the value (4.7), or to be more precise, the corresponding red shift $z_{\min,w}$, we obtained in last section[1]. In this sense, the position where w reaches its minimum can be observed, albeit not directly.

One quantity, that of direct observational relevance (especially for observations related to supernova [57, 61]), is the current value H_0 of the Hubble parameter, whose value can be fixed by fitting data with cosmological models. In principle, for our model emerged from two modes, we can get H_0 directly by fitting with data, which is cumbersome as there are many GFT parameters that being involved. We can use an easier way, however, by noting the fact that the phantom crossing only occurred recently, as we argued in last section. Therefore, compared to the single mode case, where the value of H_0 is easier to fix, the two-modes evolution can be viewed as a slight modification at late times. This modification will result in a small deviation δH_0, and approximately we can set the current Hubble value in two-modes case as $H_0 + \delta H_0$, where H_0 is the value obtained from single mode evolution.

Here we made a first step towards showing the effects of including a second mode on the quantities that can be observed directly. In fact, we can see that this will increase the preferred value of the current Hubble parameter H_0, compared to the single mode case when fitting some cosmological data. Although it's not of our concern for the moment, we need to stress that the same happens in the realistic cosmological models. In fact, L. Heisenberg et al. observed in [66] that in general the appearance of a late time phantom phase in the evolution of our universe, can increase the current Hubble parameter H_0 inferred from CMB data [132], and hence to alleviate the H_0 tension [60, 61]. In the following we will use the same methods to check the effects of the inclusion of a second mode into consideration, compared to the single mode case. But one need to be aware that unlike the case in [66], our results below don't have direct observation relevance at current stage, as we are not dealing with the realistic matter contents that fill up our universe.

To begin, noting that for a single mode, we can simply substitute equation (2.28) into equation (4.10) to obtain [45],

$$H^2_{\text{single}} = \frac{8Q_1^2}{9}\left(\frac{\varepsilon_{Q_1}}{V^4} + \frac{\varepsilon_{E_1}}{V^3} + \frac{\varepsilon_{m_1}}{V^2} + \varepsilon_{\lambda_1}\right), \tag{4.13}$$

with the parameters

$$\varepsilon_{Q_1} = -\frac{Q_1^2}{2}V_1^2, \quad \varepsilon_{E_1} = V_1 E_1, \quad \varepsilon_{m_1} = \frac{m_1^2}{2}, \quad \varepsilon_{\lambda_1} = -\frac{\lambda_1}{6V_1^2}.$$

In terms of red shift z such that $(1+z)^3 = V_0/V$ for the current volume V_0, equation (4.13)

[1] It's worth emphasizing that the comparison can be quantitate only when we are able to, in our GFT formalism, take into account the realistic matter contents, like radiation with $w = 1/3$ and more importantly the non-relativistic matter with $w = 0$.

can be written as

$$H^2_{\text{single}} = H_0^2 \left[\Omega_{Q_1}(1+z)^{12} + \Omega_{E_1}(1+z)^9 + \Omega_{m_1}(1+z)^6 + \Omega_{\lambda_1}\right], \tag{4.14}$$

where we defined

$$\begin{aligned} H_0^2 &= \frac{8Q_1^2}{9}\left(\frac{\varepsilon_{Q_1}}{V_0^4} + \frac{\varepsilon_{E_1}}{V_0^3} + \frac{\varepsilon_{m_1}}{V_0^2} + \varepsilon_{\lambda_1}\right), \\ \Omega_{Q_1} &= \frac{1}{H_0^2}\frac{8Q_1^2}{9}\frac{\varepsilon_{Q_1}}{V_0^4}, \quad \Omega_{E_1} = \frac{1}{H_0^2}\frac{8Q_1^2}{9}\frac{\varepsilon_{E_1}}{V_0^3}, \\ \Omega_{m_1} &= \frac{1}{H_0^2}\frac{8Q_1^2}{9}\frac{\varepsilon_{m_1}}{V_0^2}, \quad \Omega_{\lambda_1} = \frac{1}{H_0^2}\frac{8Q_1^2}{9}\varepsilon_{\lambda_1}, \end{aligned}$$

such that $\Omega_{Q_1} + \Omega_{E_1} + \Omega_{m_1} + \Omega_{\lambda_1} = 1$, and the value of H_0 can be determined using the observed data. Since the current volume V_0 should be very large, and in general ε_{Q_1}, ε_{E_1} and ε_{m_1} are of same order, one would expect that $\Omega_{Q_1} \ll \Omega_{E_1} \ll \Omega_{m_1}$, therefore, in practice we can just ignore Ω_{Q_1} and Ω_{E_1} for small red shift z. Following [66], when the expansion history is modified (for example by including a second GFT mode), such that[1]

$$H(H_0) = H_{\text{single}}(H_0) + \delta H, \tag{4.15}$$

the preferred value of H_0, obtained by fitting data using $H(H_0)$, will change compared to that using $H_{\text{single}}(H_0)$, and the deviation can be given through the response function $\mathcal{R}_{H_0}$ as we can see below.

4.2.1 Deviation δH in the presence of the second mode

In the presence of the second mode, the expansion history of our universe will be modified. Effectively, such modification can be viewed as adding a fictitious phantom matter ψ (as we introduced in section 3.1) with the effective EoS $w_\psi = w$, where the latter w refers to the EoS obtained in our GFT cosmology model. Then the modified expansion history in the presence of the second mode can be written in the form

$$H^2 = H_0^2 \left[\Omega_{Q_1}(1+z)^{12} + \Omega_{E_1}(1+z)^9 + \Omega_{m_1}(1+z)^6 + \Omega_{\lambda 1} \mathrm{e}^{\int_0^z \frac{3(1+w(z'))}{1+z'}\mathrm{d}z'}\right]. \tag{4.16}$$

The Hubble parameter H can already be determined numerically since we have the numerical results for the evolution of w (used to plot the red dashed line of figures 3.3 and 4.1), which proves useful in determining the deviations δH and δH_0 (as can be seen from the figure 4.2(b) and the last column of table 4.1). But the numerical results are not very informative in revealing certain properties of δH, for which an analytic formula is

[1] Note that $H = H(z)$ should be a function of the red shift z of the form (4.16). We write $H(H_0)$ to stress the fact that to fix the whole history H, one needs to infer the value of parameters, including H_0, from data.

more preferable. Therefore, we will also consider using, in sacrificing of some accuracy, the approximation (3.24) of w, which can be rewritten using red shift z as

$$\begin{aligned} w &= -1 - \frac{b}{V_0}(1+z)^3, \\ &= -1 + (1+w_0)(1+z)^3, \end{aligned} \tag{4.17}$$

where V_0 is the current volume, the red shift z satisfies $(1+z)^3 = V_0/V$, and we have defined current value w_0 of the EoS such that

$$w_0 = w(z)|_{z=0} = -1 - \frac{b}{V_0}. \tag{4.18}$$

The approximation (4.17) allows to evaluate the integral in the Hubble parameter (4.16), which results in

$$H^2 = H_0^2 \left(\Omega_{Q_1}(1+z)^{12} + \Omega_{E_1}(1+z)^9 + \Omega_{m_1}(1+z)^6 + \Omega_{\lambda_1} \exp\left\{(1+w_0)\left[(1+z)^3 - 1\right]\right\}\right). \tag{4.19}$$

Therefore, the relative modification $\delta H/H_{\text{single}}$ can be given by (for simplicity, we ignore terms proportional to Ω_{Q_1} and Ω_{E_1}, since they are small)

$$\begin{aligned} \frac{\delta H}{H_{\text{single}}} &= \frac{H - H_{\text{single}}}{H_{\text{single}}}, \\ &= -1 + \sqrt{\frac{\Omega_{m_1}(1+z)^6 + \Omega_{\lambda_1} \exp\left\{(1+w_0)\left[(1+z)^3 - 1\right]\right\}}{\Omega_{m_1}(1+z)^6 + \Omega_{\lambda_1}}}. \end{aligned} \tag{4.20}$$

Since in the presence of the second mode, the universe will enter a phantom phase, we have $1 + w_0 < 0$, which means $\delta H/H_{\text{single}}$ is negative, as shown in figure 4.2. Furthermore, we can see that the deviation is non-vanishing only around its minimal value, determined by

$$\frac{\mathrm{d}}{\mathrm{d}z}\frac{\delta H}{H_{\text{single}}} \approx \frac{3(1+w_0)\Omega_{\lambda_1}(1+z)^2\left\{\Omega_{m_1}(1+z)^3\left[(1+z)^3 - 2\right] - \Omega_{\lambda_1}\right\}}{2\left[\Omega_{m_1}(1+z)^6 + \Omega_{\lambda_1}\right]^2} = 0,$$

where we used the fact that $1 + w_0$ is small. In our model, Ω_{m_1} is usually much smaller than Ω_{λ_1}[1], hence the solution to last equation can be approximated as

$$z_{\min,\delta H} = \left(\frac{\Omega_{\lambda_1}}{\Omega_{m_1}}\right)^{\frac{1}{6}} - 1. \tag{4.21}$$

Later we will see that this value is close to the minimal position of the so-called response function $\mathcal{R}_{H_0}$ (see equation (4.30) for definition), hence the modification introduced by including a second mode will indeed change H_0, according to the integral (4.29).

[1] This is acceptable as one would expect that the contribution from free massless scalar field (which has EoS $w = 1$) should vanish faster than the radiation (which has $w = 1/3$), and the latter can already be ignored nowadays.

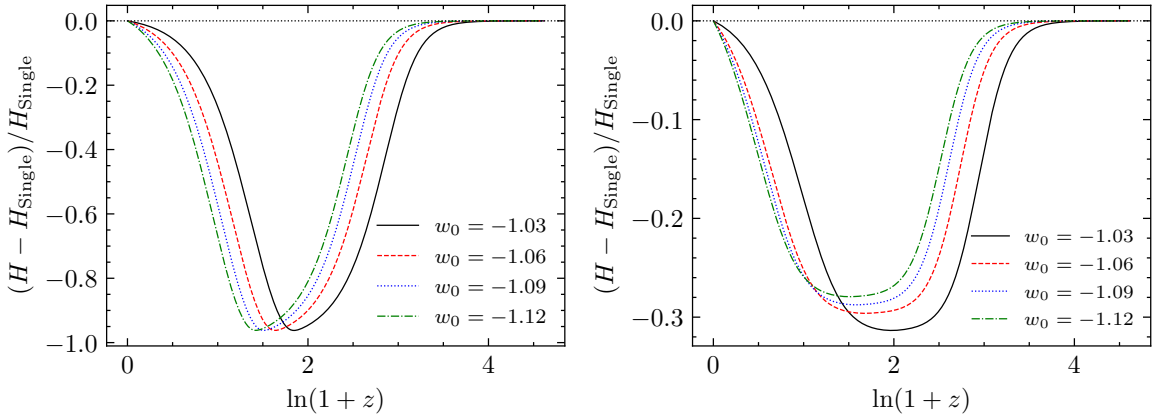

(a) Approximated result

(b) Exact result

Figure 4.2: The deviation δH in the presence of the second mode. 4.2(a): obtained from the approximated w (4.17), corresponds to black line of figure 4.1; 4.2(b): obtained from the exact result of w (calculated numerically), corresponds to red dashed line of figure 4.1. Apparently, the numerical value of w improves the accuracy of the result, but the qualitative result remains the same. Data is the same as in figure 4.1.

It's true that our approximation (4.17) of w deviates from the exact one quickly when z is large (as can be seen from figure 4.1), which results in a not that small deviation δH, as can be seen from figure 4.2(a). While from figure 4.2(b), we see that using the exact behaviour of w instead, obtained by numerical methods, indeed improves the accuracy, which results in a smaller deviation of δH and δH_0 (see the last column of table 4.1). What we would like to emphasize is, however, the qualitative feature remains the same, and the approximation (4.17) is useful when we try to determine the minimal point of the deviation, which is given by equation (4.21). It is impossible to write the result in the close analytic form if we only consider the exact yet numerical results of w.

Before we continue, we need to emphasize that in our model the choice of w_0 is not independent of other parameters. In fact, according to the relation (4.18) between w_0 and V_0, we see that the value of w_0 will determine V_0 as well, which is used in defining the red shift z. In other words, the choice of w_0 will determine what we called 'now' in our model. Correspondingly, the value of relative energy density, such as Ω_{m_1} and Ω_{λ_1} will also change, but this is not because we used a modified expansion history, instead the changed is due to that we defined a new point where $z = 0$. This is different with the case in [66], where the definition of 'now' should not change. Therefore, in our case we only need one response function (instead of two in [66]), $\mathcal{R}_{H_0}$.

4.2.2 The response function $\mathcal{R}_{H_0}$

Now, for a small deviation of the expansion history δH with the form of (4.15), the preferred value of H_0 when fitting with observed data should be changed such that [66]

$$H(H_0 + \delta H_0) = H_{\text{single}}(H_0) + \Delta H. \tag{4.22}$$

To the first order we should have [66]

$$\frac{\Delta H}{H_{\text{single}}} = \frac{H_0^2}{H_{\text{single}}^2}\frac{\delta H_0}{H_0} + \frac{\delta H}{H_{\text{single}}}. \tag{4.23}$$

And in general, every cosmological quantity $g(z)$ will have the variation as following [66]

$$\frac{\Delta g(z)}{g(z)} = I_g(z)\frac{\delta H_0}{H_{\text{single}}} + \int_0^\infty \frac{\mathrm{d}x_z}{1+x_z} R_g(x_z, z)\frac{\delta H(x_z)}{H_{\text{single}}(x_z)}. \tag{4.24}$$

In particular, for angular diameter distance [66]

$$d_A(z) = \frac{1}{1+z}\int_0^z \frac{\mathrm{d}z}{H_{\text{single}}(z)}, \tag{4.25}$$

we have

$$I_{d_A}(z) = -\frac{1}{\chi(z)}\int_0^z \mathrm{d}x_z \frac{H_0^2}{H_{\text{single}}^3}, \tag{4.26}$$

$$R_{d_A}(z) = -(1+x_z)\frac{\theta(z-x_z)}{\chi(z)H_{\text{single}}(x_z)}, \tag{4.27}$$

where $\chi(z)$ is the conformal distance

$$\chi(z) = \int_0^z \frac{\mathrm{d}x_z}{H_{\text{single}}(x_z)}. \tag{4.28}$$

Substituting equation (4.28) and the FLRW equation for single mode (4.13) into equations (4.26) and (4.27), we see that both I_{d_A} and R_{d_A} are independent of H_0.

To see how the inclusion of the second mode will change the value of H_0, we need an observable that is fixed for both single and two mode cases [66]. For example, we can consider the angular diameter distance at the end of bounce scenario (with red shift z_*)[1], whose deviation due to the modification of the expansion history is simply

$$\frac{\Delta d_A^*}{d_A^*} = I_{d_A}^*\frac{\delta H}{H_0} + \int_0^\infty \frac{\mathrm{d}x_z}{1+x_z} R_{d_A}^*\frac{\delta H}{H_{\text{single}}},$$

where we write $d_A^* = d_A(z_*)$ (and similarly for $I_{d_A}^*$ and $R_{d_A}^*$) for simplicity. Note that d_A^* is an observable and its value should not change no matter how we modify the expansion

[1] Currently, it's unclear how to determine the exact value of z_* in our GFT model, but the exact value of z_* is not important as long as it's large enough. In the following we will simply take $z_* = 1000$.

history, i.e., we require $\Delta d_A^* \simeq 0$. This provides us the variation of δH_0 due to the modification of expansion history [66]

$$\frac{\delta H_0}{H_0} = \int_0^\infty \frac{\mathrm{d}x_z}{1+x_z} \mathcal{R}_{H_0} \frac{\delta H}{H_{\text{single}}}, \tag{4.29}$$

where the response function

$$\mathcal{R}_{H_0} = -\frac{R_{d_A}^*}{I_{d_A}^*}, \tag{4.30}$$

which is also independent of H_0 as same as $I_{d_A}^*$ and $R_{d_A}^*$. Since $H(z) \geq 0$ in the whole history of our universe, we see that $\chi(z) > 0$ and $I_{d_A} < 0$, $R_{d_A} < 0$, which results in $\mathcal{R}_{H_0} < 0$ as well, as shown in figure 4.3. On the other hand, the appearance of second mode will introduce phantom crossing, which results a negative δH. Therefore, the preferred value H_0 will increase compared to the single mode case.

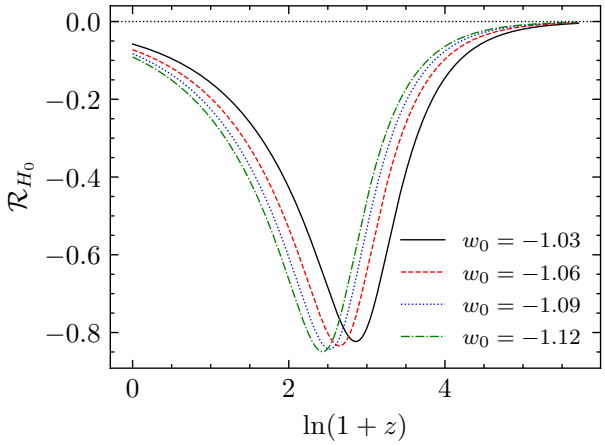

Figure 4.3: The response function $\mathcal{R}_{H_0}$. The data is same as in figure 4.1. Note that for $w_0 = -1.03$ we have $V_0 = 1.296 \times 10^8$. Then the Hubble parameter in Planck units is $H_0 = 3.5 \times 10^{-4}$, much larger than the value inferred from the Planck data, which in Planck units reads $H_0 = 1.18 \times 10^{-61}$ (in SI units the value is $H_0 = 67.4\ km\ s^{-1}\ Mpc^{-1}$ [56]). The exact estimation of H_0 in our model from CMB data requires including the non-relativistic matter into GFT, which is out of reach for the moment. And we leave this issue for future works.

Before we move on, let's take a closer look at the behaviour of response function $\mathcal{R}_{H_0}$. For $x_z < z^*$, we have

$$\frac{\mathrm{d}}{\mathrm{d}x_z} R_{d_A}^* = -\frac{1}{\chi^*} \left[\frac{1}{H_{\text{single}}(x_z)} - \frac{1+x_z}{H_{\text{single}}(x_z)^2} \frac{\mathrm{d}}{\mathrm{d}x_z} H_{\text{single}}(x_z) \right].$$

The minimal value is determined by $\dfrac{\mathrm{d}}{\mathrm{d}x_z} R_{d_A}^* = 0$, which requires

$$\frac{1}{H_{\text{single}}(x_z)} - \frac{1+x_z}{H_{\text{single}}(x_z)^2} \frac{\mathrm{d}}{\mathrm{d}x_z} H_{\text{single}}(x_z) = 0.$$

Substituting the FLRW equation for single mode (4.13), and ignore Ω_{Q_1} and Ω_{E_1} since they are small, we get

$$6\Omega_{m_1}(1+z)^6 = \Omega_{m_1}(1+z)^6 + \Omega_{\lambda_1}. \tag{4.31}$$

Therefore, at the minimal value of $\mathcal{R}_{H_0}$, we have the red shift

$$z_{\min,\mathcal{R}_{H_0}} = \left(\frac{\Omega_{\lambda_1}}{5\Omega_{m_1}}\right)^{\frac{1}{6}}, \tag{4.32}$$

around which, we have $\Omega_{\lambda_1} \simeq 5\Omega_{m_1}(1+z)^6$. Therefore, when the response function $\mathcal{R}_{H_0}$ deviates from 0 significantly, we see that in the FLRW equation (4.13) the contribution from matter term has the same order as the cosmological constant term. This is just where the universe enters phantom phase and the contribution from the second mode becomes noticeable. This can also be seen from the fact that by comparing equations (4.21) and (4.32)

$$z_{\min,\mathcal{R}_{H_0}} = \frac{1}{5^{1/6}} z_{\min,\delta H} + \frac{1}{5^{1/6}} - 1.$$

We see that $z_{\min,\mathcal{R}_{H_0}}$ and $z_{\min,\delta H}$ are close to each other, which means there would be an overlap for the regions where H deviates from H_{single} and $\mathcal{R}_{H_0}$ deviates from 0 respectively. Therefore, the preferred Hubble parameter H_0 will indeed change according to equation (4.29).

In fact, substituting equations (4.30) and (4.20) into equation (4.29) we can get the change of preferred H_0 in the presence of the second mode. Several results for different w_0 are shown in table 4.1. We see that when including a second mode into our GFT cosmology model, the value of H_0 inferred from data will increase. This is one would expect as a phantom phase (which is inevitable in GFT cosmology with two modes) can alleviate the Hubble tension by increasing H_0 inferred from CMB data [66].

Table 4.1: The deviation of H_0 in the presence of the second mode. The 4th column lists results obtained using w in the approximated form (4.17), while the last column lists the result obtained using numerical value of w from chapter 3.

w_0	V_0	Ω_{m_1}	$\delta H_0/H_0$ (approx)	$\delta H_0/H_0$ (numerical)
-1.03	1.30×10^8	1.79×10^{-8}	0.700	0.269
-1.06	6.92×10^7	6.27×10^{-8}	0.706	0.271
-1.09	4.74×10^7	1.34×10^{-7}	0.711	0.260
-1.12	3.61×10^7	2.30×10^{-7}	0.715	0.253

We emphasize again that in GFT cosmology the choice of w_0 (the current value of EoS) will also change the current volume V_0 and hence the energy density Ω_{m_1} of matter. This fact is also reflected from table 4.1.

4.3 Summary

In this chapter, we investigated several cosmological sequences when including two modes in GFT cosmology. The effects can be encoded in the effective EoS w, and based on our previous results of chapter 3 we know that in the two modes case a phantom phase will emerge in the late time evolution of the universe [50], hence there should be a point where the phantom crossing[1] occurs, i.e. w crosses the line $w = -1$. Finding the exact position of phantom crossing can be cumbersome, hence we took a detour by noting the fact that phantom crossing has to happen between the end of the Friedman phase and the minimum point of w, and shown that the latter two positions are close to each other. Therefore, approximately we can assume that the position of phantom crossing is either the end point of Friedman phase or the minimum point of w. On the other hand, soon after the phantom crossing we can use the approximation (3.24) of w, which approaches to $w = -1$ quickly. In other words, the universe will enter the de Sitter regime quickly after the phantom crossing, hence if we are experiencing a phantom phase, the phantom crossing must happen recently with a low red shift.

In the de Sitter regime, the evolution is dominated by a single mode, and we can extract the cosmological constant (4.12) using microscopic parameters from GFT. Interestingly, we see that a non-vanishing Λ will necessarily require a bounce in the very early universe. Therefore, Λ can be viewed as a remnant of the history of the universe in the far past, where we should have a bounce instead of the Big Bang singularity.

Furthermore, using the method from [66], we showed how the second mode will change the preferred value of H_0 when we fit data using our GFT cosmology model. To this end, we approximate the effects of the second mode using the fictitious field ψ we introduced in section 3.1, with EoS given by (3.24), such that the modified FLRW equation has the form of (4.16). Then we can see that the deviation δH is negative, as shown in figure 4.2, because the field ψ is phantom like. Furthermore, we see that $\delta H/H$ is non-vanishing only around its minimum point, which is also close to the minimum point of response function $\mathcal{R}_{H_0}$. Therefore, the non-vanishing region of $\delta H/H$ and $\mathcal{R}_{H_0}$ are overlapped. This is important as otherwise the current value H_0 of Hubble parameter will not change no matter how the expansion history (4.16) being modified. Finally, carrying out the integration in equation (4.29) we obtain the deviation $\delta H_0/H_0$ of current Hubble parameter as shown in table 4.1, and the deviation is positive as we expected. It's worth mentioning that we also calculated the deviation δH and δH_0 using exact w obtained by numerical calculations, indeed the accuracy is improved, but the result is qualitatively the same as the one obtained using the approximation (3.24).

[1] Which is defined as where the EoS w changes from values larger than -1 to less than -1.

Chapter 5

Generalized Amit-Roginsky model as perturbations

In the previous chapters, we have discussed the phenomenological effects of *homogeneous* and *isotropic* condensate states in GFT, with a focus on the cosmological evolution. These two requirements dramatically simplified our analysis of the GFT dynamics, by allowing us to use an effective action of the form (2.21). At the same time, however, these simplifications also hide the internal structure, especially the combinatorial ones which specify the interaction terms, of the underlying GFT models. On the one hand, this suggests that our result is quite general, valid for any GFT model that has the same effective description as we introduced before in the homogeneous and isotropic sector; on the other hand, such generality also means the lacking of the ability to distinguish or verify different microscopic GFT models from their cosmological consequences.

As we mentioned in section 1.2, these limitations can be overcome by introducing either inhomogeneities perturbations [51, 74] or anisotropic condensates represented graphically by non-equilateral tetrahedra (in the 4d case) or triangle (in the 3d case we are going to consider below) [75, 76]. In particular, for the latter improvement we need more than one spin j to specify the condensate wave function σ in the spin representation, hence the details of the combinatorial structure of the kinetic and interaction kernel of GFT action need to be taken into account, which will modify the evolution of our universe compared to the isotropic case, as well as provide new observables beyond the total volume [75, 76].

In this chapter, we are going to consider the inhomogeneous perturbations over the homogeneous but anisotropic GFT condensates. The analysis focuses on the 3d GFT model which, despite lacking of cosmological relevancies, is simpler to deal with compared to the 4d case. We emphasize again that when dealing with anisotropic condensates it's necessary to take into account the combinatorial structure, which means that we have to go beyond the effective action of the form (2.21) and consider a detailed microscopic model instead. In the 3d case, a suitable candidate is the Boulatov model [77], whose partition function represents a completion of the resummation of Ponzano-Regge amplitudes [29] of the discretized 3d gravity [78, 79].

We will see that with a suitable choice of the condensates, the dynamics of the pertur-

bations would be a generalization of the Amit-Roginsky model (whose action is given by (5.34)) [81], in the sense that the resulting action is a summation over spin j, which label different modes of the inhomogeneous perturbation over condensates under consideration, such that each summand has the similar form as the AR model. The AR model is interesting in itself as it's the only field with an interaction of odd order that admits a melonic dominance in the large-N limit[1] [82]. We won't discuss such properties in much detail, as what's important for us is the fact it's possible to obtain an effective continuum QFT in flat space from the quantum gravity model.

5.1 Boulatov model coupled to matter frame

In its original form [77], there are no reference frames in the Boulatov model, making it difficult to introduce inhomogeneous perturbations (even the concept of inhomogeneity itself) or provide a field theoretic meaning to the emergent fields [73, 80]. To overcome such difficulties we will show how to couple free massless scalar fields χ_i as *relational rods* with the Boulatov model, in the same way of introducing the relational clock ϕ into GFT formalism, as we did in chapter 2. With the help of reference frame χ_i, we can define *homogeneous* as the property that independent of χ_i. This way the homogeneous condensate wave functions, that we are going to perturb, would be those that solves the equation of motion of the original Boulatov model without coupling to matter frames. Before we dive into the details, let's start with a short review of the Boulatov model, with a focus on the materials we are going to need in the following discussion.

5.1.1 A brief introduction of the Boulatov model

The Boulatov model [77] is a 3d GFT model, which as usual is defined by functions on multi-copies of a certain group manifold. Following [77] we choose the group here to be $G = SU(2)$. Then the field under consideration would be a complex function[2] $T : SU(2)^{\times 3} \to \mathbb{C}$, which is further required to be invariant under the right action of $SU(2)$ due to geometrical considerations (same as in the 4d case, see section 2.1)

$$T(g_1 h, g_2 h, g_3 h) = T(g_1, g_2, g_3), \quad \forall h \in SU(2). \tag{5.1}$$

and to satisfy the reality condition [73]

$$T(g_1, g_2, g_3) = \bar{T}(g_3, g_2, g_1). \tag{5.2}$$

In the original paper [77], it is further required to have cyclic symmetry in the group elements g_i such that $T(g_1, g_2, g_3) = T(g_3, g_2, g_1)$. But this property plays no role for the

[1] A thorough introduction of *melonic dominance* or *large-N limit* is out the scope of current thesis, see [133] for a review of these two and other related concepts.

[2] Here we use T for the 3d group field to avoid possible confusion with the 4d case, where the field is represented by φ.

current work and even makes it difficult to find explicit solutions, so we simply ignore it and continue. But we will see that under suitable approximations, we can actually obtain the cyclic symmetric solution of the Boulatov dynamics, see equation (5.27) for the group representation or (5.28) for the spin representation.

The combinatorial structure, which is the defining property of a given GFT model, is reflected through the interaction terms. Usually the interactions are *non-local*, in the sense that each field appears in the interaction has different set of arguments, in contrary to the ordinary QFT where the Lagrangian densities, and especially the interactions, are defined for each spacetime point. With these subtleties in mind, we can write the action of the Boulatov model in the form [73, 77]

$$\begin{aligned} S[T] = &\frac{\mu^2}{2}\int \mathrm{d}g_1\mathrm{d}g_2\mathrm{d}g_3 T(g_1,g_2,g_3)\bar{T}(g_1,g_2,g_3) \\ &-\frac{\lambda}{4!}\int \prod_{i=1}^{6}\mathrm{d}g_i T(g_1,g_2,g_3)T(g_3,g_5,g_4)T(g_4,g_2,g_6)T(g_6,g_5,g_1), \end{aligned} \tag{5.3}$$

where μ is the mass of the field and λ the coupling constant. Furthermore, with the help of the reality condition (5.2), we see that the equation of motion of the field $T(g_1,g_2,g_3)$, obtained by varying the action (5.3) respect to $T(g_1,g_2,g_3)$, reads

$$\mu^2 T(g_3,g_2,g_1) = \frac{\lambda}{3!}\int \mathrm{d}g_4\mathrm{d}g_5\mathrm{d}g_6 T(g_3,g_5,g_4)T(g_4,g_2,g_6)T(g_6,g_5,g_1). \tag{5.4}$$

As we emphasized in section 2.1, for any GFT it's also possible to work in the spin representation, with the help of Peter-Weyl decomposition. In the 3d case, the invariant space $\mathrm{Inv}\{V_{j_1}\otimes V_{j_2}\otimes V_{j_3}\}$ is only 1 dimensional, hence we don't need the intertwiner label ι and the intertwiners are just $3j$ symbols (see appendix B for a basic introduction) [89]. Therefore, the basis function, or more precisely, the spin network vertex function $\kappa_{\boldsymbol{x}}$ has the form

$$\kappa^{j_1,j_2,j_3}_{m_1,m_2,m_3} = \sum_{n_1,n_2,n_3}\prod_{i=1}^{3}\sqrt{2j_i+1}D^{j_i}_{m_i n_i}(g_i)\begin{pmatrix} j_1 & j_2 & j_3 \\ n_1 & n_2 & n_3 \end{pmatrix},$$

with the $3j$ symbol $\begin{pmatrix} j_1 & j_2 & j_3 \\ n_1 & n_2 & n_3 \end{pmatrix}$ of $SU(2)$.

Therefore, under the PW decomposition, the field T can be expanded in the form (rely on the invariance property (5.1) of the T field)

$$T(g_1,g_2,g_3) = \sum_{\{j,m,n\}} T^{m_1m_2m_3}_{j_1j_2j_3}\prod_{i=1}^{3}\sqrt{2j_i+1}D^{j_i}_{m_i n_i}(g_i)\begin{pmatrix} j_1 & j_2 & j_3 \\ n_1 & n_2 & n_3 \end{pmatrix}. \tag{5.5}$$

Moreover, the sum on $\{j\}$ denotes the summation over j_1, j_2 and j_3 (respectively for $\{m\}$ and $\{n\}$). The coefficients $T^{m_1m_2m_3}_{j_1j_2j_3}$ can be computed using the orthogonality of Wigner matrices as

$$T^{m_1m_2m_3}_{j_1j_2j_3} = \int\left(\prod_{i=1}^{3}\mathrm{d}g_i\right)\sum_{\{n\}}T(g_1,g_2,g_3)\prod_{i=1}^{3}\sqrt{2j_i+1}\bar{D}^{j_i}_{m_i n_i}(g_i)\begin{pmatrix} j_1 & j_2 & j_3 \\ n_1 & n_2 & n_3 \end{pmatrix}. \tag{5.6}$$

Using this decomposition, the integral over the Wigner matrix $D^j(g)$ can be performed explicitly, allowing us to get the spin representation of the Boulatov action (5.3)[1] [77]

$$S_B[T] = \sum_{j_1,j_2,j_3} \frac{\mu^2}{2} |T^{m_1,m_2,m_3}_{j_1,j_2,j_3}|^2 - \frac{\lambda}{4!} \sum_{j_1,..,j_6} \begin{Bmatrix} j_1 & j_2 & j_3 \\ j_4 & j_5 & j_6 \end{Bmatrix} T^{4_{6j}}, \tag{5.7}$$

where the kinetic term is

$$|T^{m_1,m_2,m_3}_{j_1,j_2,j_3}|^2 = \sum_{\substack{j_1,j_2,j_3 \\ m_1,m_2,m_3}} (-1)^{\sum_{i=1}^3 (j_i - m_i)} T^{m_1,m_2,m_3}_{j_1,j_2,j_3} T^{-m_1,-m_2,-m_3}_{j_1,j_2,j_3}, \tag{5.8}$$

and in the interaction term, $T^{4_{6j}}$ encodes the contraction of the magnetic indices m_i of the field in the same manner as the $6j$ symbol (see appendix B for the convention of the $6j$ symbol used in this thesis), i.e.,

$$T^{4_{6j}} = \sum_{\{j,m\}} (-1)^{\sum_{i=1}^6 (j_i - m_i)} T^{-m_1,-m_2,-m_3}_{j_1 j_2 j_3} T^{m_3,m_5,-m_4}_{j_3 j_5 j_4} T^{m_4,m_2,-m_6}_{j_4 j_2 j_6} T^{m_1,-m_5,m_1}_{j_6 j_5 j_1}. \tag{5.9}$$

Correspondingly, the equation of motion (5.4) now becomes

$$\mu^2 T^{m_1,m_2,m_3}_{j_1,j_2,j_3} = \frac{\lambda}{3!} \sum_{j_4,j_5,j_6} \begin{Bmatrix} j_1 & j_2 & j_3 \\ j_4 & j_5 & j_6 \end{Bmatrix} T^{4_{6j}}_{\setminus\{m_1,m_2,m_3\}}, \tag{5.10}$$

where

$$T^{4_{6j}}_{\setminus\{m_1,m_2,m_3\}} = \sum_{m_4,m_5,m_6} (-1)^{\sum_{i=4}^6 (j_i - m_i)} T^{m_3,m_5,-m_4}_{j_3 j_5 j_4} T^{m_4,m_2,-m_6}_{j_4 j_2 j_6} T^{m_6,-m_5,m_1}_{j_6 j_5 j_1}, \tag{5.11}$$

is the field T where the three magnetic indices m_1,m_2 and m_3 are not summed over.

Again, it's possible to get the *algebra representation* of the Boulatov model by working with Lie algebra $su(2)$ [29], but it's irrelevant for our purpose here. In this chapter, it's also enough to have in hand the group and spin representations, just as the case in previous chapters. Moreover, as we will see the following calculations are mainly done in the spin representation, yet the group representation are mainly used for its notation simplicity.

5.1.2 Matter degrees of freedom

The Boulatov model introduced above is independent of any coordinate systems in its own, as in the case of many other quantum gravity theories. Then the problems are, again, how to extract the continuous spacetime from the model, and how to label different points of the resulting continuum in such a way that the fields, in the sense of ordinary QFT, can be defined. As we have seen in chapter 2, the physical frame can be introduced by coupling

[1] The partition function corresponds to the action (5.3) or (5.7) can be viewed as the summation of PR amplitudes [29, 77], whose semi-classical limit corresponds to the Regge action for 3d discretized gravity [78]. The detail deviation of such partition function will not concern us here, for more information see [29, 77].

GFT with matter fields, the same is true for Boulatov model. In a sense that contrary to cosmology case, for the Boulatov model of 3d gravity we can ignore the clock $\chi_0 = \phi$ and only consider *relational rods*, to help us in distinguishing different points of the space, and allow us to introduce the inhomogeneous perturbations over the condensates [51].

More precisely, in three dimensions, one uses three free massless scalar fields $\boldsymbol{\chi} = (\chi_1, \chi_2, \chi_3)$, which has no obstacle to be implemented in the GFT formalism, as relational rods that constitute the matter reference frame [51, 74]. The resulting field T now extends to the form $T(g_1, g_2, g_3; \boldsymbol{\chi}) : SU(2)^3 \times \mathbb{R}^3 \to \mathbb{C}$. One can expect that in the classical limit, the relational rods χ_i have the same Lagrangian density (2.11) as the relational time ϕ we introduced before in the cosmological setting. Therefore, the Boulatov model coupled to χ_i should also be invariant under the translations $\chi_i \to \chi_i + c_i$ and the reflections $\chi_i \to -\chi_i$ [42, 49, 51]. The corresponding derivative expansion of the kinetic term will then provide a new differential term $\nabla = \left(\frac{\partial}{\partial\chi_1}, \frac{\partial}{\partial\chi_2}, \frac{\partial}{\partial\chi_3}\right)$ respect to the matter frame, and the original action (5.3) extends to[1]

$$S[T] = \int [\mathrm{d}g]^3 \mathrm{d}^3\boldsymbol{\chi} \left[\frac{1}{2}\nabla T(g_1, g_2, g_3; \boldsymbol{\chi})\nabla\bar{T}(g_1, g_2, g_3; \boldsymbol{\chi}) + \frac{\mu^2}{2} T(g_1, g_2, g_3; \boldsymbol{\chi})\bar{T}(g_1, g_2, g_3; \boldsymbol{\chi})\right]$$
$$-\frac{\lambda}{4!}\int \prod_{i=1}^{6} \mathrm{d}g_i \mathrm{d}^3\boldsymbol{\chi} T(g_1, g_2, g_3; \boldsymbol{\chi})T(g_3, g_5, g_4; \boldsymbol{\chi})T(g_4, g_2, g_6; \boldsymbol{\chi})T(g_6, g_5, g_1; \boldsymbol{\chi}). \quad (5.12)$$

The modified equation of motion resulted from the new action (5.12) has the form

$$\nabla^2 T(g_3, g_2, g_1; \boldsymbol{\chi}) + \mu^2 T(g_3, g_2, g_1; \boldsymbol{\chi})$$
$$= \frac{\lambda}{3!}\int \mathrm{d}g_4 \mathrm{d}g_5 \mathrm{d}g_6 T(g_3, g_5, g_4; \boldsymbol{\chi})T(g_4, g_2, g_6; \boldsymbol{\chi})T(g_6, g_5, g_1; \boldsymbol{\chi}). \quad (5.13)$$

As before, we can write equations (5.12) and (5.13) in the spin representation. For the action we have

$$S_B[T(\boldsymbol{\chi})] = \sum_{j_1, j_2, j_3} \int \mathrm{d}^3\boldsymbol{\chi} \left[\frac{1}{2}\left|\nabla T^{m_1, m_2, m_3}_{j_1, j_2, j_3}(\boldsymbol{\chi})\right|^2 + \frac{\mu^2}{2}\left|T^{m_1, m_2, m_3}_{j_1, j_2, j_3}(\boldsymbol{\chi})\right|^2\right.$$
$$\left. -\frac{\lambda}{4!}\sum_{j_1, .., j_6} \begin{Bmatrix} j_1 & j_2 & j_3 \\ j_4 & j_5 & j_6 \end{Bmatrix} \int \mathrm{d}^3\boldsymbol{\chi} T(\boldsymbol{\chi})^{4_{6j}}\right]. \quad (5.14)$$

And the equation of motion in the spin representation can be written as

$$\nabla^2 T^{m_1, m_2, m_3}_{j_1, j_2, j_3}(\boldsymbol{\chi}) + \mu^2 T^{m_1, m_2, m_3}_{j_1, j_2, j_3}(\boldsymbol{\chi}) = \frac{\lambda}{3!}\sum_{j_4, j_5, j_6} \begin{Bmatrix} j_1 & j_2 & j_3 \\ j_4 & j_5 & j_6 \end{Bmatrix} T(\boldsymbol{\chi})^{4_{6j}}_{\setminus\{m_1, m_2, m_3\}}. \quad (5.15)$$

[1] Note that this action should not be confused with that of a dynamical Boulatov model of [134] where a Laplace-Beltrami operator acts on the group manifold.

5.1.3 Homogeneous but anisotropic condensates as solutions

Having introduced the relational frame and specified the dynamics of the Boulatov model above, we are ready to discuss the required homogeneous but anisotropic condensates, to be perturbed in the following. For a state to be condensate, the expectation value of the field operator respect to it, or *condensate function* in short, should be non-vanishing. And furthermore, such function should satisfy the classical equation of motion (5.13) (or (5.15)), hence can be identified with the solution T. Being homogeneous, the condensate T should be independent of the reference frame $\boldsymbol{\chi}$[1]. In this case, equation (5.13) reduces to equation (5.4). This relational rods only enter the picture later on when we consider perturbations. A one parameter family of solutions parametrized by normalized functions $f : SU(2) \to \mathbb{C}$ was proposed in [73]. The associated solution, or in other words, the condensate function T_f, can be given by

$$T_f(g_1, g_2, g_3) = \mu\sqrt{\frac{3!}{\lambda}} \int \mathrm{d}h \delta(g_1 h) f(g_2 h) \delta(g_3 h), \tag{5.16}$$

where $\delta(g)$ is the Dirac delta function over the group $SU(2)$ such that

$$\int \mathrm{d}h \delta(h) = 1, \ \int \mathrm{d}h \delta(h) f(h) = f(I), \tag{5.17}$$

with I is the identity of $SU(2)$ group. To see the meaning of the normalization of f, we can substitute the solution (5.16) back into the right hand side of the equation of motion (5.4),

$$\begin{aligned}
&\frac{\lambda}{3!} \int \mathrm{d}g_4 \mathrm{d}g_5 \mathrm{d}g_6 T_f(g_3, g_5, g_4) T_f(g_4, g_2, g_6) T_f(g_6, g_5, g_1) \\
&= \frac{\lambda\mu^3}{3!} \int \mathrm{d}g_4 \mathrm{d}g_5 \mathrm{d}g_6 \left(\frac{3!}{\lambda}\right) \sqrt{\frac{3!}{\lambda}} \int \mathrm{d}h_1 \delta(g_3 h_1) f(g_5 h_1) \delta(g_4 h_1) \\
&\quad \times \int \mathrm{d}h_2 \delta(g_4 h_2) f(g_2 h_2) \delta(g_6 h_2) \int \mathrm{d}h_3 \delta(g_6 h_3) f(g_5 h_3) \delta(g_1 h_3), \\
&= \mu^3 \sqrt{\frac{3!}{\lambda}} \int \mathrm{d}g_5 \int \mathrm{d}h_1 \mathrm{d}h_2 \mathrm{d}h_3 \delta(g_3 h_1) f(g_5 h_1) \delta(h_1 h_2^{-1}) f(g_2 h_2) \delta(h_2 h_3^{-1}) f(g_5 h_3) \delta(g_1 h_3), \\
&= \mu^3 \sqrt{\frac{3!}{\lambda}} \int \mathrm{d}g_5 \int \mathrm{d}h_3 \mathrm{d}h_2 \delta(g_3 h_2) f(g_5 h_2) f(g_2 h_2) \delta(h_2 h_3^{-1}) f(g_5 h_3) \delta(g_6 h_3), \\
&= \mu^3 \sqrt{\frac{3!}{\lambda}} \int \mathrm{d}g_5 \int \mathrm{d}h_3 \delta(g_2 h_3) f(g_5 h_3) f(g_2 h_3) f(g_5 h_3) \delta(g_1 h_3), \\
&= \int \mathrm{d}(g_5 h_3) f^2(g_5 h_3) \times \mu^2 \left[\mu \sqrt{\frac{3!}{\lambda}} \int \mathrm{d}h_3 \delta(g_1 h_3) f(g_2 h_3) \delta(g_3 h_3)\right], \\
&= \int \mathrm{d}(g_5 h_3) f^2(g_5 h_3) \times \left[\mu^2 T_f(g_1, g_2, g_3)\right],
\end{aligned}$$

[1] And that's why we didn't need to consider relational rods in the cosmological sector, as they won't change the dynamics without considering inhomogeneous perturbations.

which equals to the left hand side of the equation of motion (5.13) only if the function $f(g)$ is normalized such that

$$\int \mathrm{d}h f(h)^2 = 1. \tag{5.18}$$

In other words, the normalization of f is required for T_f given by equation (5.16) to really be a solution.

We can also write this solution in spin representation. In fact, substituting the solution (5.16) into the general PW coefficients (5.6) we obtain

$$(T_f)^{m_1,m_2,m_3}_{j_1,j_2,j_3} = \mu\sqrt{\frac{3!}{\lambda}}\sqrt{d_{j_1}d_{j_3}}\sum_{l_2} f^{j_2}_{m_2,l_2}\begin{pmatrix} j_1 & j_2 & j_3 \\ m_1 & m_2 & m_3 \end{pmatrix}, \tag{5.19}$$

where $d_j = 2j+1$ is the dimension of the spin j representation, and f^j_{mn} are the coefficients in the PW decomposition of $f(g)$

$$f^j_{mn} = \sqrt{2j+1}\int \mathrm{d}g f(g)\bar{D}^j_{mn}(g), \tag{5.20}$$

and the corresponding normalization condition becomes

$$\sum_{j,m,n}(-1)^{m-n} f^j_{mn} f^j_{-m,-n} = 1. \tag{5.21}$$

Before we move on, let us make quick remarks on this class of solutions and its special form which is regularized by the 'heat kernel'. Firstly, (5.16) is not symmetric under the permutations of the group elements g_i since g_2 plays a preferential role through f. Secondly, the presence of Dirac delta function in the expression (5.16) leads to several divergences. For example, the action (5.13) is divergent when evaluated on this solution due to the appearance of the factor $\delta(I)$ in the action. This can also be seen from the PW expansion of the Dirac delta over $SU(2)$

$$\delta(g) = \sum_{j,m}(2j+1)D^j_{mm}(g). \tag{5.22}$$

In fact, noting that $D^j_{mm}(I) = \delta_{mm} = 1$, we have

$$\begin{aligned}\delta(I) &= \sum_j \sum_{m=-j}^{m=j}(2j+1)\delta_{mm}, \\ &= \sum_j (2j+1)^2 \to \infty,\end{aligned}$$

Therefore, we need to regularize our solution, which can be achieved via different methods. For example, one possible solution would be to introduce a cut-off parameter J in the PW expansion of $T(g_1,g_2,g_3)$, thus making the action finite. Here, we will instead use a heat kernel regularization to make all quantities well-defined, at the cost of only having an approximate solution to the equations of motion. To do so, we introduce a new real

parameter ε. For any function f of $SU(2)$ with coefficients f^j_{mn} in its PW expansion, we define its heat kernel regularization as ($d_j = 2j+1$)

$$f_\varepsilon(g) = \sum_{j,m,n} \sqrt{d_j} f^j_{mn} D^j_{mn}(g) \mathrm{e}^{-\varepsilon C_j} \tag{5.23}$$

with C_j is the Casimir of the spin j representation of $SU(2)$. This function is well-defined for any $\varepsilon > 0$ and by taking the limit $\varepsilon \to 0$ we get back the initial function f. In particular, for the Dirac delta function of $SU(2)$, its heat kernel regularization is

$$\delta_\varepsilon(g) = \sum_{j,m} d_j D^j_{mm}(g) \mathrm{e}^{-\varepsilon C_j}. \tag{5.24}$$

Note that this function is not normalized in the sense of equation (5.18). If we denote its norm as α_ε^{-2}, the normalized function associated to δ_ε is ($d_j = 2j+1$)

$$\Delta_\varepsilon(g) = \sum_{j,m,n} \sqrt{d_j} (\Delta_\varepsilon)^j_{mn} D^j_{mn}(g) \mathrm{e}^{-\varepsilon C_j}, \tag{5.25}$$

where the PW coefficients $(\Delta_\varepsilon)^j_{mn}$ has the form

$$(\Delta_\varepsilon)^j_{mn} = \alpha_\varepsilon \sqrt{d_j} \delta_{mn} \mathrm{e}^{-\varepsilon C_j}. \tag{5.26}$$

Using $\Delta_\varepsilon(g)$, we can build now a regularized and symmetric field

$$T_\varepsilon(g_1, g_2, g_3) = \mu \sqrt{\frac{3!}{\lambda}} \int \mathrm{d}h \delta_\varepsilon(g_1 h) \Delta_\varepsilon(g_2 h) \delta_\varepsilon(g_3 h) = \mu \alpha_\varepsilon \sqrt{\frac{3!}{\lambda}} \int \mathrm{d}h \delta_\varepsilon(g_1 h) \delta_\varepsilon(g_2 h) \delta_\varepsilon(g_3 h). \tag{5.27}$$

We need to stress that, however, $T_\varepsilon(g_1, g_2, g_3)$ is only an approximate solution of the homogeneous equation of motion, i.e. it is a solution only at leading order in ε. The coefficients of its PW expansion are given by

$$(T_\varepsilon)^{m_1 m_2 m_3}_{j_1 j_2 j_3} = \mu \alpha_\varepsilon \sqrt{\frac{3!}{\lambda}} \prod_{i=1}^{3} \sqrt{d_{j_i}} \mathrm{e}^{-\varepsilon C_{j_i}} \begin{pmatrix} j_1 & j_2 & j_3 \\ m_1 & m_2 & m_3 \end{pmatrix}, \tag{5.28}$$

which has the same symmetric properties under permutations as $3j$ symbols. Therefore, we can see that the $3j$ symbols, accompanied by necessary coefficients, are solutions to the Boulatov dynamics. In the following we will refer equation (5.28) as the *heat kernel regularized solution*.

Let's stress that solutions obtained in this section are in general anisotropic, in the local sense that we have emphasized before, i.e., in general we need three different spins to specify a solution, which corresponds to a non-equilateral triangle with different length for each edge. This means locally (inside a build block, here the triangle) one can distinguish different directions, which is impossible for an isotropic space. On the contrary, in the cosmological sector as we illustrated in chapter 2, we only need one spin j to specify the

condensate function σ, correspondingly the directions are indistinguishable, which leads to isotropy required by the cosmological principle.

When perturbing over the solution (5.19) or (5.28), one can get the effective action for the perturbation in the AR form as we promised. But the conditions for the emergence of the AR model are actually weaker than that and independent of explicit solutions. We will see that the AR-like dynamics can emerge from the condensate function[1] T that satisfies two conditions (5.45) and (5.45). Although these conditions contain several arbitrary constants, that can only be fixed by substituting the explicit solutions, such as equations (5.19) and (5.28).

Furthermore, as one can expect that for the AR-like dynamics to emerge, we need the correct degrees of freedom that match to AR ones, which requires a suitable form of the perturbations, as we are going to discuss below.

5.1.4 Inhomogeneous perturbations over the condensates

Although we have mentioned *inhomogeneous perturbations* several times before, we didn't show explicitly what this means. In fact, one reason why we consider perturbations is that the equation of motion (5.15) is hard to solve, while we have in hand a family of explicit solutions to its homogeneous counterpart, (5.10). Therefore, as an approximation, we can assume that the whole solution $T_\psi(\boldsymbol{\chi})$, can be expressed as a homogeneous part T, which solves (5.10), and a small inhomogeneous perturbation $\psi(\boldsymbol{\chi})$.

Moreover, by taking into account that we need to match the degrees of freedom of the AR model, the two-dimensional perturbations over the group manifold, as introduced in [73], should be used. We further require matter frame dependence of the perturbation to take into account the inhomogeneity. Therefore, in the group representation, the condensate T_ψ can be written in the form

$$T_\psi(g_1, g_2, g_3; \boldsymbol{\chi}) = T(g_1, g_2, g_3) + \xi\psi(g_1, g_3; \boldsymbol{\chi}), \tag{5.29}$$

where $T(g_1, g_2, g_3)$ is a solution to the equation of motion (5.4), not necessarily to be the solution T_f we discussed above, $\psi(g_1, g_3; \boldsymbol{\chi})$ is the inhomogeneous perturbation whose dynamics will be determined below, and ξ is a real parameter with $0 < \xi \ll 1$, indicates that the perturbations is small. The PW coefficients of the perturbation are given by

$$\begin{aligned}\psi^{m_1m_2m_3}_{j_1j_2j_3}(\boldsymbol{\chi}) &= \sum_{\{n\}}\int [\mathrm{d}g]^3 \psi(g_1, g_3; \boldsymbol{\chi}) \prod_{i=1}^{3} \sqrt{2j_i+1}\bar{D}^{j_i}_{m_in_i} \begin{pmatrix} j_1 & j_2 & j_3 \\ n_1 & n_2 & n_3 \end{pmatrix} \\ &\equiv \delta^{j_2,0}\delta_{m_2,0}\delta^{j_1,j_3}\sqrt{2j_1+1}\psi^{j_1}_{m_1,m_3}(\boldsymbol{\chi}),\end{aligned} \tag{5.30}$$

where we used the fact that when $j_2 \neq 0$ the coefficients vanish, and when $j_2 = 0$ the equation (B.9) can be used for simplifications. The scaling factor $\sqrt{2j_1+1}$ in the last line

[1] It's worth emphasizing that being a condensate function, T has to solve the equation of motion (5.15), or in the homogeneous case, (5.10). Furthermore, any solution of equation (5.10) is also a solution of (5.15).

of equation (5.30) is introduced for later convenience. Therefore, in spin representation, the inhomogeneous condensate T_ψ can be written as

$$(T_\psi)^{m_1m_2m_3}_{j_1j_2j_3}(\boldsymbol{\chi}) = T^{m_1m_2m_3}_{j_1j_2j_3} + \xi\delta^{j_2,0}\delta_{m_2,0}\delta^{j_1,j_3}\psi^{j_1}_{m_1,m_3}(\boldsymbol{\chi}). \tag{5.31}$$

Substituting (5.31) into the action (5.14), we get the action for the perturbed solution

$$S_B[T_\psi(\boldsymbol{\chi})] = S_B[T] + \xi^2 \cdot S_{\text{eff}}[\psi] + \mathcal{O}(\xi^4), \tag{5.32}$$

where the first order in ξ vanishes since T is a solution to the equation of motion. The action $S_{\text{eff}}[\psi]$ represents the effective action of the perturbation field ψ^j_{mn} and contains corrections up to ξ. Therefore, $\xi^2 S_{\text{eff}}[\psi]$ contains corrections up to order ξ^3.

It is the main objective of the current chapter to get an explicit form of the effective action $S_{\text{eff}}[\psi]$. Generally, $S_{\text{eff}}[\psi]$ would be quite involving unless the homogeneous condensate T satisfies certain conditions. We will see that to get a generalization of the AR action, two conditions, (5.41) and (5.45), are required. And one can verify that these conditions are valid for the solution (5.28) automatically, and for solution (5.19) if f^j_{mn} satisfy the condition (5.55). Furthermore, since the AR model involves a field $\phi^j_m(\boldsymbol{\chi})$ (see equation (5.34) for the action and the involving fields of AR model) that transforms in a representation of $SU(2)$ and thus carrying only one magnetic index m, we will specialize the perturbations ψ under consideration to the following form

$$\psi^{j_1}_{m_1m_3}(\boldsymbol{\chi}) = \sum_m \sqrt{2j_1+1}\phi^{j_1}_m(\boldsymbol{\chi}) \begin{pmatrix} j_1 & j_1 & j_1 \\ m_1 & m & m_3 \end{pmatrix}. \tag{5.33}$$

As a mild spoiler, we will see that when two conditions (5.41) and (5.45) are satisfied, the effective dynamics of the perturbation of the form (5.33) will be determined by the action (5.49), which is a summation over AR models of different spin j. When the explicit solution (5.28) is substituted, several coefficients in the action (5.49) can be fixed, results in (5.61) and (5.62).

5.2 Amit-Roginsky model as perturbations over condensates

With the proper perturbations, we are ready to see how the AR-like action can emerge from the Boulatov model. We mentioned before that the AR model [81] is a cubic field theory, for a scalar field $\phi^j_m(\boldsymbol{\chi})$ with an internal vector symmetry, in the sense that ϕ^j_m transforms under the global $SO(3)$ (or $SU(2)$) group in the same way as vectors in the spin j representation. The $N = 2j+1$ fields ϕ^j_m coupled to themselves through the $3j$ symbol for a fixed value of the spin j, such that the interaction term is invariant under the action of $SO(3)$. In fact, we can write the action of AR model in the form [81, 82]

$$\begin{aligned} S_{AR}[\phi] = \int \mathrm{d}^d x \Bigg\{ & \frac{1}{2}\sum_m (-1)^{j-m}\left[(\nabla\phi^j_m)(\nabla\phi^j_{-m}) + \mu\phi^j_m\phi^j_{-m}\right] \\ & + \sum_{m_1,m_2,m_3} \frac{\lambda}{3!}\sqrt{2j+1}\begin{pmatrix} j & j & j \\ m_1 & m_2 & m_3 \end{pmatrix}\phi^j_{-m_1}\phi^j_{-m_2}\phi^j_{-m_3}\Bigg\}. \end{aligned} \tag{5.34}$$

The model is interesting as it's the only model whose interaction is cubic in field ϕ^j_m, and at the same time dominated by the so-called *melonic* graphs when $N = 2j + 1$ is large [82]. Melonic graphs are characterized by their distinct topology, featuring a tree-like structure with multiple internal lines connecting at a common vertex [82, 135].

The significance of melonic dominance lies in the fact that in the presense of it, the calculations and analyses of the Feynman graph can be simplified. The tree-like structure of melonic diagrams allows for certain summations and calculations to be performed analytically, leading to more tractable computations. This simplification becomes particularly advantageous when studying the renormalization properties of a theory, as it provides insights into the behavior of the theory at different energy scales [135].

However, in our generalized AR model, derived from Boulatov dynamics, we observe a loss of melonic dominance due to the inclusion of a summation over the spin j. Conducting a comprehensive renormalization analysis of the entire model goes beyond the scope of this thesis. Instead, our focus will be on demonstrating that the melonic dominance can be restored by employing appropriate approximations.

It can be seen that the effective action $S_{\text{eff}}[\psi]$ (or $S_{\text{eff}}[\phi]$) contains quadratic and cubic terms of ψ (or ϕ), which we will consider separately in the following. For simplicity, we omit from now to explicitly write the dependency on the matter frame $\boldsymbol{\chi}$.

5.2.1 Quadratic term

The quadratic term in ξ receives three kinds of contributions when substituting perturbation (5.31) into the Boulatov action (5.14). The kinetic term of Boulatov model gives rise to one contribution of the form $\psi\psi$. Then, the interaction term gives two distinct type of contributions, either of the form $TT\psi\psi$ or $T\psi T\psi$, depending on how the two perturbation fields are connected in the action. Schematically, we get the $TT\psi\psi$ term when the two perturbation fields ψ^j_{mn} share two magnetic indices, while in the $T\psi T\psi$ term they only share one. The two of them give different contribution to the effective action. In the following, we will consider the $\psi\psi$, $TT\psi\psi$ and $T\psi T\psi$ terms respectively.

$\psi\psi$ term. The kinetic term $\sum_{j_1,j_2,j_3} \left|(T_\psi)^{m_1,m_2,m_3}_{j_1,j_2,j_3}(\boldsymbol{\chi})\right|^2$ of the Boulatov action gives the following contribution to the effective action:

$$\begin{aligned}
&\sum_{\substack{j_1,j_2,j_3\\ m_1,m_2,m_3}} (-1)^{\sum_{i=1}^3 (j_i - m_i)} \left[\delta^{j_2,0}\delta_{m_2,0}\delta^{j_1,j_3}\psi^{j_1}_{m_1,m_3}\right]\left[\delta^{j_2,0}\delta_{-m_2,0}\delta^{j_1,j_3}\psi^{j_1}_{-m_1,-m_3}\right] \\
&= \sum_{\substack{j_1,m_1,m_3\\ m,m'}} (-1)^{2j_1 - m_1 - m_3}\phi^{j_1}_m\phi^{j_1}_{m'}(2j_1+1)\begin{pmatrix} j_1 & j_1 & j_1 \\ m_1 & m & m_3 \end{pmatrix}\begin{pmatrix} j_1 & j_1 & j_1 \\ -m_1 & m' & -m_3 \end{pmatrix} \\
&= \sum_{j_1,m_1} (-1)^{j_1 - m_1}\phi^{j_1}_{m_1}\phi^{j_1}_{-m_1}. \qquad (5.35)
\end{aligned}$$

This term is simply the quadratic term of the AR action (5.34). Note that this contribution is independent of the solution $T^{m_1m_2m_3}_{j_1j_2j_3}$, therefore it does not impose any restriction on the

homogeneous solution considered.

$TT\psi\psi$ term. There are four terms of type[1] $TT\psi\psi$. Each of them has the same contribution to the effective action as

$$\begin{aligned}
&\sum_{\substack{m_1,\cdots,m_6\\ j_1,\cdots,j_6}} \left\{ \begin{array}{ccc} j_1 & j_2 & j_3 \\ j_4 & j_5 & j_6 \end{array} \right\} (-1)^{\sum_i (j_i - m_i)} T^{-m_1,-m_2,-m_3}_{j_1 j_2 j_3} T^{m_3,m_5,-m_4}_{j_3 j_5 j_4} \\
&\times \delta^{j_2,0} \delta_{m_2,0} \delta^{j_4,j_6} \psi^{j_4}_{m_4,-m_6} \delta^{j_5,0} \delta_{m_5,0} \delta^{j_6,j_1} \psi^{j_6}_{m_6,m_1} \\
=& \sum_{\substack{m_1,m_3,m_4,m_6\\ j_1,j_3,j_4,j_6}} \left\{ \begin{array}{ccc} j_1 & 0 & j_3 \\ j_4 & 0 & j_6 \end{array} \right\} (-1)^{\sum_{i\neq 2,5} (j_i - m_i)} T^{-m_1,0,-m_3}_{j_1,0,j_3} T^{m_3,0,-m_4}_{j_3,0,j_4} \delta^{j_4,j_6} \delta^{j_6,j_1} \psi^{j_1}_{m_4,-m_6} \psi^{j_1}_{m_6,m_1} \\
=& \sum_{\substack{m_1,m_3,m_4,m_6\\ j_1}} (-1)^{6j_1 - \sum_{i\neq 2,5} m_i} T^{-m_1,0,-m_3}_{j_1,0,j_1} T^{m_3,0,-m_4}_{j_1,0,j_1} \psi^{j_1}_{m_4,-m_6} \psi^{j_1}_{m_1,m_6} \\
=& \sum_{j_1,m_1,m_6,m_4} \left[\sum_{m_3} (-1)^{-m_3-m_4} T^{-m_1,0,-m_3}_{j_1,0,j_1} T^{m_3,0,-m_4}_{j_1,0,j_1} \right] (-1)^{2j_1 - m_1 - m_6} \psi^{j_1}_{m_4,-m_6} \psi^{j_1}_{m_1,m_6}
\end{aligned} \tag{5.36}$$

Therefore, if the homogeneous solution $T^{m_1 m_2 m_3}_{j_1 j_2 j_3}$ satisfies the following condition

$$\sum_{m_3} (-1)^{-m_3-m_4} T^{-m_1,0,-m_3}_{j_1,0,j_1} T^{m_3,0,-m_4}_{j_1,0,j_1} = c_{1,j_1} \delta_{m_1,-m_4}, \tag{5.37}$$

for some arbitrary constants c_{1,j_1}, the contribution (5.36) from $TT\psi\psi$ term will reduce to

$$\begin{aligned}
&\sum_{\substack{m_1,\cdots,m_6\\ j_1,\cdots,j_6}} \left\{ \begin{array}{ccc} j_1 & j_2 & j_3 \\ j_4 & j_5 & j_6 \end{array} \right\} (-1)^{\sum_i (j_i - m_i)} T^{-m_1,-m_2,-m_3}_{j_1 j_2 j_3} T^{m_3,m_5,-m_4}_{j_3 j_5 j_4} \\
&\times \delta^{j_2,0} \delta_{m_2,0} \delta^{j_4,j_6} \psi^{j_4}_{m_4,-m_6} \delta^{j_5,0} \delta_{m_5,0} \delta^{j_6,j_1} \psi^{j_6}_{m_6,m_1} \\
=& \sum_{j_1,m_1,m_6,m_4} \left[\sum_{m_3} (-1)^{-m_3-m_4} T^{-m_1,0,-m_3}_{j_1,0,j_1} T^{m_3,0,-m_4}_{j_1,0,j_1} \right] (-1)^{2j_1 - m_1 - m_6} \psi^{j_1}_{m_4,-m_6} \psi^{j_1}_{m_1,m_6},
\end{aligned} \tag{5.38}$$

and when specializing to perturbations of the form (5.33) we get

$$\begin{aligned}
&\sum_{\substack{m_1,\cdots,m_6\\ j_1,\cdots,j_6}} \left\{ \begin{array}{ccc} j_1 & j_2 & j_3 \\ j_4 & j_5 & j_6 \end{array} \right\} (-1)^{\sum_i (j_i - m_i)} T^{-m_1,-m_2,-m_3}_{j_1 j_2 j_3} T^{m_3,m_5,-m_4}_{j_3 j_5 j_4} \\
&\times \delta^{j_2,0} \delta_{m_2,0} \delta^{j_4,j_6} \psi^{j_4}_{m_4,-m_6} \delta^{j_5,0} \delta_{m_5,0} \delta^{j_6,j_1} \psi^{j_6}_{m_6,m_1} \\
=& \sum_{j_1,m_1} c_{1,j_1} (-1)^{j_1 - m_1} \phi^{j_1}_{m_1} \phi^{j_1}_{-m_1}.
\end{aligned} \tag{5.39}$$

which is the kinetic term of the AR model.

[1] Which can be obtained by permutations of the fields that keeping the combinatorial structure, i.e., the four terms are $TT\psi\psi$, $\psi TT\psi$, $\psi\psi TT$ and $T\psi\psi T$ respectively.

The coefficients c_{1,j_1} remain arbitrary if we only require that T to be condensate, but can be fixed by using the explicit solutions, such as (5.19) and (5.28). On the other hand, we have to point out that the condition (5.37) is not an independent one. In fact, as we can see in the following, when the condition (5.45), obtained by the cubic term later, is satisfied, the condition (5.37) establishes automatically.

$T\psi T\psi$ term. The remaining two quadratic contributions from the interaction term of the Boulatov model are of the form[1] $T\psi T\psi$. Each of these terms contributes to the effective action as

$$\begin{aligned}
&\sum_{\substack{m_1,\cdots,m_6\\ j_1,\cdots,j_6}} (-1)^{\sum_i (j_i-m_i)} T^{-m_1,-m_2,-m_3}_{j_1 j_2 j_3} \delta^{j_5,0}\delta_{m_5,0}\delta^{j_3,j_4}\psi^{j_3}_{m_3,-m_4} \\
&\times T^{m_4,m_2,-m_6}_{j_4 j_2 j_6} \delta^{j_5,0}\delta_{m_5,0}\delta^{j_1,j_6}\psi^{j_6}_{m_6 m_1} \begin{Bmatrix} j_1 & j_2 & j_3 \\ j_4 & j_5 & j_6 \end{Bmatrix} \\
=& \sum_{\substack{m_1,m_3,m_4,m_6\\ j_1,j_3}} (-1)^{j_1+j_3-m_4-m_6} \psi^{j_3}_{m_3,-m_4}\psi^{j_1}_{m_6,m_1} \frac{1}{\sqrt{(2j_1+1)(2j_3+1)}} \\
&\times \sum_{j_2,m_2} (-1)^{\sum_{i=1}^3 (2j_i-m_i)} T^{-m_1,-m_2,-m_3}_{j_1,j_2,j_3} T^{m_4,m_2,-m_6}_{j_3,j_2,j_1}.
\end{aligned} \tag{5.40}$$

For a general solution of the equation of motion, this term leads to a non-diagonal kinetic term for the ψ fields, of different spins j_1 and j_3. To get the correct AR dynamics, we need to get rid of these non-diagonal terms, which can be achieved if the homogeneous solution T satisfies the condition

$$\sum_{j_2,m_2} (-1)^{\sum_{i=1}^3 (2j_i-m_i)} T^{-m_1,-m_2,-m_3}_{j_1,j_2,j_3} T^{m_4,m_2,-m_6}_{j_3,j_2,j_1} = c_{2,j_1} c_{2,j_3} \delta_{m_1,-m_6}\delta_{m_3,m_4}. \tag{5.41}$$

Under the condition (5.41), the contribution (5.40) becomes

$$\begin{aligned}
&\sum_{\substack{m_1,m_3,m_4,m_6\\ j_1,j_3}} (-1)^{j_1+j_3-m_4-m_6} \psi^{j_3}_{m_3,-m_4}\psi^{j_1}_{m_6,m_1} \frac{1}{\sqrt{(2j_1+1)(2j_3+1)}} \\
&\times \sum_{j_2,m_2} (-1)^{\sum_{i=1}^3 (2j_i-m_i)} T^{-m_1,-m_2,-m_3}_{j_1,j_2,j_3} T^{m_4,m_2,-m_6}_{j_3,j_2,j_1} \\
=& \left[\sum_{j_1,m_1} (-1)^{j_1-m_1} \frac{c_{2,j_1}}{\sqrt{2j_1+1}} \psi^{j_1}_{m_1,-m_1} \right]^2.
\end{aligned} \tag{5.42}$$

[1] The other term of the same type is $\psi T\psi T$.

Substituting the required form (5.33) of the perturbations to the term inside the bracket, we obtain

$$\begin{aligned}\sum_{j_1,m_1}(-1)^{j_1-m_1}\frac{c_{2,j_1}}{\sqrt{2j_1+1}}\psi^{j_1}_{m_1,-m_1} &= \sum_{j_1,m_1,m}(-1)^{j_1-m_1}c_{2,j_1}\phi^{j_1}_m\begin{pmatrix} j_1 & j_1 & j_1 \\ m_1 & m & -m_1\end{pmatrix},\\ &= \sum_{j_1}c_{2,j_1}\phi^{j_1}_0\sum_{m_1}(-1)^{j_1-m_1}\begin{pmatrix} j_1 & j_1 & j_1 \\ m_1 & 0 & -m_1\end{pmatrix},\\ &= \sum_{j_1}c_{2,j_1}\phi^{j_1}_0\delta_{j_1,0}\sqrt{2j_1+1},\\ &= c_{2,0}\phi^0_0, \end{aligned} \tag{5.43}$$

where the equation (B.8) is used. Therefore, the quadratic term obtained from $T\psi T\psi$ term can also be made diagonal under a proper choice of the condensate function T. This closes our calculations for the quadratic term, and we can now turn to the cubic term, which should have a similar form as the AR interaction in the action (5.34).

5.2.2 Cubic term

There is only one type of cubic contribution which comes from the interaction term of the Boulatov model, which can be represented by the form $T\psi\psi\psi$. There are four such terms[1], and they all contribute as

$$\begin{aligned}&\sum_{\{j,m\}}(-1)^{\sum_i(j_i-m_i)}T^{-m_1,-m_2,-m_3}_{j_1,j_2,j_3}\delta^{j_5,0}\delta_{m_5,0}\psi^{j_3}_{m_3,-m_4}\delta^{j_2,0}\delta_{m_2,0}\psi^{j_4}_{m_4,-m_6}\delta^{j_5,0}\delta_{m_5,0}\psi^{j_6}_{m_6,m_1}\begin{Bmatrix} j_1 & j_2 & j_3\\ j_4 & j_5 & j_6\end{Bmatrix}\\ =&\sum_{\substack{m_1,m_3,m_4,m_6\\ j_1}}(-1)^{-\sum_{i\neq2,5}-m_i}T^{-m_1,0,-m_3}_{j_1,0,j_1}\frac{(-1)^{2j_1}}{2j_1+1}\psi^{j_1}_{m_3,-m_4}\psi^{j_1}_{m_4,-m_6}\psi^{j_1}_{m_6,m_1}.\end{aligned} \tag{5.44}$$

If we demand the following condition for T

$$T^{-m_1,0,-m_3}_{j_1,0,j_1} = c_{3,j_1}(-1)^{-m_3}\delta_{m_1,-m_3}, \tag{5.45}$$

for some coefficient c_{3,j_1}, the contribution (5.44) becomes

$$\begin{aligned}&\sum_{\substack{m_1,m_3,m_4,m_6\\ j_1}}(-1)^{-\sum_{i\neq2,5}m_i}T^{-m_1,0,-m_3}_{j_1,0,j_1}\frac{(-1)^{2j_1}}{2j_1+1}\psi^{j_1}_{m_3,-m_4}\psi^{j_1}_{m_4,-m_6}\psi^{j_1}_{m_6,m_1}\\ =&\sum_{\substack{m_3,m_4,m_6\\ j_1}}(-1)^{2j_1-m_3-m_4-m_6}\frac{c_{3,j_1}}{2j_1+1}\psi^{j_1}_{m_3,-m_4}\psi^{j_1}_{m_4,-m_6}\psi^{j_1}_{m_6,-m_3}.\end{aligned} \tag{5.46}$$

[1] The full list of the terms under this type is $T\psi\psi\psi$, $\psi T\psi\psi$, $\psi\psi T\psi$ and $\psi\psi\psi T$.

After substituting the required form (5.33) of the perturbation, we get the desired interaction corresponds to AR model

$$
\begin{aligned}
&\sum_{\substack{m_1,m_3,m_4,m_6\\ j_1}} (-1)^{-\sum_{i\neq 2,5} m_i} T^{-m_1,0,-m_3}_{j_1,0,j_1} \frac{(-1)^{2j_1}}{2j_1+1} \psi^{j_1}_{m_3,-m_4} \psi^{j_1}_{m_4,-m_6} \psi^{j_1}_{m_6,m_1} \\
&= \sum_{\substack{m_3,m_4,m_6\\ j_1}} (-1)^{2j_1-m_3-m_4-m_6} \frac{c_{3,j_1}}{2j_1+1} \sum_{m,m',m''} \phi^{j_1}_m \phi^{j_1}_{m'} \phi^{j_1}_{m''} \\
&\quad \times \begin{pmatrix} j_1 & j_1 & j_1 \\ m_3 & m & -m_4 \end{pmatrix} \begin{pmatrix} j_1 & j_1 & j_1 \\ m_4 & m' & -m_6 \end{pmatrix} \begin{pmatrix} j_1 & j_1 & j_1 \\ m_6 & m'' & -m_3 \end{pmatrix} \\
&\quad \times (-1)^{j_1} \sum_{m_3,m_4,m_6} (-1)^{3j_1-m_3-m_4-m_6} \begin{pmatrix} j_1 & j_1 & j_1 \\ m & -m_4 & m_3 \end{pmatrix} \begin{pmatrix} j_1 & j_1 & j_1 \\ m_6 & m'' & -m_3 \end{pmatrix} \begin{pmatrix} j_1 & j_1 & j_1 \\ -m_6 & m_4 & m' \end{pmatrix} \\
&= \sum_{\substack{m,m',m''\\ j_1}} \frac{c_{3,j_1}}{2j_1+1} \begin{Bmatrix} j_1 & j_1 & j_1 \\ j_1 & j_1 & j_1 \end{Bmatrix} \phi^{j_1}_m \phi^{j_1}_{m'} \phi^{j_1}_{m''} \begin{pmatrix} j_1 & j_1 & j_1 \\ m & m' & m'' \end{pmatrix}. \qquad (5.47)
\end{aligned}
$$

In the calculation, we have used equations (B.4) and (B.11), and the fact that $(-1)^{2j_1} = 1$ since j_1 here has to be an integer for a non-vanishing $3j$ symbol.

Noting that if we substitute the condition (5.45) to the left hand side of the condition (5.37) obtained from $T\psi T\psi$ term, the result is

$$
\begin{aligned}
&\sum_{m_3} (-1)^{-m_3-m_4} T^{-m_1,0,-m_3}_{j_1,0,j_1} T^{m_3,0,-m_4}_{j_1,0,j_1} \\
&= \sum_{m_3} (-1)^{-m_3-m_4} c_{3,j_1} (-1)^{-m_3} \delta_{m_1,-m_3} \times c_{3,j_1} (-1)^{-m_4} \delta_{-m_3,-m_4}, \\
&= c^2_{3,j_1} \delta_{m_1,-m_4},
\end{aligned}
$$

which means that the condition (5.37) is satisfied automatically once we demand (5.45), and the constants c_{1,j_1} and c_{3,j_1} are related by

$$c_{1,j_1} = c^2_{3,j_1}. \qquad (5.48)$$

5.2.3 Emergence of the generalized Amit-Roginsky model

Now we are ready to extract AR model from the Boulatove action (5.14), based on two conditions (5.41) and (5.45) we discussed in last subsection. Our main result is the effective action (5.61) and (5.62) for each mode ϕ^j_m of the perturbation (defined through equation (5.33)). We can see that the form of these actions are the same as the AR ones [81, 82].

The effective action for the perturbation ψ. Putting together different terms we computed in the last subsection, we see that when the conditions (5.41) and (5.45) are satisfied, the inhomogeneous perturbation $\phi^j_m(\boldsymbol{\chi})$ of the form given by equation (5.33) would have a similar dynamics as in the AR model, such that the action can be written as

$$S[\phi^j_m] = S_0[\phi^0_0] + \sum_{j>0} S_j[\phi^j_m], \qquad (5.49)$$

where

$$S_0[\phi_0^0] = \int \mathrm{d}^3\boldsymbol{\chi}\left(\frac{1}{2}\left\{(\nabla\phi_0^0)^2 + \left[\mu^2 + \frac{\lambda}{3!}(2c_{3,0}^2 + c_{2,0}^2)\right](\phi_0^0)^2\right\} - \frac{\xi\lambda}{3!}c_{3,0}\left(\phi_0^0\right)^3\right), \tag{5.50}$$

and

$$\begin{aligned} S_j[\phi_m^j] = \int \mathrm{d}^3\boldsymbol{\chi}\Bigg\{&\frac{1}{2}\left[|\nabla\phi_n^j|^2 + \left(\mu^2 + \frac{\lambda}{3!}c_{3,j}^2\right)|\phi_n^j|^2\right] \\ &-\frac{c_{3,j_1}}{2d_j}\frac{\xi\lambda}{3!}\begin{Bmatrix} j & j & j \\ j & j & j \end{Bmatrix}\sum_{m_1,m_2,m_3}\phi_{m_1}^j\phi_{m_2}^j\phi_{m_3}^j\begin{pmatrix} j & j & j \\ m_1 & m_2 & m_3 \end{pmatrix}\Bigg\}, \end{aligned} \tag{5.51}$$

where $\sum_n |\phi_n^j|^2 = \sum_n (-1)^{j-n}\phi_n^j\phi_{-n}^j$. The fields ϕ_m^j with different spin label j decouple and each of them has the form of the AR action with j-dependent mass and coupling terms. And again, the coefficients $c_{2,j}$ and $c_{3,j}$ can be given explicitly after substituting solutions (5.19) and (5.28).

Computing coefficients c_i. We compute explicitly here the coefficients $c_{1,j}$, $c_{3,j}$ and $c_{2,j}$ for the homogeneous solution (5.16) to check that these conditions are compatible with our homogeneous solution. Substituting (5.16) into condition (5.45), we obtain

$$\mu\sqrt{\frac{3!}{\lambda}}d_{j_1}f_{00}^0\begin{pmatrix} j_1 & 0 & j_1 \\ -m_1 & 0 & -m_3 \end{pmatrix} = \mu\sqrt{\frac{3!d_{j_1}}{\lambda}}f_{00}^0(-1)^{j_1+m_3}\delta_{m_1,-m_3} = c_{3,j_1}(-1)^{-m_3}\delta_{m_1,-m_3}, \tag{5.52}$$

which leads to

$$c_{3,j} = \begin{cases} (-1)^j\mu\sqrt{\dfrac{3!d_j}{\lambda}}f_{00}^0 & \text{if } j \in \mathbb{N} \\ 0 & \text{otherwise} \end{cases}. \tag{5.53}$$

On the other hand, condition (5.41) yields

$$\begin{aligned} &\frac{3!\mu^2}{\lambda}\sum_{j_2,m_2}(-1)^{\sum_{i=1}^3(4j_i-m_i)}d_{j_1}d_{j_3}\sum_{n_2,l_2}f_{-m_2,-n_2}^{j_2}f_{m_2,l_2}^{j_2}\begin{pmatrix} j_1 & j_3 & j_2 \\ m_1 & m_3 & n_2 \end{pmatrix}\begin{pmatrix} j_1 & j_3 & j_2 \\ -m_6 & m_4 & l_2 \end{pmatrix} \\ &= c_{2,j_1}c_{2,j_3}\delta_{m_1,-m_6}\delta_{m_3,m_4}, \end{aligned} \tag{5.54}$$

which leads to the condition for $f_{m_2n_2}^{j_2}$

$$\sum_{m_2}(-1)^{n_2-m_2}f_{-m_2,-n_2}^{j_2}f_{m_2,l_2}^{j_2} = d_{j_2}c_{f,j_2}^2\delta_{n_2,l_2}, \tag{5.55}$$

for some new constants c_{f,j_2}. Together with the normalization condition (5.18) for f_{mn}^j, we get the condition that these new constants should satisfy

$$\begin{aligned} 1 &= \sum_{j_2,m_2,n_2,l_2}(-1)^{n_2-m_2}f_{-m_2,-n_2}^{j_2}f_{m_2,l_2}^{j_2}\delta_{n_2,l_2}, \\ &= \sum_{j_2}d_{j_2}^2c_{f,j_2}^2. \end{aligned} \tag{5.56}$$

And we can get the explicit form (5.58) of c_{f,j_2} by substituting the heat kernel regularized solution (5.28).

Using the heat kernel regularized solution. It's true that we can't fix the coefficients $c_{2,j}$ and $c_{3,j}$ completely with only the explicit solution (5.19), because (5.19) still contains an arbitrary function f. Therefore, to fix these coefficients completely, we need to use the solution (5.28) instead. Substituting the PW coefficients (5.26) of the regularized delta function Δ_ε into the equation (5.53), we see that for $j \in \mathbb{N}$, the constants $c_{3,j}$ become

$$c_{3,j} = (-1)^j \mu \sqrt{\frac{3! d_j}{\lambda}} (\Delta_\varepsilon)^0_{00} = (-1)^j \mu \sqrt{\frac{3! d_j}{\lambda}} \alpha_\varepsilon. \tag{5.57}$$

And the coefficients $c_{f,j}$ would have the form

$$c_{f,j} = \alpha_\varepsilon \mathrm{e}^{-\varepsilon C_j}. \tag{5.58}$$

Since equation (5.28) is only an approximate solution, we see that the condition (5.41) can only be satisfied approximately at first order in ε. Indeed, at first order in ε, equation (B.7) gives

$$\sum_{j,m} d_j \mathrm{e}^{-2\varepsilon C_j} \begin{pmatrix} j_1 & j_2 & j \\ m_1 & m_2 & m \end{pmatrix} \begin{pmatrix} j_1 & j_2 & j \\ m_1' & m_2' & m \end{pmatrix} \approx \delta_{m_1' m_1} \delta_{m_2' m_2}. \tag{5.59}$$

Hence the coefficients $c_{2,j}$ of the condition (5.41) can then be determined as

$$c_{2,j} = \mu d_j \alpha_\varepsilon \sqrt{\frac{3!}{\lambda}}. \tag{5.60}$$

This way we have fixed all the arbitrary coefficients appear in the conditions that T should satisfy, and it follows that the effective action obtained by using heat kernel regularized homogeneous solution (5.28) is

$$S_0[\phi_0^0] = \int \mathrm{d}^3\boldsymbol{\chi} \left\{ \frac{1}{2} \left[(\nabla \phi_0^0)^2 + \mu^2 \left(1 + 3\alpha_\varepsilon^2\right) (\phi_0^0)^2 \right] - \frac{\sqrt{\lambda}\xi\mu\alpha_\varepsilon}{\sqrt{3!}} \left(\phi_0^0\right)^3 \right\}, \tag{5.61}$$

$$\begin{aligned} S_j[\phi_m^j] = \int \mathrm{d}^3\boldsymbol{\chi} \Bigg\{ & \frac{1}{2} \left[|\nabla \phi_n^j|^2 + \mu^2 \left(1 + d_j \alpha_\varepsilon^2\right) |\phi_n^j|^2 \right] \\ & - \frac{(-1)^j}{\sqrt{3!}} \frac{\sqrt{\lambda}\xi\mu\alpha_\varepsilon}{2\sqrt{d_j}} \begin{Bmatrix} j & j & j \\ j & j & j \end{Bmatrix} \sum_{m_1,m_2,m_3} \phi^j_{m_1} \phi^j_{m_2} \phi^j_{m_3} \begin{pmatrix} j & j & j \\ m_1 & m_2 & m_3 \end{pmatrix} \Bigg\}, \end{aligned} \tag{5.62}$$

where the first equation corresponds to a massive scalar without internal degree of freedom, while the second equation is exactly the AR action for spin j, with mass and interaction coupling depend on fundamental GFT coupling and the spin index j. This shows that the AR model can be obtained as a particular perturbation (of the form (5.33)) around classical solutions of the Boulatov model, provided that the homogeneous solution T satisfies conditions given by equations (5.41) and (5.45).

5.3 Melonic dominance

As already mentioned before, an important feature of AR model is the dominance of melonic graphs at large $N = 2j + 1$ limit. However, the main difference between the effective action (5.49) and the original AR action is the presence of the sum over spins j. Therefore, we have to check whether this new summation spoils the existence of a melonic limit or not. Even though the general behaviour of $\{3nj\}$ symbols as functions of j is an open issue [136–139], one can qualitatively study the behaviour of the Feynman amplitudes of the model and give additional constraints to ensure the existence of the melonic limit.

One thing to be noted is that in the action (5.49) we deal with the $j = 0$ and $j \neq 0$ cases separately, as technically ϕ_0^0 for $j = 0$ is just an ordinary scalar field and can't be regarded as an AR one. In the following discussions, however, it's not of much different whether we take into account ϕ_0^0 or not, and including such field will make it easier in performing summations. Therefore, in the following we will set ϕ_0^0 at the same footing as other fields ϕ_m^j, for simplicity. And without further specification the summation over j are assumed to start from $j = 0$.

5.3.1 Feynman amplitudes for the non-regularized solution

For simplicity reasons, we will drop below the heat kernel regularization and work with the actions given by Equation (5.51), including the sum over spin labels j. As in the AR model, each Feynman diagram γ of our new model consists of isoscalar part I_γ and isospin part A_γ [81, 82]

$$\mathcal{A}_\gamma = \sum_j c_\gamma \left(\frac{\lambda\{6j\}}{3!\sqrt{2j+1}} \right)^v I_\gamma A_\gamma, \tag{5.63}$$

where c_γ is the combinatorial factor of the diagram. The melonic graphs are fully 2-particle reducible (F2PR) diagrams, i.e. they always admit a 2-cut which gives another melonic graph with fewer vertices, until the trivial graph is reached. For a F2PR diagram, the corresponding amplitude decomposes to [82]

$$\mathcal{A}_{\text{F2PR}} = \sum_j (2j+1)^{1-3n} \{6j\}^{2n}, \tag{5.64}$$

with for a graph with $v = 2n$ vertices. For a graph that is not fully 2-particle reducible (NF2PR), on the other hand, the Feynman amplitude can be factorized as a product of 2-particle irreducible graphs

$$\mathcal{A}_{\text{NF2PR}} = \sum_j (2j+1)^{-n_0-2n} \prod_{i=1}^{k} A_{\{3n_i j\}} \{6j\}^{2n}, \tag{5.65}$$

where n is one half of the number of vertices v, which also has the form

$$n = 1 + n_0 - k + \sum_{i=1}^{k} n_i, \tag{5.66}$$

and $A_{\{3n_ij\}}$ is the amplitude of a three-particle irreducible diagrams with $2n_i$ vertices, constituted by $\{3n_ij\}$ symbols [82].

When $N = 2j + 1$ goes to infinity, the amplitudes $\mathcal{A}_{\text{F2PR}}$ is conjectured to obey the following bound [81]

$$\mathcal{A}_{\text{NF2PR}} \leq \sum_j (2j+1)^{1-3n-\alpha} \{6j\}^{2n}, \tag{5.67}$$

for some positive real number $\alpha > 0$. Asymptotically, when $N \to \infty$, both $n \geq 1$ and the $6j$ symbol are small with respect to N. Therefore, we get the following bound

$$\mathcal{A}_{\text{F2PR}} < \sum_j N^{1-3n} = \sum_j (2j+1)^{1-3n} = \left(1 - 2^{1-3n}\right) \zeta(3n-1), \tag{5.68}$$

where ζ is the Riemann zeta function, which is a monotonically decreasing finite function of n. In performing the summation we have used the fact that $\sum_j \frac{1}{(2j+1)^\alpha} = \left(1 - 2^{-\alpha}\right) \zeta(\alpha)$, which can be deduced from the following observation

$$\begin{aligned} \zeta(\alpha) &= \sum_{n=1}^{\infty} \frac{1}{n^\alpha}, \\ &= \sum_{j=0}^{\infty} \frac{1}{(2j+1)^\alpha} + \sum_{j=1}^{\infty} \frac{1}{(2j)^\alpha}, \\ &= \sum_{j=0}^{\infty} \frac{1}{(2j+1)^\alpha} + \frac{1}{2^\alpha} \zeta(\alpha), \end{aligned}$$

If one assumes that the bound (5.67) holds for any value of $N = 2j + 1$, then the amplitude of a NF2PR graphs is also finite. If the bound (5.67) fails to hold for values of N satisfying $N < N_t$ for some bound N_t, then the sum from $N = 1$ to $N = N_t$ is still a finite number, while the sum from $N = N_t$ is finite as well. Therefore, it is possible that $\mathcal{A}_{\text{NF2PR}}$ is comparable with $\mathcal{A}_{\text{F2PR}}$ since the maximal value of $\zeta(3n-1)$ is only $\pi^2/6 \simeq 1.645$.

One can thus conclude that the sum over j can dramatically change the amplitude of a Feynman graphs of the AR model and spoil the melonic limit at large j. In fact, it is one can expect as there is no melonic dominance in the Feynman expansions in the theory of ordinary scalar field ϕ^0_0, and for other fields ϕ^j_m with finite j, the situation is not of much different. The melonic limit can only be obtained if we take the limit $j \to \infty$. Such observation also provides us a way to restore the melonic dominance with suitable approximations, as we are going to illustrate in the following subsection.

5.3.2 Restoring the melonic dominance

One naive way to restore the melonic dominance is to further specialize the form of the perturbation (5.31) in order to enforce the selection of one spin j, thus getting rid of the sum over spin labels and leading to the original AR model

$$(T_\psi)^{m_1 m_2 m_3}_{j_1 j_2 j_3}(\boldsymbol{\chi}) = T^{m_1 m_2 m_3}_{j_1 j_2 j_3} + \delta^{j_1 j} \delta^{j_2, 0} \delta_{m_2, 0} \psi^{j_1}_{m_1, m_3}(\boldsymbol{\chi}), \tag{5.69}$$

such that we get exactly the AR model without any generalization, which possesses the property of melonic dominance in the limit of large $N = 2j + 1$ [81, 82].

Another way to recover melonic dominance is to work with the approximate solution (5.27). Indeed, when $j_2 = 0$ the solution takes the form:

$$(T_\varepsilon)^{m_1 m_2 m_3}_{j_1 j_2 j_3} = \mu\alpha_\varepsilon \sqrt{\frac{3!}{\lambda}} \mathrm{e}^{-2\varepsilon C_{j_1}} \sqrt{2j_1+1}(-1)^{j_1-m_1}\delta_{j_1,j_3}\delta_{m_1,-m_3}. \tag{5.70}$$

For $\varepsilon = \dfrac{1}{2N(N+1)}$, the expression above scales as $\sqrt{2j_1+1}$ for $j_1 < N$. Hence, in the PW expansion, the coefficients with larger j are dominant, and the coefficients $(T_\varepsilon)^{m_1 m_2 m_3}_{j_1 j_2 j_3}$ with $j_i < N_0$ for some threshold N_0 can be neglected. At first order in ε one then has

$$(T_\psi)^{m_1 m_2 m_3}_{j_1 j_2 j_3}(\boldsymbol{\chi}) \simeq \begin{cases} T^{m_1 m_2 m_3}_{j_1 j_2 j_3} + \delta^{j_1 j}\delta^{j_2,0}\delta_{m_2,0}\psi^{j_1}_{m_1,m_3}(\boldsymbol{\chi}), & N_0 \le j_i \le N \\ 0, & \text{otherwise} \end{cases}.$$

Such perturbations ϕ^j_m will lead to the isospin part of the amplitude of the form

$$\mathcal{A}_\gamma = \sum_{j=N_0}^{j=N} c_\gamma \left(\frac{\lambda\{6j\}}{3!\sqrt{2j+1}}\right)^v I_\gamma A_\gamma, \tag{5.71}$$

which becomes an infinitesimal again for large N_0 and N, while the NF2PR graphs are higher order infinitesimals as in the original AR model. The melonic dominance is thus restored under suitable approximations.

5.4 Summary

In this chapter, we showed how a homogeneous but anisotropic condensate state looks like in GFT, and how to introduce inhomogeneous perturbations over such states. For simplicity, we considered a 3d GFT, the Boulatov model, instead of the 4d case. In fact, what we relied on is a slightly generalized version of the original Boulatov model, with the additional coupling with free massless scalar fields $\boldsymbol{\chi}$, served as matter reference frame, which is required to introduce properly the notion of *inhomogeneity*. The condensate can be represented by a function T, corresponds to the expectation value of GFT field operator, and has to be a solution of the classical equation of motion. Generally, without imposing isotropic condition on purpose, such solutions would be anisotropic, hence the combinatorial structure of the interaction term is important in determining the GFT dynamics [73], in contrast to the cosmological sector we discussed previously.

Furthermore, with a proper choice of the inhomogeneous perturbations, one can show that a generalized version of AR model emerges if the condensate T satisfies certain conditions. Although the study of classical solutions to GFT dynamics (including the Boulatov model) is basically an unknown area, with only a few exceptions [29, 73, 80], our result is

quite general without using any explicit solutions, i.e., to get an AR-like action it's sufficient to require T to be a solution. The explicit solutions are only needed later when we try to fix several coefficients appearing in such action.

The main difference between our effective action (5.49) for the perturbation and the usual AR model is the presence of the summation on the spin index j. This difference, have significant consequences on the Feynman expansions of the AR model. Most notably, in our generalized version, the Feynman graph is not dominated by melonic diagrams when we take the large $N = 2j + 1$ limit. This is actually what one can expect, though, as even for the original AR model, the melonic dominance can only be obtained when N is large, and is absent for a finite N [82]. This observation also provides us a way to restore the melonic dominance, i.e., the limit can be restored if we remove the modes with finite spin j. We can achieve this either by specializing the type of perturbation considered, or by making use of the heat kernel regularization and taking a double scaling limit.

Chapter 6

Discussion

In this thesis, we have shown how to extract physical consequences of quantum gravity effects from GFT condensates, including both isotropic and anisotropic ones. We emphasize again that in thesis the terms *isotropic* and *anisotropic* are defined locally, used to distinguish situations whether we can characterize the condensate function by identical spins, such that the combinatorial structure of GFT interactions can be ignored in the isotropic case. They are not necessarily related to the corresponding properties of the emerged spacetime, and in particular an isotropic spacetime allows triangulations based on anisotropic building blocks [76].

The isotropic condensate. As we have seen in chapter 2, the way we implement isotropy by forcing spins to be identical could simplify our analysis of the GFT dynamics significantly. The main reason is the decoupling of dynamics for different modes under such simplification, which made it possible to consider the contribution to volume of each mode individually, without affecting the dynamics of other modes. In other words, we can safely set most of the modes to vanish without changing the evolution of one or two modes of interest, making it easier to extract some useful information of the cosmological evolution from the modified FLRW equations (2.28) and (2.29).

Based on the volume and its derivatives, we can introduce a useful quantity, the effective equation of state w, to reveal properties of the evolution otherwise hard to identify. In particular, some previous results in GFT condensate cosmology can be rewritten using w, and we can see that at the bounce $w \to -\infty$, corresponds to an expansion with infinite accelerations, but such accelerating phase won't last long before we enter the Friedmann phase. The inclusion of other modes doesn't change the qualitative behaviour of the expansion, which can be viewed as a consistency check of the GFT formalism, since in the early universe the volume is small and no mode should be taken dominant.

At late times of the universe evolution, the volume is large and GFT interactions should be taken into account. The equation of motion (2.26) for each mode can be solved approximately at the large volume limit, and the solution (3.17) diverges at finite relational time $\phi = \phi_{j\infty}$ for each mode ρ_j. This indicates that asymptotically there is indeed only a single mode, which has the smallest $\phi_{j\infty}$, becomes dominant. The EoS w also approaches

to a constant value as the volume grows, and in particular, for interactions with $n = 6$, we see that $w \to -1$, which corresponds to the cosmological constant. Including other modes won't change the asymptotic value of w, but the way how the asymptote is reached. For example, as we discussed in chapter 3, in the two modes case with $n = 6$ interaction term, a phantom phase can emerge where $w < -1$ and the EoS reaches -1 from below, which is impossible for the single mode case. The appearance of the phantom phase in our model is of purely quantum gravity origin. Furthermore, with a slightly more complicate interaction kernel, it's also possible to combine inflationary and phantom phases together, without the need of inflaton nor dark energy field.

The nature of the phantom behaviour can be investigated further with suitable approximations. For example, we are able to show that the phantom crossing should happen recently in our model, and its position should also close to the location where w reaches its minimum. This result suggests that the evolution in the two modes case can be seen as a small deviation at late times compared to the single mode case. When fitting the model with possible data, such modifications will increase the value of current Hubble parameter H_0 as shown in table 4.1. In standard ΛCDM model, such increasing is required to alleviate the H_0 tension [66], which reveals the discrepancy between CMB and supernova data [61]. At current stage, we are not able to couple the full realistic matter content of our universe to GFT, making it hard to test our formalism by actual observations. But at least our result shows the potential of solving cosmological puzzles based on quantum gravity effects.

The anisotropic condensate. When we come to the anisotropic condensates, whose wave function can't be labelled by identical spins, the dynamics of different modes couple together in the interaction term and one is not allowed to separate a certain mode out. To be more precise, it's not possible to assume as before that only a few modes contribute while set other modes to vanish, as the equation of motion would be invalid under such assumptions. One can imagine how complicated it could be if one tries to calculate geometric quantities, such as the total volume we introduced in the cosmological sector.

Fortunately, it's possible to reveal interesting physical information from the anisotropic condensate without considering these geometrical quantities. As we have seen in chapter 5, by considering perturbations over the condensate, we are able to extract dynamics of matter fields, in particular the AR model of a scalar field with internal $SO(3)$ symmetry [81, 82]. The emergence of the AR model based on the perturbations of the form (5.33) which matches degrees of freedom of the AR field, and the fact that condensate function T is a solution of equation of motion and satisfy two conditions (5.41) and (5.45). In fact, what we obtain is a slightly generalized version of the AR model, with an additional summation over spins in the effective action of the perturbations. There are arbitrary coefficients in the action (which can be traced back to the conditions (5.41) and (5.45)), that can only be fixed by substituting explicit solutions. The important lesson that worth mentioning is that, the matter field we extracted this way can be massive, which is interesting from the GFT perspective as it's usually hard to implement massive fields in our context [72].

The AR model, and our generalization to it, are field theories in the ordinary QFT, and in particular, they are defined over flat space. This is one can expect as for 3d, gravity has no local degree of freedom, and the solution of Einstein equations without matter can only be flat [140, 141]. What's puzzling is how the flat space, which is isotropic as well, would emerge from the complicated contributions of the modes that constitute the solution. Indeed, we can say that even an isotropic space admits anisotropic triangulations, but how exactly it works is still unclear.

Outlooks. More generally, one may ask what kind of spacetime can be extracted from GFT formalism, or how can we identify the structure of a spacetime corresponds to a given solution (hence should correspond to a condensate as well) of the GFT dynamics? The simple examples illustrated previously in this thesis can only show that it's possible to extract the macroscopic phenomena from the underlying microscopic quantum gravity theories, but not able to answer such questions in a more general setting. In particular, can we get any concrete criterion on the condensates such that the emerged spacetime would be isotropic?

The proper definition of isotropy seems to relate to the way we embed the building blocks into the emerged spacetime [75, 76]. In the 4d case, for example, one can define the isotropy using equilateral tetrahedra and then the introduction of condensate corresponds to non-equilateral ones would result in anisotropies [76]. But this doesn't explain *why* we need to consider the equilateral tetrahedra in the first place, and as we have seen in the case of Boulatov mode, the space resulted from a bunch of non-equilateral building blocks can still be isotropic. In the later case, although it's possible to extract phenomenological results without using geometrical quantities, they are required for a detailed analysis of the underlying spacetime. One needs to find a proper way to work out the summation over spins when different modes coupled together. At the current stage, the few examples available in the GFT community didn't provide many clues to address these issues.

Besides the above issue regarding the emerged spacetime, the use of isotropic condensate in the cosmological setting also introduces other simplifications or limitations.

One technical point is that in such case we are allowed to use an effective interaction kernel (2.22), in the sense that under the isotropic restriction, our dynamics only incorporates some aspects of known models in the isotropic restriction (for example, the fact that different spin modes decouple, as in the EPRL model), but not their detailed expression. In other words, as we noted, the approach we have taken is rather phenomenological, not working with any specific GFT model but with a rather general expression. On the one hand, this has the advantage of ensuring a certain degree of generality for our results, but on the other the method followed in this thesis should be complemented by a careful analysis of specific GFT models (including the study of their renormalization group flow), to make sure that our expression captures their relevant features at this cosmological level, or to extract new ingredients that need to be added to the phenomenological expression, as potentially changing the resulting cosmological evolution.

As a basis for such effective phenomenological approach, we also used the mean-field

approximation, which may not be trusted at late times, where the interactions become large (indeed, recent analyses confirm this worry [92]). But, we emphasize again, in our work the only true relevant ingredients are encoded in the choice of effective action. We used the simplest (mean field) approximation to it for simplicity, and for a closer contact with previous works in the literature, but one can easily consider a more general setting. The main point of our results is that including more than one mode in such effective action can indeed change the evolution of the universe, especially at late times, before one single mode becomes dominating.

More precisely, in order to obtain the expression (2.27) for the total volume, we used the mean-field approximation based on coherent states. However, for more general states, we do not expect that the template for the derivation of relational volume observable and its dynamics would be much different. Like in ordinary quantum field theory, the generic quantum effective action for GFTs is also a function of the effective mean field corresponding to the expectation value of the field operator in the true vacuum/ground state of the theory (rather than the simple coherent state we used), and a similar approximation in which such mean field is suitably peaked with respect to the relational clock would lead to the desired expression for corresponding observables as well. In this sense, as we have already pointed out in chapter 2, the effective action we used actually takes into account already the quantum corrections, and shouldn't be viewed simply as obtaining from the mean-field approximation and subjecting modifications from quantum fluctuations.

From an even broader perspective, our universe is way too simple to be fully realistic. At least we need to improve our analysis to include additional matter content, starting from general interacting scalar fields [72] but including then also the typical fluid components used in standard cosmological scenarios, such as radiation and the non-relativistic matter. Furthermore, in our analysis of the cosmological evolution we only considered isotropic and homogeneous universes spacetime, thus ignored the effects from anisotropies and inhomogeneities, even at a perturbative level, on the evolution of the universe. Interesting work in both these directions have been done, in the GFT cosmology literature [51, 74–76, 142, 143]. A possible way to see how the massive matter fields will change the cosmological evolution is to use the matter emerged from inhomogeneities, as we have seen in chapter 5, albeit for the Boulatov model of 3d gravity. If we can implement the same procedure in the more realistic 4d case, the cosmological effects come from massive matter can then be viewed as back reactions of perturbations to the background homogeneous condensate, similarly as in the standard cosmological scenario [144, 145].

Ideally, we should combine the methods used in this thesis together, i.e., working in a microscopic GFT model without ignoring the combinatorial structure of the interaction term, as well as studying the behaviour of the full geometric quantity like the total volume in this case where different modes coupled to each other. The isotropic property of our universe could emerge more naturally without enforcing the equilateral constrain. Based on which, a proper description of the cosmological inhomogeneities is also needed to make solid contact with cosmological observations and truly embed physical cosmology within our quantum gravity framework. This remains our main goal.

Appendix A

Effective equation of state, convergence of total volume and $\phi_{j\infty}$

In this appendix, we show in detail the derivation of several results in 3, which omitted in the main text. We will show how the EoS in relational language can be derived, how the boundedness of the mass term of GFT is resulted from the requirement that the total volume should be finite, and how the value of $\phi_{j\infty}$ can be corrected by comparison with the case where $n_j = 4$.

A.1 The effective equation of state

We want to define the EoS of the content in the universe using only geometrical quantities. From the FLRW equation in a universe filled with different matter contents (represented by i)

$$H^2 = \frac{1}{3}\sum_i \rho_i,\ \ \dot{H} = -\frac{1}{2}\sum_i(\rho_i + p_i) = -\frac{1}{2}\sum_i(1+w_i)\rho_i,$$

where $H = \frac{\dot{a}}{a}$ is the Hubble parameter, $\dot{}$ represents derivative respect to commoving time, and $w_i = p_i/\rho_i$ is the EoS for matter species. We can define an effective EoS as

$$1 + w = -\frac{2\dot{H}}{3H^2}. \tag{A.1}$$

In the relational time ϕ, we have

$$H = \frac{\dot{a}}{a} = \frac{1}{3}\frac{\mathcal{V}'}{\mathcal{V}}\dot{\phi}. \tag{A.2}$$

Using the fact that $\pi_\phi = \dot{\phi}\mathcal{V}$ is a conserved quantity, we have $0 = \ddot{\phi}\mathcal{V} + \dot{\phi}\dot{\mathcal{V}} = \ddot{\phi}\mathcal{V} + \dot{\phi}^2 V'$, and $\ddot{\phi}$ can be solved as

$$\ddot{\phi} = -\frac{\mathcal{V}'}{\mathcal{V}}\dot{\phi}^2.$$

Therefore we have [45]

$$\dot{H}=\frac{1}{3}\frac{\mathrm{d}}{\mathrm{d}\phi}\frac{\mathcal{V}'}{\mathcal{V}}\dot{\phi}^2+\frac{1}{3}\frac{\mathcal{V}'}{\mathcal{V}}\ddot{\phi}=\frac{1}{3}\frac{\mathcal{V}''}{\mathcal{V}}\dot{\phi}^2-\frac{1}{3}\left(\frac{\mathcal{V}'}{\mathcal{V}}\right)^2-\frac{1}{3}\left(\frac{\mathcal{V}'}{\mathcal{V}}\right)^2\dot{\phi}^2=\frac{1}{3}\dot{\phi}^2\left[\frac{\mathcal{V}''}{\mathcal{V}}-2\left(\frac{\mathcal{V}'}{\mathcal{V}}\right)^2\right].$$

And the EoS can be rewritten as

$$w=-\frac{2}{3}\frac{\dot{H}}{H^2}-1=-2\left[\frac{\mathcal{V}\mathcal{V}''}{(\mathcal{V}')^2}-2\right]-1=3-\frac{2\mathcal{V}\mathcal{V}''}{(\mathcal{V}')^2}\quad. \tag{A.3}$$

When the evolution of the EoS is known, the evolution of volume of universe can be recovered. To do this, we first introduce the relational Hubble parameter[1]

$$G=\frac{\mathcal{V}'}{\mathcal{V}}\quad. \tag{A.4}$$

Then the effective EoS (A.3) can be written by

$$w=1-\frac{2G'}{G^2}\quad. \tag{A.5}$$

Suppose that w is known, the equation is an ordinary differential equation of G and can be solved by

$$G=\left(\int_{\phi_0}^{\phi}\frac{w(\chi)-1}{2}\mathrm{d}\chi+\frac{1}{G_0}\right)^{-1}, \tag{A.6}$$

where $G_0=G(\phi_0)$ is the initial value of G. Then the definition (A.4) of G becomes a differential equation of volume $\mathcal{V}$, and can be solved as

$$\ln\mathcal{V}=\int_{\phi_0}^{\phi}\mathrm{d}\kappa\left(\int_{\phi_0}^{\kappa}\frac{w(\chi)-1}{2}\mathrm{d}\chi+\frac{1}{G_0}\right)^{-1}+\ln\mathcal{V}_0, \tag{A.7}$$

with $\mathcal{V}_0=\mathcal{V}(\phi_0)$. Hence, the evolution of volume respect to relational time ϕ is recovered.

A.2 The consequences of the convergence of total volume $\mathcal{V}$

In this appendix we consider how the convergence of $\mathcal{V}$ will constrain parameters in our model. When ϕ is large, we will have

$$\sqrt{E_j^2+m_j^2Q_j^2}\cosh(2m_j\phi)-E_j>\sqrt{E_j^2+m_j^2Q_j^2}.$$

[1] Using the relation between volume and scale factor $\mathcal{V}=a^3$, we see that the relation between Hubble parameter H and the relational one G is $H=\frac{\dot{a}}{a}=\frac{a'}{a}\dot{\phi}=\frac{G}{3}\dot{\phi}$.

Therefore, if $\mathcal{V}$ is convergent, the series

$$\sum_j \frac{\mathcal{V}_j}{m_j^2}\sqrt{E_j^2 + m_j^2 Q_j^2} \tag{A.8}$$

must also be convergent. Then if m_j is unbounded in the sense that $m_j \to \infty$ for $j \to \infty$, $\mathcal{V}$ would certainly be divergent cause in terms with sufficient large j, we will have $\cosh(2m_j\phi) \to \infty$ for non-zero ϕ. Therefore, the convergence of $\mathcal{V}$ also requires m_j to be bounded.

Conversely, if series (A.8) is convergent and $\forall j,\ m_j \leq m$ with a given m, then

$$\cosh(2m_j\phi) \leq \cosh(2m\phi),$$

which leads to the convergence of series

$$\sum_j \left[\frac{\mathcal{V}_j}{m_j^2}\sqrt{E_j^2 + m_j^2 Q_j^2}\cosh(2m\phi)\right] = \cosh(2m\phi)\sum_j \frac{\mathcal{V}_j}{m_j^2}\sqrt{E_j^2 + m_j^2 Q_j^2},$$

since its right hand side is convergent according to our assumption. Therefore, series

$$\sum_j \left[\frac{\mathcal{V}_j}{m_j^2}\sqrt{E_j^2 + m_j^2 Q_j^2}\cosh(2m_j\phi)\right] \tag{A.9}$$

converges as well. Furthermore, since $E_j < \sqrt{E_j^2 + m_j^2 Q_j^2}$, we see that $\sum_j \frac{\mathcal{V}_j E_j}{m_j^2}$ is also convergent.

In conclusion, if we require $\rho_j' = 0$ at the bounce for all j, then $\mathcal{V}$ is convergent if and only if $\sum_j \frac{\mathcal{V}_j}{m_j}\sqrt{E_j^2 + m_j Q_j^2}$ converges and m_j's are bounded. Just as we referred in section 3.2.

A.3 Behaviour of $\phi_{j\infty}$ in $n_j = 4$ case for small λ_j

Here we consider the large ρ_j behaviour for $n_j = 4$ case, where we have an exact solution. In fact, for $n_j = 4$, the solution of equation of motion (3.5) with $\mu_j = 0$ can be expressed using elliptic functions. With the convention that $F(\phi, m) = \int_0^\phi \frac{1}{\sqrt{1 - m\sin^2(\theta)}}\mathrm{d}\theta$, we have the solution for a given mode j with $\lambda_j < 0$ [146]

$$\phi = \sqrt{\frac{2}{-\lambda(\omega_3 - \omega_1)}}F\left(\sin^{-1}\left(\sqrt{\frac{\rho_j^2 - \omega_3}{\rho_j^2 - \omega_2}}\right), \frac{\omega_2 - \omega_1}{\omega_3 - \omega_1}\right), \tag{A.10}$$

where $\omega_3 > \omega_2 > \omega_1$ are three real roots of the polynomial

$$P(\chi) = \chi^3 - \frac{m^2}{2\lambda}\chi^2 - \frac{E}{\lambda}\chi + \frac{2Q^2}{\lambda} \qquad , \tag{A.11}$$

and the solution valid for $\rho_j > \sqrt{\omega_3}$. Note that $|\lambda_j|$ should be small enough such that the three roots of the polynomial (A.11) are all real. Setting $\rho_j \to \infty$ in the solution (A.10), we get the exact asymptotic value $\phi_{j\infty}$ in $n_j = 4$ case

$$\phi_{j\infty} = \sqrt{\frac{2}{-\lambda_j(\omega_3 - \omega_1)}} K\left(\frac{\omega_2 - \omega_1}{\omega_3 - \omega_1}\right). \tag{A.12}$$

Now we consider the behaviour of this $\phi_{j\infty}$ for small $|\lambda_j|$. To do this, we need first find the approximate roots for the polynomial (A.11). At the first order of λ_j, these roots are

$$\begin{aligned}
\omega_1 &= \frac{2m_j^2}{2\lambda_j} + \frac{2E_j}{m_j^2} + \frac{2E_j^2}{m_j^6}\lambda_j, \\
\omega_2 &= E_j - \sqrt{E_j^2 + m_j^2 Q_j^2} + \frac{Q_j^4\left(1 + \frac{E_j}{\sqrt{E_j^2+m_j^2Q_j^2}}\right)}{4m_j^2\left(E_j - \sqrt{E_j^2 + m_j^2 Q_j^2}\right)^2}\lambda_j, \\
\omega_3 &= \frac{Q_j^2}{E_j + \sqrt{E_j^2 + m_j^2 Q_j^2}} + \frac{Q_j^4\left(1 - \frac{E_j}{\sqrt{E_j^2+m_j^2Q_j^2}}\right)}{4m_j^2(E_j + \sqrt{E_j^2 + m_j^2 Q_j^2})^2}\lambda_j.
\end{aligned}$$

Then, putting these approximations of roots into equation (A.12), we can further expand $\phi_{j\infty}$ with respect to small λ_j using the expansion $K(x) \to \ln\frac{4}{\sqrt{1-x}}$ for $x \to 1$, and we will obtain the same result as given by the corrected value (3.22) of $\phi_{j\infty}$.

Appendix B

Definitions and identities from $SU(2)$ recoupling theory

We give several definitions and properties related to $SU(2)$ recoupling theory used in the article. All those properties are classical results on recoupling theory of $SU(2)$, and we refer the interested reader to Ilkka Mäkinen's introduction [89] on the topic for more details.

B.1 Haar measure and Wigner matrices

From the Peter-Weyl theorem, the Wigner matrices $D^j_{mn}(g)$ form an orthogonal basis of the functions $f : SU(2) \to \mathbb{C}$. This orthogonality relation is encoded in the Haar measure via the relation

$$\int \mathrm{d}g D^j_{mn}(g)\bar{D}^{j'}_{m'n'}(g) = \frac{1}{(2j+1)}\delta^{jj'}\delta_{mm'}\delta_{nn'}, \tag{B.1}$$

where the Wigner matrices satisfy

$$D^j_{mn}(g) = (-1)^{m-n}\bar{D}^j_{-m,-n}(g). \tag{B.2}$$

B.2 $3j$-symbol and its properties

The $3j$ symbol is invariant under the action of $SU(2)$ group,

$$D^{j_1}_{m_1n_1}D^{j_2}_{m_2n_2}D^{j_3}_{m_3n_3}\begin{pmatrix} j_1 & j_2 & j_3 \\ n_1 & n_2 & n_3 \end{pmatrix} = \begin{pmatrix} j_1 & j_2 & j_3 \\ m_1 & m_2 & m_3 \end{pmatrix}. \tag{B.3}$$

It's also invariant under the even permutations of indices, while it acquires an additional phase under odd permutations

$$\begin{pmatrix} j_1 & j_2 & j_3 \\ m_1 & m_2 & m_3 \end{pmatrix} = (-1)^{\sum_{i=a}^{3}(j_a - m_a)}\begin{pmatrix} j_1 & j_3 & j_2 \\ m_1 & m_3 & m_2 \end{pmatrix}. \tag{B.4}$$

The same phase also appear if we replace m_i by their negative

$$\begin{pmatrix} j_1 & j_2 & j_3 \\ -m_1 & -m_2 & -m_3 \end{pmatrix} = (-1)^{\sum_{i=a}^{3}(j_a - m_a)} \begin{pmatrix} j_1 & j_2 & j_3 \\ m_1 & m_2 & m_3 \end{pmatrix}. \tag{B.5}$$

The $3j$ symbols satisfy two orthonormal relations

$$(2j_3+1)\sum_{m_1,m_2} \begin{pmatrix} j_1 & j_2 & j_3 \\ m_1 & m_2 & m_3 \end{pmatrix} \begin{pmatrix} j_1 & j_2 & j_3' \\ m_1 & m_2 & m_3' \end{pmatrix} = \delta_{j_3,j_3'}\delta_{m_3,m_3'}, \tag{B.6}$$

$$\sum_{j_3,m_3} (2j_3+1) \begin{pmatrix} j_1 & j_2 & j_3 \\ m_1 & m_2 & m_3 \end{pmatrix} \begin{pmatrix} j_1 & j_2 & j_3 \\ m_1' & m_2' & m_3 \end{pmatrix} = \delta_{m_1,m_2'}\delta_{m_2,m_2'}, \tag{B.7}$$

Finally, when one of the magnetic moment (say m_3) vanishes, then the $3j$ symbol vanishes unless $m_1 = -m_2$, and we have

$$\sum_m (-1)^{j-m} \begin{pmatrix} j & j & k \\ m & -m & 0 \end{pmatrix} = \sqrt{2k+1}\delta_{k,0}. \tag{B.8}$$

And in particular for $k = 0$ we have

$$\begin{pmatrix} j_1 & 0 & j_3 \\ n_1 & 0 & n_3 \end{pmatrix} = \delta^{j_1,j_3} \frac{1}{\sqrt{2j_1+1}} (-1)^{j_1+n_1}\delta_{n_1,-n_3} \tag{B.9}$$

B.3 $6j$-symbol and its properties

The $6j$ symbol is defined as

$$\begin{Bmatrix} j_1 & j_2 & j_3 \\ j_4 & j_5 & j_6 \end{Bmatrix} = \sum_{j_i,m_i} (-1)^{\sum_{a=1}^{6}(j_a - m_a)} \begin{pmatrix} j_1 & j_2 & j_3 \\ -m_1 & -m_2 & -m_3 \end{pmatrix} \begin{pmatrix} j_1 & j_5 & j_6 \\ m_1 & -m_5 & m_6 \end{pmatrix} \cdot \begin{pmatrix} j_4 & j_2 & j_6 \\ m_4 & m_2 & -m_6 \end{pmatrix} \begin{pmatrix} j_4 & j_5 & j_3 \\ -m_4 & m_5 & m_3 \end{pmatrix}. \tag{B.10}$$

It enjoys several symmetries properties that we do not make use of in the main body. We refer the interested reader to [89] where they are explicitly mentioned.

Using the $6j$ symbol we have

$$\sum_{n_1,n_2,n_3} (-1)^{\sum_{a=1}^{3}(k_a - n_a)} \begin{pmatrix} j_1 & k_2 & k_3 \\ m_1 & -n_2 & n_3 \end{pmatrix} \begin{pmatrix} k_1 & j_2 & k_3 \\ n_1 & m_2 & -n_3 \end{pmatrix} \begin{pmatrix} k_1 & k_2 & j_3 \\ -n_1 & n_2 & m_3 \end{pmatrix} = \begin{Bmatrix} j_1 & j_2 & j_3 \\ k_1 & k_2 & k_3 \end{Bmatrix} \begin{pmatrix} j_1 & j_2 & j_3 \\ m_1 & m_2 & m_3 \end{pmatrix}. \tag{B.11}$$

Finally, when one of the spin index (say j_6) vanishes we have

$$\begin{Bmatrix} j_1 & j_2 & j_3 \\ j_4 & j_5 & 0 \end{Bmatrix} = \frac{\delta_{j_1,j_5}\delta_{j_2,j_4}}{\sqrt{d_{j_1}d_{j_2}}} (-1)^{j_1+j_2+j_3} \{j_1\ j_2\ j_3\}. \tag{B.12}$$

Acknowledgements

The completion of this thesis and my PhD study won't be possible without the help and support I have received during these chaotic yet impressive four years.

First and foremost, I need to thank my supervisor, Dr. Daniele Oriti, for giving me the opportunity to work in his quantum gravity group. His insights on quantum gravity, and more generally, on physics, are of great importance in shaping my research. At the same time Daniele is also a very relaxing person, made it more than enjoyable to work with him. The financial support from China Scholarship Council is deeply appreciated as well.

I need also to thank all colleagues working together in quantum gravity group of LMU, especially Dr. Jibril Ben Achour, Dr. Eugenia Colafranceschi, Roukaya Dekhil, Simon Langenscheidt, Dr. Luca Marchetti, Dr. Andreas Pithis and Yili Wang for numerous illuminating discussions on quantum gravity and physics. Special thanks to Simon for the translation of *die Zusammenfassung*.

Furthermore, I need to thank Victor Nador and Prof. Adrian Tanasa for their hospitality in LaBRI, University of Bordeaux, where part of the work in this thesis is done. I also appreciate the financial support from Bordeaux-LMU joint grant for my stay in Bordeaux.

We are living in hard times due to the long-lasting pandemic, and my life would be much miserable without the support from many friends. I need to thank Dr. Yuxuan Feng, Siyang Gu, Chenhao Li, Hong Luo, Dr. Yao Jin, Nan Qiu, Bishan Yang, Hao Yu, and Hanlin Zhang for their help during my stay here in Munich, especially when I was knocked down by the virus. I also need to thank my friends back in China, especially Ruiming Chen and Wenbin Sun, for their encouragements when I'm struggling to finish the thesis.

Finally, I need to thank my parents for their support on everything, emotionally and financially. It's certainly not possible for me to complete my PhD study without their understanding and encouragement.

Xiankai Pang
May 8, 2023 in Munich

Bibliography

[1] D. Oriti, *Approaches to Quantum Gravity*, Cambridge University Press (Mar, 2009), 10.1017/CBO9780511575549.

[2] R.P. Woodard, *How Far Are We from the Quantum Theory of Gravity?*, *Reports Prog. Phys.* **72** (2009) 126002 [0907.4238v1].

[3] A. Ashtekar, M. Reuter and C. Rovelli, *From General Relativity to Quantum Gravity*, 1408.4336.

[4] B.S. Dewitt, *Quantum Theory of Gravity. 1. The Canonical Theory*, *Phys.Rev.* **160** (1967) 1113.

[5] G. 't Hooft and M.J.G. Veltman, *One loop divergencies in the theory of gravitation*, *Ann. Inst. H. Poincare Phys. Theor. A* **20** (1974) 69.

[6] M.H. Goroff and A. Sagnotti, *The ultraviolet behavior of Einstein gravity*, *Nucl. Phys. B* **266** (1986) 709.

[7] C. Rovelli, *Notes for a brief history of quantum gravity*, *Recent Dev. Theor. Exp. Gen. Relativ. Gravit. Relativ. F. Theor. Proceedings, 9th Marcel Grossmann Meet. MG'9, Rome, Italy, July 2-8, 2000. Pts. A-C* (2000) 742 [gr-qc/0006061].

[8] A. Shomer, *A pedagogical explanation for the non-renormalizability of gravity*, 0709.3555.

[9] S. Bose, A. Mazumdar, G.W. Morley, H. Ulbricht, M. Toroš, M. Paternostro et al., *A Spin Entanglement Witness for Quantum Gravity*, *Phys. Rev. Lett.* **119** (2017) 240401 [1707.06050].

[10] C. Marletto and V. Vedral, *Gravitationally-induced entanglement between two massive particles is sufficient evidence of quantum effects in gravity*, *Phys. Rev. Lett.* **119** (2017) 240402 [1707.06036].

[11] T.D. Galley, F. Giacomini and J.H. Selby, *A no-go theorem on the nature of the gravitational field beyond quantum theory*, *Quantum* **6** (2022) 779 [2012.01441].

[12] K. Eppley and E. Hannah, *The necessity of quantizing the gravitational field*, *Found. Phys.* **7** (1977) 51.

[13] C. Isham, *Structural Issues in Quantum Gravity*, *Present.* (1995) 167 [gr-qc/9510063].

[14] S. Carlip, *Quantum gravity: A Progress report*, *Rept. Prog. Phys.* **64** (2001) 885 [gr-qc/0108040].

[15] S. Carlip, *Is quantum gravity necessary?*, *Class. Quant. Grav.* **25** (2008) 154010.

[16] S. Carlip, D.-W. Chiou, W.-T. Ni and R. Woodard, *Quantum gravity: A brief history of ideas and some prospects*, *Int. J. Mod. Phys. D* **24** (2015) 1530028 [1507.08194].

[17] A. Belenchia, R.M. Wald, F. Giacomini, E. Castro-Ruiz, Č. Brukner and M. Aspelmeyer, *Quantum Superposition of Massive Objects and the Quantization of Gravity*, *Phys. Rev. D* **98** (2018) [1807.07015].

[18] E. Rydving, E. Aurell and I. Pikovski, *Do Gedanken experiments compel quantization of gravity?*, *Phys. Rev. D* **104** (2021) 086024 [2107.07514].

[19] M. Bronstein, *Quantum theory of weak gravitational fields*, *Gen.Rel.Grav.* **44** (2012) 267.

[20] C. Rovelli and F. Vidotto, *Covariant Loop Quantum Gravity*, Cambridge University Press (2014).

[21] T. Thiemann, *Modern Canonical Quantum General Relativity*, Cambridge University Press (Sep, 2007), 10.1017/CBO9780511755682, [gr-qc/0110034].

[22] S.W. Hawking, *Black hole explosions?*, *Nature* **248** (1974) 30.

[23] S.W. Hawking, *Particle creation by black holes*, *Commun. Math. Phys.* **43** (1975) 199.

[24] A. Eichhorn, *Status of the asymptotic safety paradigm for quantum gravity and matter*, *Found. Phys.* **48** (2018) 1407 [1709.03696].

[25] K.S. Stelle, *String Theory, Unification and Quantum Gravity*, *Lect. Notes Phys.* **863** (2013) 3 [1203.4689].

[26] C. Rovelli, *Quantum gravity*, Cambridge university press (2004).

[27] A. Perez, *The Spin Foam Approach to Quantum Gravity*, *Living Rev. Rel.* **16** (2013) 3 [1205.2019].

[28] T. Krajewski, *Group Field Theories*, in *Proc. 3rd Quantum Gravity Quantum Geom. Sch. — PoS(QGQGS 2011)*, (Trieste, Italy), p. 005, Sissa Medialab, Jan, 2013, DOI [1210.6257].

[29] D. Oriti, *The microscopic dynamics of quantum space as a group field theory*, 1110.5606.

[30] D. Oriti, *Disappearance and emergence of space and time in quantum gravity*, *Stud. Hist. Phil. Sci.* **B46** (2014) 186 [1302.2849].

[31] D. Oriti, *Levels of spacetime emergence in quantum gravity*, 1807.04875.

[32] S. Carrozza, *Flowing in Group Field Theory Space: a Review*, *SIGMA* (2016) [1603.01902].

[33] D. Oriti, *Group field theory and loop quantum gravity*, in *Loop Quantum Gravity*, pp. 125–151 (2017), DOI [1408.7112].

[34] V. Rivasseau, *The Tensor Track: an Update*, in *29th Int. Colloq. Group-Theoretical Methods Phys.*, 2012 [1209.5284].

[35] V. Rivasseau, *Random Tensors and Quantum Gravity*, *SIGMA* **12** (2016) 69 [1603.07278].

[36] V. Rivasseau, *Tensor Field Theory*, *Proc. Proc. Corfu Summer Inst. 2015 — PoS(CORFU2015)* **CORFU2015** (2016) 106 [1604.07860].

[37] N. Delporte and V. Rivasseau, *The Tensor Track V: Holographic Tensors*, in *17th Hellenic School and Workshops on Elementary Particle Physics and Gravity*, Apr, 2018 [1804.11101].

[38] M. Finocchiaro and D. Oriti, *Renormalization of Group Field Theories for Quantum Gravity: New Computations and Some Suggestions*, *Front. Phys.* **8** (2021) [2004.07361].

[39] A.G.A. Pithis and J. Thürigen, *Phase transitions in TGFT: Functional renormalization group in the cyclic-melonic potential approximation and equivalence to $O(N)$ models*, *JHEP* **2020** (2020) [2009.13588].

[40] L. Freidel, *Group field theory: An Overview*, *Int. J. Theor. Phys.* **44** (2005) 1769 [hep-th/0505016].

[41] S. Gielen, D. Oriti and L. Sindoni, *Homogeneous cosmologies as group field theory condensates*, *JHEP* **06** (2014) 13 [1311.1238].

[42] D. Oriti, L. Sindoni and E. Wilson-Ewing, *Emergent Friedmann dynamics with a quantum bounce from quantum gravity condensates*, *Class. Quant. Grav.* **33** (2016) 224001 [1602.05881].

[43] S. Gielen and L. Sindoni, *Quantum Cosmology from Group Field Theory Condensates: a Review*, *SIGMA* (2016) [1602.08104].

[44] D. Oriti, *The universe as a quantum gravity condensate*, *Comptes Rendus Phys.* **18** (2017) 235 [1612.09521].

[45] M. de Cesare, A.G.A. Pithis and M. Sakellariadou, *Cosmological implications of interacting Group Field Theory models: cyclic Universe and accelerated expansion*, *Phys. Rev.* **D94** (2016) 64051 [1606.00352].

[46] M. de Cesare and M. Sakellariadou, *Accelerated expansion of the Universe without an inflaton and resolution of the initial singularity from Group Field Theory condensates*, *Phys. Lett. B* **764** (2017) 49 [1603.01764].

[47] A.G.A. Pithis and M. Sakellariadou, *Group Field Theory Condensate Cosmology: An Appetizer*, *Universe* **5** (2019) 147 [1904.00598].

[48] L. Marchetti and D. Oriti, *Quantum Fluctuations in the Effective Relational GFT Cosmology*, *Front. Astron. Sp. Sci.* **8** (2021) [2010.09700].

[49] L. Marchetti and D. Oriti, *Effective relational cosmological dynamics from quantum gravity*, *JHEP* **2021** (2021) 25 [2008.02774].

[50] D. Oriti and X. Pang, *Phantom-like dark energy from quantum gravity*, *JCAP* **2021** (2021) 040 [2105.03751].

[51] L. Marchetti and D. Oriti, *Effective dynamics of scalar cosmological perturbations from quantum gravity*, *JCAP* **2022** (2022) 004 [2112.12677].

[52] M. Bojowald, *Absence of a Singularity in Loop Quantum Cosmology*, *Phys. Rev. Lett.* **86** (2001) 5227 [gr-qc/0102069v1].

[53] A. Ashtekar and P. Singh, *Loop Quantum Cosmology: A Status Report*, *Class. Quant. Grav.* **28** (2011) 213001 [1108.0893].

[54] M. Bojowald, *Critical evaluation of common claims in loop quantum cosmology*, *Universe* **6** (2020) 36 [2002.05703].

[55] J. Martin, *Cosmic Inflation: Trick or Treat?*, 1902.05286.

[56] N. Aghanim, Y. Akrami, M. Ashdown, J. Aumont, C. Baccigalupi, M. Ballardini et al., *Planck 2018 results: VI. Cosmological parameters*, *Astron. Astrophys.* **641** (2020) [1807.06209].

[57] J. Martin, *Everything You Always Wanted To Know About The Cosmological Constant Problem (But Were Afraid To Ask)*, *Comptes Rendus Phys.* **13** (2012) 566 [1205.3365].

[58] S. Weinberg, *The cosmological constant problem*, *Rev. Mod. Phys.* **61** (1989) 1.

[59] G.-B. Zhao, M. Raveri, L. Pogosian, Y. Wang, R.G. Crittenden, W.J. Handley et al., *Dynamical dark energy in light of the latest observations*, *Nat. Astron.* **1** (2017) 627 [1701.08165].

[60] W. Yang, S. Pan, E. Di Valentino, O. Mena and A. Melchiorri, *2021-H_0 Odyssey: Closed, Phantom and Interacting Dark Energy Cosmologies*, *JCAP* **2021** (2021) 008 [2101.03129].

[61] L. Perivolaropoulos and F. Skara, *Challenges for ΛCDM: An update*, *New Astron. Rev.* **95** (2021) 101659 [2105.05208v3].

[62] D.L. Shafer and D. Huterer, *Chasing the phantom: A closer look at type Ia supernovae and the dark energy equation of state*, *Phys. Rev. D* **89** (2014) 063510 [1312.1688].

[63] Y. Wang, L. Pogosian, G.-B. Zhao and A. Zucca, *Evolution of Dark Energy Reconstructed from the Latest Observations*, *Astrophys. J.* **869** (2018) L8 [1807.03772].

[64] A.G. Riess, S. Casertano, W. Yuan, L.M. Macri and D. Scolnic, *Large Magellanic Cloud Cepheid Standards Provide a 1Determination of the Hubble Constant and Stronger Evidence for Physics beyond ΛCDM*, *Astrophys. J.* **876** (2019) 85 [1903.07603].

[65] E. Di Valentino, A. Mukherjee and A.A. Sen, *Dark Energy with Phantom Crossing and the H_0 tension*, *Entropy* **23** (2020) [2005.12587].

[66] L. Heisenberg, H. Villarrubia-Rojo and J. Zosso, *Can late-time extensions solve the H_0 and σ_8 tensions?*, *Phys. Rev. D* **106** (2022) 043503 [2202.01202].

[67] R. Caldwell, *A phantom menace? Cosmological consequences of a dark energy component with super-negative equation of state*, *Phys. Lett. B* **545** (2002) 23 [astro-ph/9908168].

[68] S.M. Carroll, M. Hoffman and M. Trodden, *Can the dark energy equation-of-state parameter w be less than -1?*, *Phys. Rev. D* **68** (2003) 023509 [astro-ph/0301273].

[69] R. Saitou and S. Nojiri, *Stable phantom-divide crossing in two scalar models with matter*, *Eur. Phys. J. C* **72** (2012) 1 [1203.1442].

[70] A. Ashtekar, B. Gupt, D. Jeong and V. Sreenath, *Alleviating the Tension in the Cosmic Microwave Background using Planck-Scale Physics*, *Phys. Rev. Lett.* **125** (2020) 051302 [2001.11689].

[71] A. Ashtekar, B. Gupt and V. Sreenath, *Cosmic Tango Between the Very Small and the Very Large: Addressing CMB Anomalies Through Loop Quantum Cosmology*, *Front. Astron. Sp. Sci.* **8** (2021) [2103.14568].

[72] Y. Li, D. Oriti and M. Zhang, *Group field theory for quantum gravity minimally coupled to a scalar field*, *Class. Quant. Grav.* **34** (2017) 195001 [1701.08719].
[73] W.J. Fairbairn and E.R. Livine, *3D spinfoam quantum gravity: matter as a phase of the group field theory*, *Class. Quant. Grav.* **24** (2007) 5277 [gr-qc/0702125].
[74] S. Gielen and D. Oriti, *Cosmological perturbations from full quantum gravity*, *Phys. Rev.* **D98** (2018) 106019 [1709.01095].
[75] M. de Cesare, D. Oriti, A.G.A. Pithis and M. Sakellariadou, *Dynamics of anisotropies close to a cosmological bounce in quantum gravity*, *Class. Quant. Grav.* **35** (2018) 015014 [1709.00994].
[76] A. Calcinari and S. Gielen, *Towards anisotropic cosmology in group field theory*, *Class. Quant. Grav.* **40** (2023) 085004 [2210.03149].
[77] D. Boulatov, *A Model of Three-Dimensional Lattice Gravity*, *Mod. Phys. Lett. A* **07** (1992) 1629 [hep-th/9202074].
[78] G. Ponzano and T. Regge, *Semiclassical limit of Racah coefficients*, *Spectrosc. Gr. Theor. methods Phys.* (1968) 1.
[79] L. Freidel, *A Ponzano-Regge model of Lorentzian 3-dimensional gravity*, *Nucl. Phys. B - Proc. Suppl.* **88** (2000) 237 [gr-qc/0102098].
[80] F. Girelli, E.R. Livine and D. Oriti, *4d Deformed Special Relativity from Group Field Theories*, *Phys. Rev. D* **81** (2009) [0903.3475].
[81] D.J. Amit and D.V. Roginsky, *Exactly soluble limit of ϕ^3 field theory with internal Potts symmetry*, *J.Phys.A* **12** (1979) 689.
[82] D. Benedetti and N. Delporte, *Remarks on a melonic field theory with cubic interaction*, *JHEP* **2021** (2020) [2012.12238].
[83] S. Gielen, D. Oriti and L. Sindoni, *Cosmology from Group Field Theory Formalism for Quantum Gravity*, *Phys. Rev. Lett.* **111** (2013) 31301 [1303.3576].
[84] D. Oriti, L. Sindoni and E. Wilson-Ewing, *Bouncing cosmologies from quantum gravity condensates*, *Class. Quant. Grav.* **34** (2017) 04LT01 [1602.08271].
[85] J. Engle, R. Pereira and C. Rovelli, *Consistently solving the simplicity constraints for spinfoam quantum gravity*, *Phys. Rev. Lett.* **99** (2007) 1 [0705.2388].
[86] J. Engle, E. Livine, R. Pereira and C. Rovelli, *LQG vertex with finite Immirzi parameter*, *Nucl. Phys. B* **799** (2007) 136 [0711.0146].
[87] M. Dupuis and E.R. Livine, *Lifting SU(2) Spin Networks to Projected Spin Networks*, *Phys.Rev.D* **82** (2010) [1008.4093].
[88] M. Finocchiaro, Y. Jeong and D. Oriti, *Quantum geometric maps and their properties*, *Class. Quant. Grav.* **39** (2022) 135014 [2012.11536].
[89] I. Mäkinen, *Introduction to SU(2) recoupling theory and graphical methods for loop quantum gravity*, 1910.06821.
[90] D. Oriti, *Group field theory as the 2nd quantization of Loop Quantum Gravity*, *Class. Quant. Grav.* **33** (2016) 85005 [1310.7786].
[91] E. Wilson-Ewing, *A relational Hamiltonian for group field theory*, *Phys. Rev. D* **99** (2018) [1810.01259].
[92] S. Gielen and A. Polaczek, *Generalised effective cosmology from group field theory*, *Class. Quant. Grav.* **37** (2019) [1912.06143].

[93] S. Gielen, *Frozen formalism and canonical quantization in group field theory*, *Phys. Rev. D* **104** (2021) 106011 [2105.01100].

[94] E. Colafranceschi and D. Oriti, *Quantum gravity states, entanglement graphs and second-quantized tensor networks*, *JHEP* **2021** (2021) 52 [2012.12622].

[95] J. Tambornino, *Relational Observables in Gravity: a Review*, *SIGMA* **8** (2011) 17 [1109.0740].

[96] P.A. Höhn, A.R.H. Smith and M.P.E. Lock, *Trinity of relational quantum dynamics*, *Phys. Rev. D* **104** (2021) 066001 [1912.00033].

[97] J. Engle, R. Pereira and C. Rovelli, *Flipped spinfoam vertex and loop gravity*, *Nucl. Phys. B* **798** (2008) 251 [0708.1236].

[98] G. Chirco, I. Kotecha and D. Oriti, *Statistical equilibrium of tetrahedra from maximum entropy principle*, *Phys. Rev. D* **99** (2019) 086011 [1811.00532].

[99] I. Kotecha, *On Generalised Statistical Equilibrium and Discrete Quantum Gravity*, Springer Theses, Springer International Publishing, Cham (Oct, 2022), 10.1007/978-3-030-90969-7, [2010.15445].

[100] S. Gielen, *Quantum cosmology of (loop) quantum gravity condensates: An example*, *Class. Quant. Grav.* **31** (2014) [1404.2944v3].

[101] A. Baratin and D. Oriti, *Group field theory and simplicial gravity path integrals: A model for Holst-Plebanski gravity*, *Phys. Rev. D* **85** (2011) [1111.5842].

[102] S. Gielen, *Emergence of a low spin phase in group field theory condensates*, *Class.Quant.Grav.* **33** (2016) 224002 [1604.06023].

[103] A.G.A. Pithis and M. Sakellariadou, *Relational evolution of effectively interacting group field theory quantum gravity condensates*, *Phys. Rev.* **D95** (2017) 64004 [1612.02456].

[104] A.G. Pithis, M. Sakellariadou and P. Tomov, *Impact of nonlinear effective interactions on group field theory quantum gravity condensates*, *Phys. Rev. D* **94** (2016) 064056 [1607.06662].

[105] S. Perlmutter, G. Aldering, G. Goldhaber, R.A. Knop, P. Nugent, P.G. Castro et al., *Measurements of Omega and Lambda from 42 High-Redshift Supernovae*, *Astrophys. J.* **517** (1998) 565 [9812133v1].

[106] A.G. Riess, A.V. Filippenko, P. Challis, A. Clocchiatti, A. Diercks, P.M. Garnavich et al., *Observational Evidence from Supernovae for an Accelerating Universe and a Cosmological Constant*, *Astron. J.* **116** (1998) 1009 [astro-ph/9805201].

[107] S. Weinberg, *Cosmology*, Oxford University Press (2008).

[108] D.N. Spergel, R. Bean, O. Dore, M.R. Nolta, C.L. Bennett, J. Dunkley et al., *Three-Year Wilkinson Microwave Anisotropy Probe (WMAP) Observations: Implications for Cosmology*, *Astrophys. J. Suppl. Ser.* **170** (2007) 377 [astro-ph/0603449].

[109] A.D. Sakharov, *Vacuum quantum fluctuations in curved space and the theory of gravitation*, *Sov.Phys.Dokl.* **12** (1968) 1040.

[110] A. Eichhorn, *On unimodular quantum gravity*, *Class. Quant. Grav.* **30** (2013) [1301.0879].

[111] R. Percacci, *Unimodular quantum gravity and the cosmological constant*, *Found. Phys.* **48** (2017) 1364 [1712.09903].
[112] P. Brax, *What makes the Universe accelerate? A review on what dark energy could be and how to test it*, *Reports Prog. Phys.* **81** (2018) 016902.
[113] S. Tsujikawa, *Dark energy: Investigation and modeling*, in *Dark Matter and Dark Energy: A Challenge for Modern Cosmology*, S. Matarrese, M. Colpi, V. Gorini and U. Moschella, eds., (Dordrecht), pp. 331–402, Springer Netherlands (2011).
[114] F.K. Anagnostopoulos, S. Basilakos, G. Kofinas and V. Zarikas, *Constraining the Asymptotically Safe cosmology: Cosmic acceleration without dark energy*, *JCAP* **2019** (2019) [1806.10580].
[115] G. Dvali, G. Gabadadze and M. Porrati, *4D gravity on a brane in 5D Minkowski space*, *Phys. Lett. B* **485** (2000) 208 [hep-th/0005016].
[116] D. Samart and B. Gumjudpai, *Phantom field dynamics in loop quantum cosmology*, *Phys. Rev. D* **76** (2007) [0704.3414].
[117] R.R. Caldwell, M. Kamionkowski and N.N. Weinberg, *Phantom Energy and Cosmic Doomsday*, *Phys. Rev. Lett.* **91** (2003) 071301 [astro-ph/0302506].
[118] M. Bouhmadi-Lopez, A. Errahmani, P. Martin-Moruno, T. Ouali and Y. Tavakoli, *The little sibling of the big rip singularity*, *Int. J. Mod. Phys. D* **24** (2014) [1407.2446].
[119] S. Nojiri and S.D. Odintsov, *Quantum de Sitter cosmology and phantom matter*, *Phys. Lett. B* **562** (2003) 147 [hep-th/0303117].
[120] S. Nojiri, S.D. Odintsov and S. Tsujikawa, *Properties of singularities in the (phantom) dark energy universe*, *Phys. Rev. D* **71** (2005) 063004 [hep-th/0501025].
[121] A. Vikman, *Can dark energy evolve to the Phantom?*, *Phys. Rev. D* **71** (2004) [astro-ph/0407107].
[122] J.M. Cline, S. Jeon and G.D. Moore, *The phantom menaced: Constraints on low-energy effective ghosts*, *Phys. Rev. D* **70** (2004) 043543 [hep-ph/0311312].
[123] S. Nesseris and L. Perivolaropoulos, *Crossing the Phantom Divide: Theoretical Implications and Observational Status*, *JCAP* (2006) [astro-ph/0610092].
[124] G. Alestas, L. Kazantzidis and L. Perivolaropoulos, *H_0 Tension, Phantom Dark Energy and Cosmological Parameter Degeneracies*, *Phys. Rev. D* **101** (2020) [2004.08363].
[125] S. Nojiri and S.D. Odintsov, *Modified gravity and its reconstruction from the universe expansion history*, *J. Phys. Conf. Ser.* **66** (2006) [hep-th/0611071].
[126] P. Singh, *Effective state metamorphosis in semi-classical loop quantum cosmology*, *Class. Quant. Grav.* **22** (2005) 4203 [gr-qc/0502086].
[127] J. Haro, J. Amoros and E. Elizalde, *Fate of the phantom dark energy universe in semiclassical gravity*, *Phys. Rev. D* **83** (2011) 123528.
[128] B. McInnes, *The dS/CFT Correspondence and the Big Smash*, *JHEP* **2002** (2002) 029 [hep-th/0112066].
[129] H. Zhang, *Crossing the phantom divide*, 0909.3013.
[130] A.A. Starobinsky, *Spectrum of relict gravitational radiation and the early state of the universe*, *JETP Lett.* **30** (1979) 682.

[131] V.F. Mukhanov, H.A. Feldman and R.H. Brandenberger, *Theory of cosmological perturbations. Part 1. Classical perturbations. Part 2. Quantum theory of perturbations. Part 3. Extensions*, *Phys.Rept.* **215** (1992) 203.

[132] Planck Collaboration, P.A.R. Ade, N. Aghanim, M. Arnaud, F. Arroja, M. Ashdown et al., *Planck 2015 results. XX. Constraints on inflation*, *Astron. Astrophys.* **594** (2016) A20 [1502.02114].

[133] R. Gurau, *A review of the large N limit of tensor models*, *Symmetries Groups Contemp. Phys.* (2012) 109 [1209.4295].

[134] J.B. Geloun, *On the finite amplitudes for open graphs in Abelian dynamical colored Boulatov–Ooguri models*, *J. Phys. A Math. Theor.* **46** (2013) 402002 [1307.8299v1].

[135] I.R. Klebanov, F. Popov and G. Tarnopolsky, *TASI Lectures on Large N Tensor Models*, *PoS* **TASI2017** (2018) 004 [1808.09434].

[136] H.M. Haggard and R.G. Littlejohn, *Asymptotics of the Wigner* $9j$*-symbol*, *Class. Quant. Grav.* **27** (2010) 135010 [0912.5384v1].

[137] F. Costantino and J. Marché, *Generating series and asymptotics of classical spin networks*, *J. Eur. Math. Soc.* **17** (2015) 2417 [1103.5644].

[138] V. Bonzom and P. Fleury, *Asymptotics of Wigner* $3nj$*-symbols with small and large angular momenta: an elementary method*, *J. Phys. A Math. Theor.* **45** (2012) 075202 [1108.1569v1].

[139] P. Donà, M. Fanizza, G. Sarno and S. Speziale, *SU(2) graph invariants, Regge actions and polytopes*, *Class. Quant. Grav.* **35** (2018) 045011 [1708.01727v3].

[140] S. Weinberg, *Gravitation and Cosmology*, John Wiley and Sons, New York (1972).

[141] L.D. Landau and E.M. Lifschits, *The Classical Theory of Fields*, Pergamon Press, Oxford (1975).

[142] S. Gielen, *Inhomogeneous universe from group field theory condensate*, *JCAP* **2019** (2019) 013 [1811.10639].

[143] F. Gerhardt, D. Oriti and E. Wilson-Ewing, *Separate universe framework in group field theory condensate cosmology*, *Phys. Rev. D* **98** (2018) 066011 [1805.03099].

[144] R.H. Brandenberger, *The Early Universe and Observational Cosmology*, vol. 646 of *Lecture Notes in Physics*, Springer Berlin Heidelberg, Berlin, Heidelberg (Jun, 2004), 10.1007/b97189, [hep-th/0306071].

[145] T. Buchert, *Dark Energy from structure: a status report*, *Gen. Rel. Grav.* **40** (2007) 467 [0707.2153].

[146] I.S. Gradshteyn, A. Jeffrey and I.M. Ryzhik, *Table of Integrals, Series, and Products*, Elsevier (2015), 10.1016/C2010-0-64839-5.